

Medical University of South Carolina

**MEDICA**

---

MUSC Theses and Dissertations

---

1998

## **Clear Cell Sarcoma of the Kidney and Congenital Mesoblastic Nephroma: Cellular and Molecular Characterization of Primary Tumors, Tumor Cell Lines, and Nude Mouse Xenografts Delineate Wilms' Tumor-Distinct Histopathogenetic Properties**

Noel Anderson Brownlee  
*Medical University of South Carolina*

Follow this and additional works at: <https://medica-musc.researchcommons.org/theses>

---

### **Recommended Citation**

Brownlee, Noel Anderson, "Clear Cell Sarcoma of the Kidney and Congenital Mesoblastic Nephroma: Cellular and Molecular Characterization of Primary Tumors, Tumor Cell Lines, and Nude Mouse Xenografts Delineate Wilms' Tumor-Distinct Histopathogenetic Properties" (1998). *MUSC Theses and Dissertations*. 174.

<https://medica-musc.researchcommons.org/theses/174>

This Dissertation is brought to you for free and open access by MEDICA. It has been accepted for inclusion in MUSC Theses and Dissertations by an authorized administrator of MEDICA. For more information, please contact [medica@musc.edu](mailto:medica@musc.edu).

Clear Cell Sarcoma of the Kidney and Congenital Mesoblastic Nephroma: Cellular and  
Molecular Characterization of Primary Tumors, Tumor Cell Lines, and Nude Mouse Xenografts  
Delineate Wilms' Tumor-Distinct Histopathogenetic Properties

Noel Anderson Brownlee

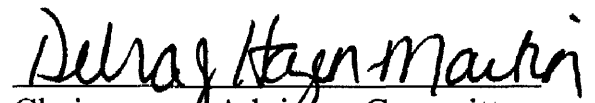
A dissertation submitted to the faculty of the Medical University of South Carolina in  
partial fulfillment for the degree of Doctor of Philosophy in the College of Graduate Studies

Medical University of South Carolina

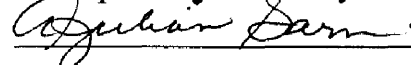
Department of Pathology and Laboratory Medicine

1998

Approved by:



Chairperson, Advisory Committee


















## Acknowledgments

I would like to first thank my parents for their support, encouragement, and patience during my tenure at the Medical University of South Carolina. Without these, I would not have been able pursue my interests in pathology.

Dr. Debra Hazen-Martin, my mentor and chairperson of my advisory committee deserves many thanks for listening to my concerns over the years. She has consistently offered invaluable advice and assistance in many aspects of my training. Because of her excellent teaching skills, I was able to learn many aspects of tissue culture, electron microscopy, and histochemistry. I also appreciate her commitment to improving graduate education in experimental pathology and for encouraging my future endeavors into this field. More than anything, she will always be valued as a good friend.

I would like to thank Dr. Gian Re for his patience and dedication to teaching me the ropes of the molecular biology laboratory. Dr. Re is also an invaluable friend who has offered me sound advice regarding subjects both on and off of campus. Dr. Re is also a natural teacher whose expertise is not always duly recognized; he has a lot to offer to any student who becomes a part of this department.

Dr. Garvin has been an invaluable committee member. He has provided me with specimens that have enabled me to initiate cell cultures for all of my studies on clear cell sarcoma of the kidney and congenital mesoblastic nephroma. I would especially like to thank him for remaining on my committee even after he relocated to Wake Forest University School of Medicine and taking the time out of his busy schedule to attend all of my committee meetings.

I would like to thank Drs. Willingham, Gattoni-Celli, and Fernandes for all of their helpful input regarding my project, particularly in the realm of cell cycle analysis and evaluation of apoptosis in CMN and CCSK. I also would like to thank Dr. Allen for his helpful input regarding gel electrophoresis. I would especially like to thank Dr. Willingham for remaining on my committee and making the trips from Winston-Salem to Charleston over the past year.

Carol Moskos, Sadie Green, and Margaret Romano deserve many thanks not only for their technical expertise, but also for their valued friendship. Carol worked very hard in trying to help me finish my transmission and scanning electron micrographs, Sadie assisted me greatly in maintaining my cell lines in my absence, and Margaret always did a nice job in preparing, cutting, and staining tissue in the histology laboratory. I would also like to thank Linda McC Carson for her excellent Word Processing pointers regarding the preparation of this dissertation.

## Table of Contents

Acknowledgments. . . . .	.ii
Table of Contents. . . . .	.iii
List of Tables. . . . .	.vi
List of Figures. . . . .	.vii
List of Abbreviations. . . . .	.ix
Abstract. . . . .	.xi

### Chapter 1: Introduction

I. General Introduction. . . . .	.2
II Historical Background. . . . .	.3
1. Genetic Etiology of Wilms' Tumor:Initiating Factors. . . . .	.3
2. p53 Signal Transduction: Cell Cycle Control and Apoptosis. . . . .	.11
3. p53 and Anaplastic Progression in Wilms' Tumor. . . . .	.14
4. Genetic Basis of Kidney Development with Implications for16 Pediatric Renal Tumor Histogenesis. . . . .	.17
5. All-trans Retinoic Acid Induced Differentiation of Tumor Cells. . . . .	.22
6. Congenital Mesoblastic Nephroma: Molecular Biology and 265 Histogenesis. . . . .	.24
7. Clear Cell Sarcoma of the Kidney: Molecular Biology and Histogenesis. . . . .	.26

### Chapter 2: Materials and Methods

I. Tumor Specimens. . . . .	.41
II Chemicals. . . . .	.41
III. Nude Mouse Heterotransplantation. . . . .	.42
IV. Tumor and Heterotransplant Tissue Fixation, Processing, and Hematoxylin and Eosin Staining. . . . .	.42
V. Transmission Electron Microscopic Evaluation of Tumor Cell Cultures. . . . .	.43
VI. Scanning Electron Microscopic Evaluation of Tumor Cell Cultures. . . . .	.44
VII. Initiation of Tumor Cell Culture. . . . .	.44
VIII. Cis-diamminedichloroplatinum (II) DNA Damage Response Assay. . . . .	.47
IX. All-trans Retinoic Acid Induced Cell Differentiation Assay. . . . .	.47
X. Immunocytochemistry Using Peroxidase Labelled Secondary Antibodies. . . . .	.48
XI. Immunofluorescence Cytochemistry. . . . .	.49
XII. Flow Cytometry: Cell Cycle Analysis. . . . .	.50
XIII. SDS-Polyacrylamide Gel Electrophoresis and Western Blotting. . . . .	.51
XIV. RNA Extraction-Agarose Gel Electrophoresis-Northern Blotting. . . . .	.52
XV. cDNA Probe Labelling and Nucleic Acid Hybridization. . . . .	.53
XVI. p53 Polymerase Chain Reaction-Single Stranded Conformation Polymorphism and DNA Sequencing. . . . .	.55

### **Chapter 3: Morphologic and Molecular Characterization of an In Vitro and In Vivo Model for the Study of Clear Cell Sarcoma of the Kidney and Congenital Mesoblastic Nephroma**

I.	Introduction.	.58
II.	Results.	.61
	1. In Vitro Characteristics of CCSK and CMN.	.61
	2. Light and Electron Microscopic Analysis of CCSK and CMN Nude Mouse Xenografts.	.61
	3. Immunofluorescent Cytochemical Analysis of Intermediate Filament Proteins in CCSK and CMN Cells.	.63
	4. WT-1 and IGF-2 Northern Analysis.	.64
III.	Discussion.	.65

### **Chapter 4: Characterization of the p53 Signal Transduction Pathway in Clear Cell Sarcoma of the Kidney, Congenital Mesoblastic Nephroma, and Anaplastic Wilms' Tumor**

I.	Introduction.	.87
II.	Results.	.91
	1. p53 Immunocytochemistry, SSCP, and DNA Sequencing Analysis.	.91
	2. mRNA Induction in Cisplatin Treated Tumor Cells.	.92
	3. Stabilization of p53 Protein in Cisplatin Treated Cells.	.94
	4. Flow Cytometric Evaluation of G1 Cell Cycle Arrest.	.95
	5. Steady-state mRNA Expression of p53, p21, MDM-2, and MDR-1 in CCSK and CMN Primary Tumors.	.95
III.	Discussion.	.97

### **Chapter 5: Steady-state and Retinoic Acid Induced Gene Expression Analysis of Clear Cell Sarcoma of the Kidney and Congenital Mesoblastic Nephroma: A Model of Tumor Histogenesis**

I.	Introduction.	.132
II.	Results.	.138
	1. Expression of Genes Involved in Normal Nephrogenesis in CCSK and CMN Primary Tumors.	.138
	2. Phase Contrast Microscopy of all-trans Retinoic Acid Treated CCSK and CMN Tumor Cells.	.138

**Chapter 5(continued)**

	3. Transmission and Scanning Electron Microscopic Analysis of all-trans Retinoic Acid Treated CCSK and CMN Cell Cultures.	.139
	4. All-trans Retinoic Acid Induced Gene Expression Alterations in CCSK and CMN Cells.	.140
III.	Discussion.	.142
	<b>Chapter 6: Summary and Conclusions.</b>	.172
	<b>Chapter 7: List of References.</b>	.178







**CHAPTER 5 (continued)**

Figure 6.	.	.	.	.	.	.	.	.159
Figure 7.	.	.	.	.	.	.	.	.161
Figure 8.	.	.	.	.	.	.	.	.163
Figure 9.	.	.	.	.	.	.	.	.165
Figure 10.	.	.	.	.	.	.	.	.167
Figure 11.	.	.	.	.	.	.	.	.169

**CHAPTER 6**

No Figures

**CHAPTER 7**

No Figures

## LIST OF ABBREVIATIONS

ABC	Avidin-Biotin-horseradish peroxidase complex
AE1/AE3	monoclonal antibody to cytokeratin intermediate filaments
atRA	all-trans retinoic acid
aWT	anaplastic Wilms' tumor
Bax	pro-apoptotic gene
Bcl-2	B-cell lymphoma-2 gene
Bcl-x <sub>L</sub>	B-cell lymphoma-x-long gene
BF-2	winged-helix transcription factor specific to developing renal stroma
BP2	insulin-like growth factor binding protein 2
CCSK	clear cell sarcoma of the kidney
CMN	congenital mesoblastic nephroma
DAB	3,3'- diaminobenzidine
dCTP	deoxycytosine triphosphate
DMEM	Dulbecco's modified Eagle's Medium
EDTA	ethylenediaminetetracetic acid
EGR	early growth response
F12	Ham's F12 Medium
FCS	fetal calf serum
GAPD	glyceraldehyde phosphate dehydrogenase
HBSS	Hank's balanced salt solution
IGF-1R	type I insulin-like growth factor receptor
IGF-2	insulin-like growth factor 2
kb	kilobase
MDM-2	murine double minute-2 gene
NBF	neutral buffered formalin
OCT	frozen tissue embedding compound
p21	cyclin-dependent kinase inhibitor p21 <sup>waf-1/cip-1</sup>

p53	tumor suppressor protein 53
PBS	phosphate buffered saline
PCR	polymerase chain reaction
RAR- $\alpha$	retinoic acid receptor alpha
RTK	rhabdoid tumor of the kidney
SDS	sodium dodecyl sulfate
SEM	scanning electron microscopy
SMA	smooth muscle actin
SSC	standard saline citrate
SSCP	single-stranded conformation polymorphism analysis
TBE	tris borate EDTA
TEM	transmission electron microscopy
TEMED	N,N,N',N'-tetramethylethylenediamine

## ABSTRACT

NOEL ANDERSON BROWNLEE. Clear Cell Sarcoma of the Kidney and Congenital Mesoblastic Nephroma: Cellular and Molecular Characterization of Primary Tumors, Tumor Cell Lines, and Nude Mouse Xenografts Delineate Wilms' Tumor Distinct Histopathogenetic Properties. (Under the direction of Dr. DEBRA J. HAZEN-MARTIN)

Clear cell sarcoma of the kidney (CCSK) and Congenital mesoblastic nephroma (CMN) are both pediatric renal tumors that differ from Wilms' tumor based on their distinctive histopathologic characteristics and clinical behavior. CCSK is a very malignant tumor characterized by a propensity for bone metastases, contrasting the relatively benign course characteristic of the majority of Wilms' tumors. CMN, in contrast, is a tumor of the newborn usually diagnosed within the first three months of life that is generally cured with surgery alone. To investigate further the cellular and molecular relationships of CCSK, CMN, and Wilms' tumor, a nude mouse xenograft and cell culture system was established for both CCSK and CMN; the immunohistochemical, gene expression, and functional analysis of the p53 tumor suppressor in cell cycle control signal transduction was performed; and Northern blot analysis of genes relevant to normal nephrogenesis was examined.

The histologic, ultrastructural, and molecular features of CCSK and CMN nude mouse xenografts, some of which have been passaged over several years, retained the characteristics of the primary tumors. Similarly, cell cultures derived from either primary tumors or mouse xenografts maintained cellular and molecular profiles consistent with findings for primary tumors.

p53 mutation is a marker for poor prognosis in Wilms' tumors. p53 immunoreactivity was absent from a large panel of CCSK and CMN primary tumor specimens examined. However, immunohistochemical analysis of CCSK and CMN tumor cell lines surprisingly

revealed p53 immunoreactivity in both CMN cell lines but in none of the CCSK cells examined suggesting that p53 was mutated in the benign CMN tumors. Functional analysis of p53 in the same CCSK and CMN cell culture system using a DNA damaging agent cis-diamminedichloroplatinum (100  $\mu$ M) demonstrated the presence of functional p53 as determined by the upregulation of *p21<sup>Waf-1/Cip-1</sup>* mRNA and G1 cell cycle arrest over an eight hour period.

The histogeneses of CCSK and CMN is not known. CCSK and CMN primary tumor tissue was examined for mRNA expression of the genes *WT-1*, *PAX-2*, *Pax-8*, and tenascin-C, all genes relevant to normal kidney development. CCSK and CMN were generally negative for WT-1, PAX-2, and Pax-8 expression. CMN, but not CCSK tumor specimens, were positive for tenascin-C mRNA. To evaluate further the histogenesis of these tumors, cultured CCSK and CMN cells were treated with the differentiation agent all-*trans* retinoic acid (1 $\mu$ M) over three days. Induction of several genes were noted during this period such as *PAX-2* and *tenascin*. The expression of *IGF-2*, *IGF-BP2*, and *p21<sup>waf-1/cip-1</sup>* were also modulated by this treatment. There were no light microscopically evident changes in cellular morphology in either CCSK or CMN cells. However, transmission and scanning electron microscopic analysis of the cells demonstrated closer cellular juxtaposition and flattening.

These studies indicate that the *in vivo* and *in vitro* model system for CCSK and CMN will be useful in further investigating the molecular pathological relationships and tumorigenic mechanisms in pediatric renal tumors. The apparent absence of p53 functional impairment in CCSK distinguishes this aggressive tumor type from anaplastic Wilms'

tumors which often bear mutation of p53 and suggests an alternative genetic explanation for the poor prognosis of CCSK. Further, a deeper understanding of the gene expression profile of pediatric renal tumors and renal development will be useful in the diagnosis and treatment of CCSK, CMN, and Wilms' tumor. Both the CCSK and CMN xenografts and cell lines also have potential utility in understanding the pathobiology of the developing fetal kidney as well as other pathologies affecting both children and adults.

# **Chapter 1**

## **Introduction**

## **I. General Introduction**

Pediatric renal tumors represent the sixth most common childhood malignancy following leukemias, brain tumors, neuroblastic tumors, and soft tissue sarcomas (Parham,1996). Wilms' tumor, or nephroblastoma, is by far the most common renal tumor of childhood, representing 85% of all reported cases (Murphy *et al.*, 1994). Other renal tumors with distinct histological and prognostic features also affect the young child. These tumors have been classified based on these distinguishing features by the National Wilms' Tumor Study (NWTs) group. They include the benign, congenital mesoblastic nephroma, (CMN) comprising 5% of all childhood renal tumors, the potentially metastatic clear cell sarcoma of the kidney (CCSK) comprising an additional 5% of cases, and the malignant rhabdoid tumor of the kidney (RTK) which comprises 2% of all renal tumors of childhood and usually metastasizes widely leading to patient death (Murphy *et al.*, 1994). The histological differences between the childhood renal tumors are noted in Figure 1. Both CMN and CCSK and their relationships with Wilms' tumor will be the subject of the present study.

Wilms' tumor has been extensively characterized at the morphological, immunohistochemical, cytogenetic, and molecular levels ( Grundy *et al.*, 1995). In contrast, both CMN and CCSK have not been evaluated thoroughly except for a few reports describing the light and electron microscopic distinction of these tumors from Wilms' tumor. In addition, there are very few studies which have evaluated the molecular pathology of these



two neoplasms. Therefore, questions as to the relationship between these two tumors and their possible relationship with Wilms' tumor remain unknown. One report has suggested that CMN represents the benign counterpart of the more aggressive CCSK (Yun, 1993). This theory is based primarily upon the similar stromal histology of these two neoplasms which differs from the triphasic histology (i.e., consisting of stroma, immature tubuli, and blastema) of Wilms' tumor. Although light and electron microscopic studies can provide valuable clues to the histogenetic origins of these two tumors, additional cellular and molecular based investigations will need to be applied to address this question thoroughly.

The present study is an effort to address the cellular and molecular biology of CMN and CCSK, determine if and how these tumor types are related to Wilms' tumor, and investigate their histogenetic origins. To address the pathology of CMN and CCSK, the following hypotheses are derived from the current literature and preliminary findings:

1. Both nude mouse xenografts (heterotransplants) and cultured cells derived from CMN and CCSK tumor tissue will maintain the characteristics of their respective primary tissue and provide models for the future study of these neoplasms.
2. Both CMN and CCSK cells exhibit different molecular biological aberrations which are distinct from those in Wilms' tumor; and,
3. CMN, CCSK, and Wilms' tumor have distinct histogenetic origins within the human developing kidney.

## **II. Historical Background**

### **1. Genetic Etiology of Wilms' Tumor: Initiating Factors**

Wilms' tumorigenesis is thought to occur during the formation of the metanephric

kidney because the histology of this tumor closely parallels the appearance of the structures visible during the course of normal development (Figure 2 ). Specifically, these structures include closely opposed blastematos tissue characterized by basophilia and high nuclear to cytoplasmic ratio, the formation of immature renal tubular elements, and the presence of cells of stromal lineage (e.g., fibroblastic cells, muscle cells, etc.) (Parham, 1996). In addition, nephrogenic rests represent foci of undifferentiated renal tissue that are found in 0.01% of all infant autopsies (Murphy *et al.*, 1994). Nephrogenic rests are also found in 0.40% of unilateral Wilms' tumor cases and 1.2% of synchronous bilateral Wilms' tumors and are thought to be tumor precursor lesions (Park *et al.*, 1993). Although Wilms' tumor is widely accepted as an aberrancy of normal renal morphogenesis, the genetic etiology of this neoplasm is very complex.

The genetic basis of Wilms' tumor was initially thought to follow the pattern of another embryonal neoplasm, retinoblastoma. Both retinoblastoma and Wilms' tumor may occur either sporadically or be familial in nature. This feature led Knudson to describe his classical "two-hit hypothesis" years before the actual identification of either the *Rb* or *WT-1* tumor suppressor genes. His hypothesis stated that those children with bilateral tumors inherited one defective allele (i.e., mutated, deleted, etc.) and acquired one additional somatic mutation before the development of a tumor. In contrast, mutations in both alleles occurred somatically in children with sporadic, unilateral cases of retinoblastoma and nephroblastoma (Knudson *et al.*, 1972).

The genetic etiology of Wilms' tumorigenesis first became evident upon the

karyotypic observation that patients with WAGR syndrome (i.e., a genetic syndrome characterized by Wilms' tumor, aniridia, genitourinary malformations, and mental retardation) harbored large germline deletions on one chromosome 11p13 allele (Grundy *et al.*, 1979). Patients with the WAGR syndrome were later reported to harbor point mutations in the other WT-1 allele (Baird *et al.*, 1992). Evidence for a putative Wilms' tumor gene mounted later with the observation that some sporadic cases of Wilms' tumors, those not associated with the WAGR syndrome, demonstrated loss of heterozygosity (LOH) at chromosome 11p13 (Fearon *et al.*, 1984; Koufos *et al.*, 1984). The localization of a small 11p13 deletion led to the identification of a gene encoding a (Cys)<sub>2</sub>-(His)<sub>2</sub> zinc finger transcription factor at this locus which was designated *WT-1* (Call *et al.*, 1990). Later work showed that alternative RNA splicing at two sites, one of which created a three amino acid (KTS) addition between the third and the fourth zinc fingers and the other which deletes exon 5, produced four discrete *WT-1* transcripts (Haber *et al.*, 1991). The role(s) of the four transcripts remain(s) unclear.

Additional evidence later came with the observation that patients having Denys-Drash syndrome, a genetic disease characterized by genitourinary malformations and a predilection for Wilms' tumor, harbored dominant point mutations that affect the WT-1 zinc fingers (Pelletier *et al.*, 1991). *WT-1* germline mutations have also been identified in Denys-Drash patients and in several cases of bilateral Wilms' tumor (Pelletier *et al.*, 1991; Huff *et al.*, 1991).

*WT-1* mutations were later described in nephrogenic rests, foci of primitive renal

cells that are found admixed with normal renal tissue in children with or without Wilms' tumor and areas thought to represent precursor lesions of Wilms' tumor (Park *et al.*, 1993). In this study, two separate cases of nephrogenic rests harbored a somatic mutation in *WT-1* that was identical to the mutation in the primary Wilms' tumors. *WT-1* knockout mice studies further demonstrated the involvement of *WT-1* in urogenital development as those mice without functional *WT-1* failed to form a functioning metanephros due to the absence of ureteric bud outgrowth. Defects in the mesothelium, heart, and lungs were also reported in these same *WT-1* knockout mice indicating the importance of this gene in other organs, as well (Kreidberg, *et al.*, 1993). Surprisingly, however, constitutional and tumor-specific *WT-1* mutations occur in only 10% of sporadic Wilms' tumor. In addition, many tumors contained only one *WT-1* mutation, with the other allele being apparently normal (Haber *et al.*, 1990). Because most Wilms' tumors overexpress *WT-1* mRNA and lack any demonstrable mutation, other, unexplored mechanisms which inactivate the function of *WT-1* may exist.

Insulin-like growth factor II (*IGF-2*), a fetal mitogen, is reportedly overexpressed in Wilms' tumor and several other childhood tumor types (Reeve *et al.*, 1985). Further, the use of a monoclonal antibody,  $\alpha$ IR3, directed against the cognate receptor of IGF-2, the insulin-like growth factor type I receptor (IGF-1R) inhibited the growth of cultured Wilms' tumor cells and the growth of heterotransplanted Wilms' tumors in nude mice (Gansler *et al.*, 1989). In addition, the use of suramin, a polysulfated naphthyl urea compound which is thought to interfere with IGF-2 binding with its cognate receptor, IGF-1R, inhibited the

growth of Wilms' tumor both *in vitro* and in tumor xenografted mice (Stein, 1993; Vincent *et al.*, 1996a). This information suggests a role for an IGF-2 autocrine growth loop in Wilms' tumor cell growth.

The *in vivo* target genes of the WT-1 transcription factor during normal renal organogenesis remain largely unknown. However, putative target genes have been identified predominantly through *in vitro* transactivation experiments. WT-1 appeared to bind promoters with guanine-cytosine (GC)-rich DNA sequences such as the early growth response (*EGR*)-1 consensus site, and led to transcriptional repression (Rauscher *et al.*, 1990). One of the presumptive WT-1 targets is the *IGF-2* gene. The major *IGF-2* promoter was defined in transient transfection assays as a region spanning from nucleotides -295 to +135, relative to the transcription start site. WT-1 bound to multiple sites within this region and functioned as a potent transcriptional repressor of *IGF-2 in vivo* (Drummond *et al.*, 1992). WT-1 also modulates the expression of the insulin-like growth factor one receptor (*IGF-1R*), a receptor which mediates the cellular action of the mitogen IGF-2. In a series of tumors examined, *IGF-1R* mRNA levels were inversely correlated with the expression of *WT-1*. Further, in the same study, cotransfection of Chinese hamster ovary cells with rat and human *IGF-1R* gene promoter constructs driving luciferase reporter genes and *WT-1* expression vectors demonstrated that the *WT-1* gene product represses *IGF-1R* promoter activity (Werner *et al.*, 1993). This evidence suggests a role for an IGF-2 autocrine growth loop as a transforming mechanism in Wilms' tumor cells.

WT-1 modulation of cell growth is not limited to the insulin-like growth factors and

their receptors. In transient transfection assays, WT-1 inhibited transcription of the platelet-derived growth factor A-chain (*PDGF-A*) gene, a growth factor overexpressed in many tumor types, by binding to a highly GC-rich region of the *PDGF-A* promoter as assessed by gel mobility shift assays (Wang *et al.*, 1992). WT-1 also repressed transforming-growth factor beta one (*TGF- $\beta$* ) gene expression (Dey *et al.*, 1994). In other studies, WT-1 repressed the *Bcl-2*, *c-myc*, and epidermal growth factor receptor promoters suggesting a role for WT-1 in the complex control of programmed cell death, or apoptosis (Hewitt *et al.*, 1995; Englert *et al.*, 1995).

The WT-1 gene product is reported to form a physical complex with another tumor suppressor protein, p53. This association depends upon the structural integrity of both proteins and has implications for both tumor suppressors' function. In the absence of functional p53 protein, WT1 appeared to attain potent transcriptional activation properties. In addition, WT1 synergized with p53 by enhancing its transactivating properties in one report (Maheswaran *et al.*, 1993). A later study found that the WT-1 gene product stabilized the p53 protein and inhibited p53 mediated apoptosis without affecting G1 cell cycle arrest (Maheswaran *et al.*, 1995). More recently, WT-1 has been shown to induce the expression of the cyclin-dependent kinase inhibitor *p21<sup>Waf-1/Cip-1</sup>* preceding apoptosis, apparently in a p53-independent manner suggesting a role for p21 in a WT-1 dependent programmed cell death pathway (Englert *et al.*, 1997). Table 1A summarizes the action of WT-1 on its various target genes.

Other potential Wilms' tumor loci have been suggested and include sites located on

chromosomes 11p15, 16q, and a familial locus at chromosome 17q ( Pritchard-Jones *et al.*, 1997). The 11p15 locus, the site of the putative WT-2 gene, was initially identified as a region of specific allele loss in Wilms' tumors and later found to contain the genes responsible for Beckwith-Wiedemann syndrome (BWS), an autosomal dominant genetic disease characterized by fetal overgrowth ( Moulton *et al.*, 1996). Children with BWS have a much greater chance of developing malignant tumors including hepatoblastomas and nephroblastomas relative to the general population. Approximately 10% of BWS children developed a childhood neoplasm in one report (Junien, 1992).

Several chromosome 11p15.5 imprinted genes have been implicated in the development of both Wilms' tumor and BWS. One of the genes residing at this locus was the paternally expressed autocrine growth factor *IGF-2* gene, a gene that showed pathological biallelic expression in some tissues due to loss of imprinting (Weksberg *et al.*, 1993). *IGF-2* is overexpressed at both the mRNA and protein levels in most cases of Wilms' tumor examined (Reeve *et al.*, 1985; Scott *et al.*, 1985), *H19* is a maternally expressed, untranslated RNA that may serve as a tumor suppressor gene also located at chromosome 11p15. In one study, the inactivation of *H19* correlated with the reciprocal activation of the *IGF-2* maternal allele in Wilms' tumor and contributed to tumorigenesis either by its *cis* effect on *IGF2* expression or via elimination of a *trans* growth-inhibiting effect of *H19* mRNA, or via both mechanisms (Hao *et al.*, 1993). The actual role of *H19* in the modulation of *IGF2* expression, however, is unclear.

More recently, attention has focused on another 11p15 gene, the cyclin-dependent

kinase inhibitor  $p57^{KIP2}$  as a candidate for the WT-2 tumor suppressor.  $p57^{KIP2}$  was reported as a structurally distinct member of the cyclin-dependent kinase inhibitor family which also includes  $p21^{Waf-1/Cip-1}$  and mapped to chromosome 11p15.5 in the vicinity of reported BWS breakpoints (Matsuoka *et al.*, 1995; Hoovers *et al.*, 1995). Analysis of the entire coding sequence and intron-exon boundaries of  $p57^{KIP2}$  in 40 unrelated cases of BWS revealed that only two patients (5%) harbored mutations, both of which were frameshift mutations in exon two (Lee *et al.*, 1997). Another report which analyzed nine patients with BWS demonstrated that 22% of the cases harbored  $p57^{KIP2}$  mutations (Hatada *et al.*, 1996). Whereas only a few cases of BWS reportedly harbor  $p57^{KIP2}$  mutations, an analysis of twelve primary Wilms' tumors revealed no mutations in this cyclin-dependent kinase inhibitor gene (O'Keefe *et al.*, 1997). Others have suggested that non-mutation cases of BWS and Wilms' tumor might still be caused by down-regulation of  $p57^{KIP2}$  expression via uni-parental paternal disomy (Henry *et al.*, 1991).

A recent study of one Wilms' tumor pedigree by linkage analysis has suggested another potential predisposition gene located at chromosome arm 17q12-q21 (Rahman *et al.*, 1996). This study conceded, however, that chromosome 17 can be excluded as the site of a predisposing gene in several smaller pedigrees which were examined.

The initiating genetic factors leading to Wilms' tumor are undoubtedly very heterogeneous. *WT-1*, once thought to be the sole initiating factor for Wilms' tumorigenesis is deleted or mutated in only 10% of cases. Likewise, genes located at chromosome 11p15 including *IGF2*, *H19*, and  $p57^{KIP2}$  still have unclear roles in the development of Wilms'



tumor. The variability and large number of genetic lesions found in Wilms' tumors to date testifies to the fact that the tumorigenic factors responsible for the development of this childhood neoplasm are very complex and poorly understood.

## **2. p53 Signal Transduction: Cell Cycle Control and Apoptosis**

The p53 tumor suppressor gene is located on the short arm of chromosome 17 and encodes a 53 kiloDalton (kD) nuclear phosphoprotein that is a negative regulator of cellular proliferation (Levine *et al.*, 1991). p53 mutations were relatively common in a large number of adult-onset tumor types including breast, lung, and colon carcinomas, but relatively rare in childhood malignancies (Nigro *et al.*, 1989). Wild-type p53 was present in extremely small quantities in most cell types analyzed due to rapid turnover mediated by the ubiquitin-dependent degradation pathway (Kastan, 1991). In contrast, tumor cells with a mutant p53 molecule demonstrated over-expression of p53 protein using either Western blotting or immunohistochemistry due to increased stability of the protein (Esrig *et al.*, 1993). Therefore, p53 protein overexpression is routinely used as a marker for a mutated p53 gene.

p53 is a mediator of diverse cellular processes including cell growth arrest, repair of DNA damage, and induction of programmed cellular death or apoptosis. p53 protein was induced following exposure to DNA damaging chemotherapeutic agents, ionizing radiation, and ultraviolet irradiation (Ko *et al.*, 1996). Several studies have suggested that p53 'senses' DNA damage by signalling through an upstream initiating factor ATM, or *mutated in ataxia telangiectasia* protein, a protein that is homologous to members of the DNA-protein kinase gene family (Hawley *et al.*, 1996). p53 mediates cell cycle arrest and programmed cell death

via several downstream effector genes. A substantial number of genes containing p53 response elements within their promoters have been identified (Table 1B).

The *p21<sup>waf-1/cip-1</sup>* is a cyclin-dependent kinase inhibitor which is transactivated by the wild-type p53 protein to effect cell cycle arrest. In seminal reports, p21 prevented cell cycle progression by binding to cyclin-cyclin dependent kinase complexes and preventing phosphorylation of proteins further downstream including the retinoblastoma protein Rb (El-Diery *et al.*, 1993; Xiong *et al.*, 1993). p21 also blocked the activity of the proliferating cell nuclear antigen which is important for S-phase cell cycle entry (Waga *et al.*, 1994). Additional evidence demonstrated that DNA damage created by gamma irradiation induces p53-dependent G1 cell cycle arrest that is mediated, at least in part, by the induction of *p21* mRNA (El-Diery *et al.*, 1994). Induction of *p21* is often used as a measure of p53 function. In a comprehensive report on over 120 cell lines treated with radiation and different chemotherapeutic agents, *p21* induction at both the mRNA and protein levels were used as determinants of the functional integrity of the p53 tumor suppressor gene (O'Connor *et al.*, 1997). *p21* is also upregulated by p53-independent mechanisms after exposure to differentiating agents such as all-trans retinoic acid, butyrate, or dimethylsulfoxide in HL-60 cells (Steinman *et al.*, 1994).

A variety of other p53 mediators have been described. Other genes which contain p53 response elements include *Bax* and *MDM-2*. In a seminal report, *Bax* was induced in response to p53 expression and encoded a pro-apoptotic protein with homology to the cellular survival factor Bcl-2 (Miyashita *et al.*, 1995). The induction of *Bax* in response to

ionizing radiation appeared to correlate with the mutational status of *p53* in human cells. Cells with wild-type *p53* actively induced *Bax* expression whereas mutant *p53* protein failed to do so (Zhan *et al.*, 1994). Initiation of the apoptotic cascade appears to depend upon the ratios of *Bax* to *Bcl-2* protein. *Bax-Bax* homodimers favored apoptosis, whereas *Bax-Bcl-2* heterodimers were inhibitors of programmed cell death (Oltvai *et al.*, 1993). *Bax* is, therefore, a link between *p53* and the initiation of apoptosis in those cells that are subject to stress signals, such as gamma irradiation or challenge with chemotherapeutic agents.

*MDM-2* is a protein which complexes with *p53* and inhibits its transcriptional activation ability (Oliner *et al.*, 1993). The *MDM-2* gene itself was shown to be a transcriptional target of *p53* which is activated in response to cell damaging signals. The latter is suggestive of an auto-regulatory feedback loop which exists between *p53* and *MDM-2* (Wu *et al.*, 1993; Burak *et al.*, 1993). In addition, *MDM-2* overexpression is known to inhibit *p53*-dependent G1 cell cycle arrest in response to irradiation. A peak in *MDM-2* protein occurs later than *p21* protein offering evidence that *MDM-2* can down-regulate *p53* after the cell has repaired DNA damage (Chen *et al.*, 1994). Crystallography experiments have recently identified the exact location of the *p53-MDM-2* interaction. An alpha-helical section of the *p53* transactivational domain interacts with a deep hydrophobic cleft of the *MDM-2* protein leading to the suppression of *p53*-mediated transactivation (Kussie *et al.*, 1996). More recently, *MDM-2* has been demonstrated to promote the rapid degradation of *p53* protein counteracting its accumulation following genotoxic stress (Haupt *et al.*, 1997).

The role of the MDM-2 proto-oncogene in the development of human tumors is well studied. The *MDM-2* gene is amplified in approximately 30-40% of all human sarcomas analyzed but rarely amplified in a large number of pediatric solid tumors examined (Oliner *et al.*, 1992; Waber *et al.*, 1993). *MDM-2* was over-expressed, however, in a number of pediatric cases of rhabdomyosarcoma (Kaletti *et al.*, 1996)

Others p53 target genes include the DNA repair gene *GADD45*, *cyclin-G*, the *insulin-like growth factor binding protein-3*, an anti-angiogenic molecule, *Thrombospondin-1*, *cyclin-D*, and several others (Ko *et al.*, 1996).

### **3. p53 and Anaplastic Progression in Wilms' Tumor**

The vast majority of classical Wilms' tumors are cured with the successful combination of chemotherapy, radiation therapy, and surgery. A small minority of Wilms' tumors (approximately 5.0%) are believed to progress to a more malignant phenotype characterized by the development of morphological anaplasia (Parham, 1996). Anaplastic cells are defined as those having extremely large nuclei with multipolar mitotic figures, hyperchromasia, and great variability in cell size. Anaplasia is associated with a high degree of chemotherapeutic resistance, but not necessarily increased tumor aggressiveness. Classical Wilms' tumors that have been successfully propagated in nude mice demonstrated no evidence of progression to morphological anaplasia after numerous passages. Therefore, direct evidence of anaplastic conversion has not been substantiated. One report, however, indicated that a metachronous anaplastic tumor developed within the tumor bed of a treated classical Wilms' tumor patient, thereby suggesting that classical tumors may progress into

its more malignant anaplastic counterpart (Oesterling *et al.*, 1987). Therefore, this study links these tumor histologies together in a continuum of time. More recent molecular biological assessment of Wilms' tumors has upheld the putative link between classical and anaplastic Wilms' tumors. Figure 3 represents a genetic model of Wilms' tumorigenesis and anaplastic progression.

Several studies have examined the mutational status of the *p53* tumor suppressor in Wilms' tumor. In one study, *p53* was mutated in two out of 21 cases examined, or 9.5% of all cases. One of the cases harbored morphological features of focal anaplasia (Malkin *et al.*, 1994). In another more comprehensive study of 140 cases, *p53* mutations were documented in eight of eleven anaplastic Wilms' tumors; the remaining 129 cases that did not exhibit anaplasia did not harbor *p53* mutations. The latter suggested that *p53* is a marker of anaplasia and is a gene, when defective, that is responsible for the poor outcome in patients with morphological features of anaplasia (Bardeesy *et al.*, 1994). In another study of three anaplastic Wilms' tumors, *p53* mutations were documented in two of the three cases. One mutation created a truncated protein that was undetectable using immunohistochemical methods suggesting that immunochemistry should not be used alone in assessing the mutational status of *p53* in these tumors. The other mutation was a point mutation at codon 273, a "hotspot" mutation, which rendered the protein product more stable and thus detectable using immunochemistry. The third case affected an older patient but no mutation was detected in this tumor even though immunohistochemical analysis using fixed primary tumor tissue suggested the presence of *p53* mutations (El Bahtimi *et al.*, 1996).

Additionally, Lahoti demonstrated a tendency for *p53* mutations to occur in the majority of a series of invasive and metastatic Wilms' tumors using immunohistochemistry. *p53* immunoreactivity was not, however, limited to either anaplastic or metastatic cases of Wilms' tumor. Lahoti suggested that the presence of other *p53* binding proteins were responsible for the latter immunophenotype in the classical Wilms' tumors (Lahoti *et al.*, 1996). However, amplification or overexpression of the *p53* binding protein MDM-2, which can bind to and stabilize the *p53* protein creating an immunophenotype similar to a mutated form of the protein, was not an alternative means for *p53* inactivation in a large series of Wilms' tumors examined (Bardeesy *et al.*, 1994).

Anaplastic Wilms' tumors are potentially aggressive tumors that are more resistant to the conventional Wilms' tumor chemotherapeutic treatment regimen of vincristine, vinblastine, and actinomycin D. A link between *p53* mutation and the development of a drug resistant phenotype has recently been described. The anaplastic Wilms' tumor cell line W4 contained a thymine deletion at codon 212 which is responsible for a frame shift leading to a TGA stop signal at codon 246. The resulting *p53* protein was truncated and non-functional (El Bahtimi *et al.*, 1996). The W4 anaplastic Wilms' tumor cell line also overexpressed the *MDR-1* gene in a separate study (Re *et al.*, 1997). *MDR-1* was not amplified in case W4 as assessed by Southern blotting, but was overexpressed at the mRNA level. P-glycoprotein function in the W4 cell line was inhibited by the calcium channel blocker verapamil in an *in vitro* daunomycin nuclear fluorescence accumulation assay. Mutation of *p53* and overexpression of *MDR-1* in this anaplastic Wilms' tumor was found to be consistent with

the clinical outcome of patient W4, as the patient died of multiple metastatic lesions.

The *MDR-1* and *p53* genes are functionally linked. *In vitro* transactivation studies containing a reporter gene under the control of the *MDR-1* promoter indicated that wild-type *p53* acts as a transcriptional repressor of the *MDR-1* gene and inactivating mutations of *p53* released this gene from repression (Chin *et al.*, 1992; Nguyen *et al.*, 1994). Evidence from studies of the W4 cell line supported these latter findings and suggested that *p53* and *MDR-1* are linked to both anaplastic progression and the development of a drug resistant phenotype in Wilms' tumors.

Although *p53* is mutated in a high percentage of the anaplastic Wilms' tumor cases, other chromosomal linkage studies have suggested the presence of other genes which predispose patients to a poor outcome. LOH at chromosome 16q was a non-random chromosomal abnormality in a series of Wilms' tumors. Significant loss of areas on chromosome 16q were present in nine of 45 informative cases (Maw *et al.*, 1992). Another report indicated that patients with deletions on chromosome 16q had relapse rates 3.3 times and mortality rates 12 times that of those patients that do not demonstrate LOH at chromosome 16q (Grundy *et al.*, 1994). The latter study also reported that chromosome 1p LOH in Wilms' tumor was a non-random event and linked to mortality rates three times higher than rates for patients without LOH.

#### **4. Genetic Basis of Kidney Development with Implications for Pediatric Renal Tumor Histogenesis**

The development of the kidney begins around embryonic day 19 and progresses through the pronephric, mesonephric, and metanephric stages before reaching maturity. The

definitive, functioning kidney of the postnatal period and beyond is the metanephros which forms as a result of a mesenchymal-epithelial transition. Around embryonic day 28, the metanephric kidney is induced in the sacral intermediate mesoderm (nephrotomes) of the trilaminar embryo by the ureteric buds, outgrowths of the distal portions of the Wolffian duct (mesonephric ducts). The ureteric buds subsequently penetrate beds of mesenchymal tissue termed the metanephric blastema spurring the mesenchyme to condense around the apical aspects of the ureteric bud. The ureteric bud and the metanephric blastema exert reciprocal inductive effects during this period causing continuation of mesenchymal condensation and further bifurcation of the ureteric buds. Later in development, remnants of the ureteric bud will constitute the collecting duct system whereas the condensed mesenchymal tissue continues to differentiate through several distinct stages including the comma-shaped and s-shaped bodies to eventually form the non-vascular elements of the glomerulus, the proximal and distal convoluted tubules, and the loops of Henle (Larsen, 1998). Recent studies have begun to elucidate the cellular and molecular mechanisms underlying the normal nephrogenesis and will undoubtedly offer new information which may be used to interpret renal abnormalities including the development of pediatric renal neoplasia. Figure 4 presents a diagrammatic representation of normal nephrogenesis.

The *WT-1* gene, first described in 1990, was localized to an area of chromosome 11 that was often deleted in Wilms' tumor (Call *et al.*, 1990). Besides its mutation or deletion in Wilms' tumors, *WT-1* plays a pivotal role in the development of the mammalian urogenital system. In a study of homozygous mutant *WT-1* mice, the ureteric buds failed to form properly leading to degradation of the metanephric mesenchyme and renal agenesis.



(Kreidberg *et al.*, 1993). In the mouse fetal kidney, *WT-1* gene expression was relatively low in the uninduced metanephric mesenchyme. Coincident with ureteric bud induction, the mesenchyme expressed increased levels of *WT-1* indicating the importance of this gene in this developmental stage (Pritchard-Jones *et al.*, 1990; Armstrong *et al.*, 1992). *WT-1* expression remained high during the formation of the early nephron precursors, but as the kidney matured, expression was limited to the glomerular podocytes (Ryan, 1995).

The *Pax* genes are other important mediators of the developmental regulation of the kidney (Gruss *et al.*, 1992). The *Pax* gene family encodes evolutionary conserved transcription factors which share a common motif, the paired box, which acts as a DNA-binding domain. Some of the first experiments which addressed the function of *Pax-2* in kidney development used gene knockout. *Pax-2* knockout mice, specifically *Pax2*<sup>-/-</sup> mice, failed to develop both kidneys and genitourinary tracts (Torres *et al.*, 1995). In addition, antisense *Pax-2* oligonucleotides used in kidney organ culture experiments demonstrated mesenchymal condensation failure and absence of epithelial differentiation (Rothenpieler *et al.*, 1993).

Additional studies of *Pax-2* function have been addressed in gene expression studies of the fetal kidney and Wilms' tumors. In the metanephric mesenchyme, *Pax-2* was expressed in the early condensates and comma-shaped bodies, but expression declined in the S-shaped bodies and was not expressed in mature nephron structures (Dressler *et al.*, 1990). Using in situ hybridization experiments, *Pax-2* has also been localized in condensed blastema cells of Wilms' tumors (Eccles *et al.*, 1995). Another report has also indicated that *Pax-2* is

abundantly expressed in a series of Wilms' tumors examined (Dressler *et al.*, 1992).

Both *WT-1* and *Pax-2* appear to be involved in a reciprocal modulation pathway. Expression of *Pax-2* is repressed in the presence of increasing amounts of a *WT-1* expression vector as assessed by chloramphenicol-acetyl transferase reporter gene assays (Ryan *et al.*, 1995). More recently, another report using deletion mutagenesis experiments indicated that *Pax-2* positively modulated the expression of *WT-1* by binding to a sequence between 33 and 71 base pairs upstream of the *WT-1* start site (Dehbi, *et al.*, 1996b).

Additional members of the *Pax* gene family implicated in early kidney development include *Pax-8*. Somewhat different from *Pax-2*, *Pax-8* was expressed in condensed mesenchyme, comma-shaped bodies, S-shaped bodies, and immature tubular structures as assessed by in situ hybridization studies. *Pax-8* is also expressed in the developing thyroid gland and in Wilms' tumors (Poleev *et al.*, 1992). A later study indicated that *Pax-8* expression was localized, in particular, to the condensed blastema cells of Wilms' tumors (Eccles *et al.*, 1995). Additionally, in transient transfection and gel-shift assays, *Pax-8* was demonstrated to transactivate *WT-1* by binding to a 38 base pair conserved motif within both mouse and human promoters, similar to that which was described for *Pax-2* (Dehbi *et al.*, 1996a). Members of the myc family of transcription factors are expressed at different stages of the kidney in a pattern similar to that of the *Pax* genes. In particular, *N-Myc* is highly expressed in the condensing mesenchymal tissue during normal nephrogenesis (Mugrauer, *et al.*, 1991).

In addition to the large number of transcription factors involved in kidney

morphogenesis, a variety of cellular adhesion molecules and extracellular matrix proteins play a role in the proper development of the nephron. One of these extracellular matrix proteins with relevance to understanding the histogenesis of CMN and CCSK is tenascin-C. Tenascin-C, also termed cytotactin, is a large hexameric glycoprotein that exhibits site-restricted expression patterns during the development of several organs and retains expression in selected adult organs including the kidney. In addition to the normal expression pattern of tenascin in the adult, it may be re-expressed in a number of pathologic conditions such as sites of inflammation, wound repair, and some tumors (Crossin, 1996). The actual function of tenascin is not clearly understood, as tenascin knockout mice have not demonstrated apparent pathologies (Saga *et al.*, 1992).

In the developing kidney, the expression pattern of tenascin is restricted. In one study, tenascin was not expressed by uninduced renal mesenchymal tissue, but was detectable in the extracellular matrix of mesenchymal cells which surrounded the developing epithelial cells. Additionally, tenascin seemed to be restricted only to those cells which gave rise to the stroma (Aufderheide *et al.*, 1987). The latter observations are consistent with the importance of this molecule in mesenchymal to epithelial transitions which occur during the developmental process. As nephrogenesis ceases, tenascin disappeared from the renal cortex and was only expressed in the interstitial cells of the deep medulla (Aufderheide *et al.*, 1987). In another study, tenascin immunoreactivity was not limited to the renal medullary interstitium, but was also found in the glomerulus, presumably secreted by the glomerular mesangial cells. In the same report, glomerular tenascin immunoreactivity was found

increased in the active phase of glomerulopathies and interstitial nephritides (Koukoulis *et al.*, 1991; Gould *et al.*, 1992; Truong *et al.*, 1996). Tenascin immunoreactivity is absent from loose mesenchymal cells even though the latter cells are positive for fibronectin and neural cell adhesion molecules (Ekblom *et al.*, 1991). The expression of tenascin is distinct from the cellular adhesion molecule expression pattern of kidney epithelial cells. These cells are negative for tenascin while positive for E-cadherin and laminin-A (known markers of epithelial cells in many tissue types). Tenascin, therefore, appears to be a marker for stromal cells. The distribution of this protein may be useful in understanding the histogenesis of pediatric renal tumors, particularly those which supposedly have stromal origins like CMN and CCSK. A summary of the gene expression characteristics of the developing kidney and pediatric renal tumors is summarized in Table II.

Intermediate filament proteins are also useful in understanding the derivation of tumors and are employed most frequently by pathologists attempting to define the origin of a tumor. For example, desmin and smooth muscle actin proteins are markers for smooth muscle cells, while vimentin is a marker for cells of mesenchymal origin. The latter intermediate filament proteins are useful in the diagnosis of connective tissue tumors, or sarcomas. In contrast, cytokeratins are markers for epithelial cells and are often useful in the diagnosis of carcinomas (Junquiera *et al.*, 1992)

## **5. All-trans Retinoic Acid (atRA) Induced Differentiation of Tumor Cells**

Retinoic acid is a well-known morphogen (Maden, 1985). As such, it has been used

as a chemopreventive agent and a therapeutic agent in some types of leukemia. Retinoic acid molecules along with their respective metabolites are analogs of Vitamin A, or retinol, an agent with many cellular functions. Of particular importance in the analysis of tumor histogenesis are the *all-trans* (atRA) and *9-cis* retinoic acid molecules. The latter agents effect their molecular and cellular modulations within the cell by binding to different types of nuclear receptors termed retinoic acid receptor (RAR) and the retinoid-X receptor (RXR). Both the RAR and RXR are heterocomplexes containing  $\alpha$ ,  $\beta$  and  $\gamma$  subunits. Transcription of a number of target genes are influenced by binding of either a retinoid-RAR or retinoid-RXR receptor complexes to retinoid acid response elements (RAREs) within their promoters.

Two tumor cell types, neuroblastoma and the promyelocytic leukemia cells HL-60, are particularly amenable to atRA induced differentiation and have constituted the subject of many studies regarding the mechanisms for this process. For example, atRA induced growth arrest and neurite formation, structures which resembled axons and dendrites, in many neuroblastoma cell lines in conjunction with downregulation of *N-myc* gene expression (Wada *et al.*, 1992). Decreased expression of the *c-myc* oncogene also occurred upon atRA induced differentiation in neuroblastoma cells (Thiele *et al.*, 1988). The levels of p53 mRNA and protein declined in atRA stimulated LAN-5 human neuroblastoma cells consistent with the notion that p53 is no longer needed in non-dividing cells (Davidoff *et al.*, 1992). Upon stimulation with atRA, HL-60 promyelocytic leukemia cells were induced to differentiate into cells of the granulocytic lineage (Olsson *et al.*, 1982).

More recently, atRA has been investigated in Wilms' tumor for its ability to initiate differentiation in a blastemal predominant cell line (Vincent *et al.*, 1996b). AtRA arrested

the proliferation of Wilms' tumor cells as assessed by tritiated thymidine incorporation experiments. Arrest of cellular proliferation was associated with downregulation of *N-myc*. However, light microscopic and ultrastructural analysis of these Wilms' tumor cells did not exhibit any morphological signs of epithelial differentiation as assessed by the development of cell polarity, microvilli, or junctional complexes.

### **5. Congenital Mesoblastic Nephroma : Molecular Biology and Histogenesis**

CMN is the most common renal neoplasm of infants and was first distinguished from the more common Wilms' Tumor by Bolande in 1967 (Bolande *et al.*, 1967). CMN comprised approximately five percent of all pediatric renal tumors in one report with over 60 percent being diagnosed before three months of age (Murphy *et al.*, 1994). The majority of CMNs are benign, with surgery alone proving to be curative. Exceptions to this rule include the clinical behavior of cellular (or atypical) CMN which had the ability to recur and metastasize following incomplete resection of tumor at surgery (Beckwith *et al.*, 1986). Histologically, the tumor is composed of interlacing fascicles of spindle-shaped fibroblasts and myofibroblasts with round nuclei in its classical form (Pettinato *et al.*, 1989). Atypical mesoblastic nephroma, also known as the cellular CMN, is a potentially aggressive variant of CMN with dense cellularity, many mitotic figures, necrosis, and hemorrhage (Joshi *et al.*, 1986).

The histogenetic origin of CMN remains controversial. Nevertheless, it has been proposed that this tumor arises from secondary mesenchyme (i.e. mesenchyme no longer capable of differentiating into epithelial cells of the nephron, but into cells which form the renal interstitium) (Yoon-Jung *et al.*, 1994). CMNs are generally positive for the

intermediate filament proteins desmin and smooth muscle actin, both of which are markers for skeletal and smooth muscle differentiation, respectively. CMN is not immunoreactive for markers of epithelial cells such as the cytokeratins (Pettinato *et al.*, 1989). One report demonstrated immunoreactivity for the Thy-1 antigen in both CMN and renal interstitium, but not in CCSK or Wilms' Tumor (Hazen-Martin *et al.*, 1993). Some reports suggested that CCSK may arise from a progression of the more benign CMN due to similarities in histological and ultrastructural appearance (Haas *et al.*, 1984). Others have proposed that CMNs and CCSKs are one tumor with the potential to differentiate anywhere along the stromal lineage of embryonic development into CMN, atypical (cellular) CMN, or CCSK (Yoon-Jung *et al.*, 1994). In other words, because all of these tumor types resemble different stages of stromal cell differentiation during fetal kidney development, tumorigenic events may develop at key points in this developmental process resulting in either the cellular or classical CMN, or CCSK.

Cytogenetic studies of CMN are relatively uncommon. Several studies have shown that CMNs are often trisomic or tetrasomic for chromosome 11 (Kaneko *et al.*, 1991). Another report using fluorescence *in situ* hybridization studies of CMN also indicated that chromosome 11 trisomy or tetrasomy is a common, non-random finding in a number of CMN cases (Schofield *et al.*, 1993). This study also reported an association of extra copies of chromosome 11 with the cellular or mixed variant of CMN. In another report, northern analysis indicated that two cases of CMN overexpressed *IGF-2*, a gene localized to chromosome 11p15 (Tomlison *et al.*, 1992). Overexpression of *IGF-2* is consistent with the extra copies of chromosome 11 in these tumors and may represent a tumorigenic mechanism

in CMN.

Molecular evidence for the concept that CMNs derive from the stromal lineage of renal stem cells is incomplete. One study reported a lack of *N-myc* and *WT-1* mRNA in two cases of CMN, contrasting with the presence of *WT-1* and *N-myc* mRNA in Wilms' tumors (Tomlison *et al.*, 1992). In addition, *WT-1* is not expressed in the stromal component of triphasic, classical Wilms' tumors (Eccles *et al.*, 1995). The latter observation is consistent with the hypothesis that CMN, being stromal in nature, arises from the same renal stem cell as the stromal cell present in Wilms' tumors.

## **6. Clear Cell Sarcoma of the Kidney: Molecular Biology and Histogenesis**

CCSK is a rare renal tumor affecting young children primarily between the ages of one and three years, having a characteristic histologic appearance composed of clear nuclei, abundant extracellular matrix production, and a fine interweaving network of blood vessels. The latter features distinguish CCSK from the more common Wilms' tumor which is usually composed of blastema, immature tubuli, and stromal cells. Clinically, CCSK is separated from Wilms' tumors due to a marked propensity to recur after initial treatment and metastasize to bone (Murphy *et al.*, 1994). CCSK was first reported as a separate entity by Kidd in 1970 when he described the "sarcoma of the kidney" as having a higher incidence of bone metastases compared to the relatively benign Wilms' tumor which generally did not metastasize (Kidd, 1970). Due to the latter, Kidd emphasized the distinction of CCSK from Wilms' tumor in the diagnostic process. Since the initial report in 1970, other reports have followed describing this tumor. The term clear cell sarcoma of the kidney as a descriptive term for this neoplasm was first suggested in a subsequent paper (Beckwith *et al.*, 1978). In



the same year, Marsden and Morgan described this same tumor type and termed the tumor bone metastasizing renal tumor of childhood and undifferentiated sarcoma of the kidney, respectively (Marsden *et al.*, 1978; Morgan *et al.*, 1978). All of these reports found that this tumor was distinguishable from Wilms' tumor based on its distinct histology and predilection for the development of metastatic bone lesions.

The treatment of children with CCSK has been dramatically improved with the addition of actinomycin D to the chemotherapeutic and radiation regimen. CCSK patients now routinely receive vincristine, actinomycin D, doxorubicin, and cyclophosphamide in addition to radiation therapy. Actinomycin D increased the six-year relapse-free survival from 25.0% to 63.5% with the overall survival rate now approaching 70%. However, this report noted that CCSK had the ability to recur several years after the initial diagnosis, therefore necessitating the need for close patient follow-up years after the initial diagnosis. This same report has further noted that etoposide and ifosfamide have been used successfully in the treatment of CCSK patients (Green *et al.*, 1994).

Previous studies of the immunohistochemical and electron microscopic features of CCSK have further distinguished this tumor from Wilms' tumors. Ultrastructurally, CCSK contained round to oval nuclei with little heterochromatin, small nucleoli, primitive cellular junctions, sparse Golgi apparatus and endoplasmic reticulum, and a lack of epithelial differentiation (Haas *et al.*, 1984). Ishii, however, noted that CCSK had a latent epithelial nature evidenced by the fact that CCSK grown in culture produced mucin, had an eosinophilic cytoplasm, and contained intracellular canaliculi (Ishii *et al.*, 1989). The latter report further noted that some CCSKs, like Wilms' tumors with primitive epithelium, were

immunoreactive for cytokeratins 8 and 19, markers of renal tubular epithelium. Other immunohistochemical studies indicated that CCSKs were negative for epithelial membrane antigen as well as for markers of smooth muscle, endothelial cells, neural tissue, and cells of the immune system. CCSK cells were only positive for vimentin consistent with the mesenchymal character of this tumor (Looi *et al.*, 1993).

The cytogenetic and molecular genetic characteristics of CCSK remain relatively scanty. A few case reports do exist, however. Punnett reported the first cytogenetic study of CCSK (Punnett *et al.*, 1989). This study demonstrated a consistent karyotype of 46,XY,t(10;17)(q22;p13) in all cells examined of an individual patient. The constitutional karyotype of peripheral blood lymphocytes from the same patient was normal 46,XY, however. Punnett further speculated that p53 may be involved in the tumorigenic events of CCSK since this tumor suppressor is located at 17p13, the region involved in the chromosomal breakpoint. Another potential gene interrupted by this translocation was the early growth response gene-2 (EGR-2) located at chromosome 10q22. Other reports indicated extensive cytogenetic abnormalities in CCSK including a loss of the short arm of chromosome 11 (Wang-Wuu *et al.*, 1990). Another report analyzed four cases of CCSK and found that the majority of cases were normal. However, one case in which the patient eventually died was found to have a chromosomal 22 translocation t(2;22)(q21;q11) (Kaneko *et al.*, 1991). Deletion of chromosome 22 in CCSK has also been reported (Douglass *et al.*, 1990). Cytogenetic aberrations or LOH at chromosome 22q loci also occur in the RTK, another renal tumor of childhood with a poor prognosis (Douglass *et al.*, 1990; Schofield *et al.*, 1996). This association may suggest a common origin for both CCSK and RTK.

Molecular biologic characterization of CCSK is limited . Yun used Northern analysis and *in situ* hybridization and demonstrated that CCSK did not express WT-1 mRNA, a gene with known involvement in the early development of the kidney, but was positive for *IGF-2* mRNA (Yun, 1993). Based on these findings along with immunohistochemistry and electron microscopy, Yun speculated that CCSK is derived from either loose metanephric mesenchyme or from stromal cells at an early stage of differentiation. One study reported that the WT-1 gene contains no gross abnormalities (i.e. gene rearrangements) in five CCSKs examined by Southern blotting (Kikuchi *et al.*, 1992). More recently, an immunohistochemical examination of several cases of CCSK demonstrated strong nuclear immunoreactivity using monoclonal antibodies directed against p53, suggesting mutations in these tumors types (Cheah *et al.*, 1996). No molecular biological or functional confirmation has been performed for these tumors.

**Figure 1.** Hematoxylin and eosin stained sections of pediatric renal tumors. **A**, cellular congenital mesoblastic nephroma; **B**, clear cell sarcoma of the kidney (m = collagenous extracellular matrix material; the arrow indicates the characteristic empty appearing nuclei of this tumor); **C**, classical, triphasic Wilms' tumor (s = stromal tissue, b = blastema, and t = immature tubuli), and **D**, Malignant rhabdoid tumor of the kidney. All micrographs at 250X.

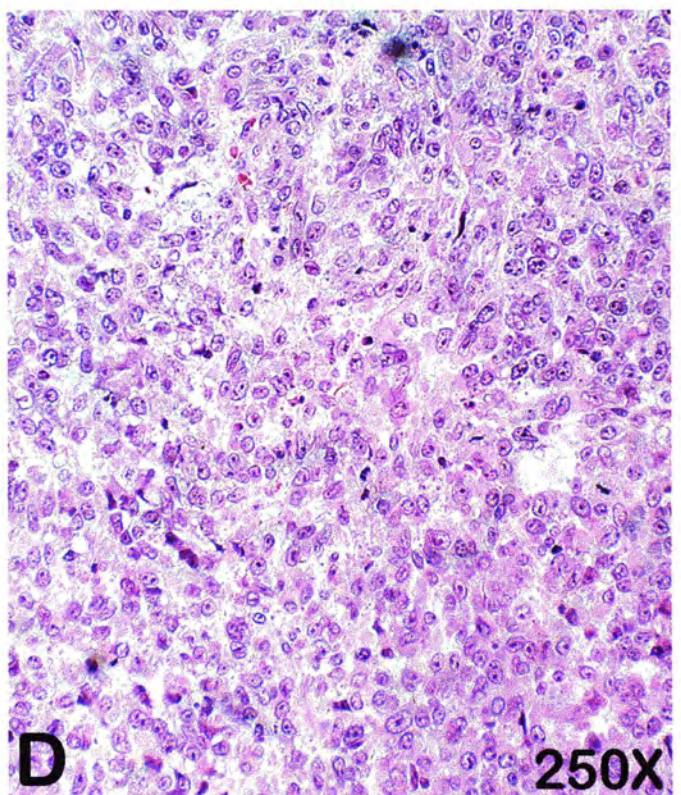
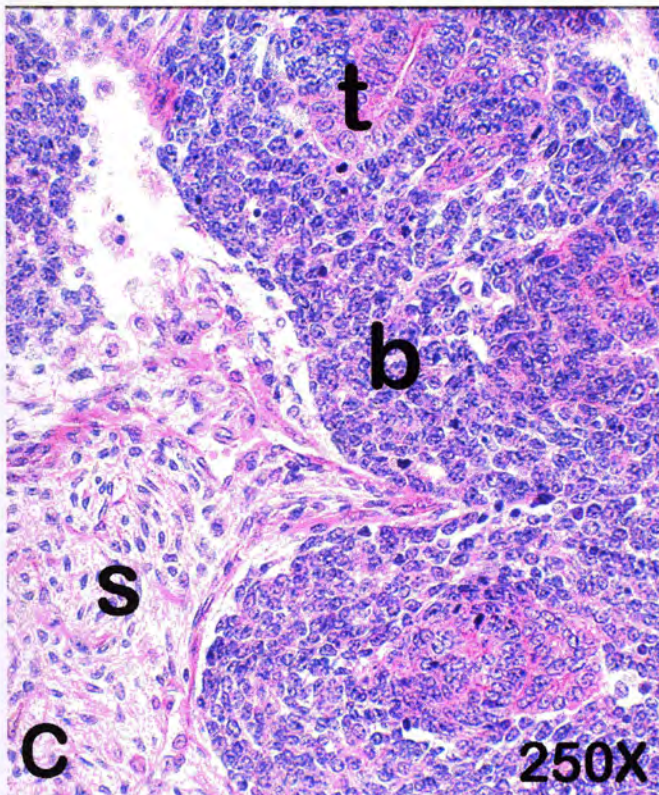
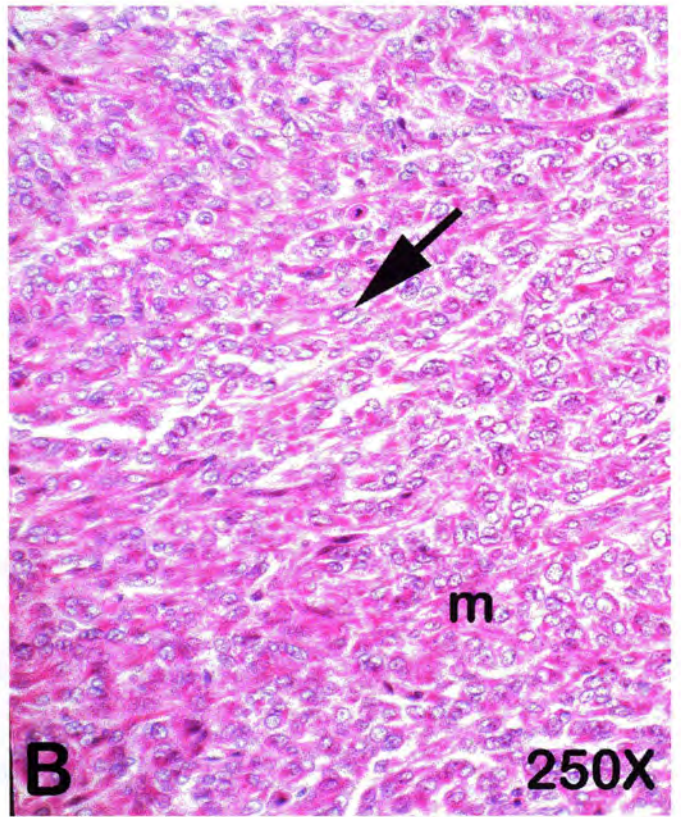
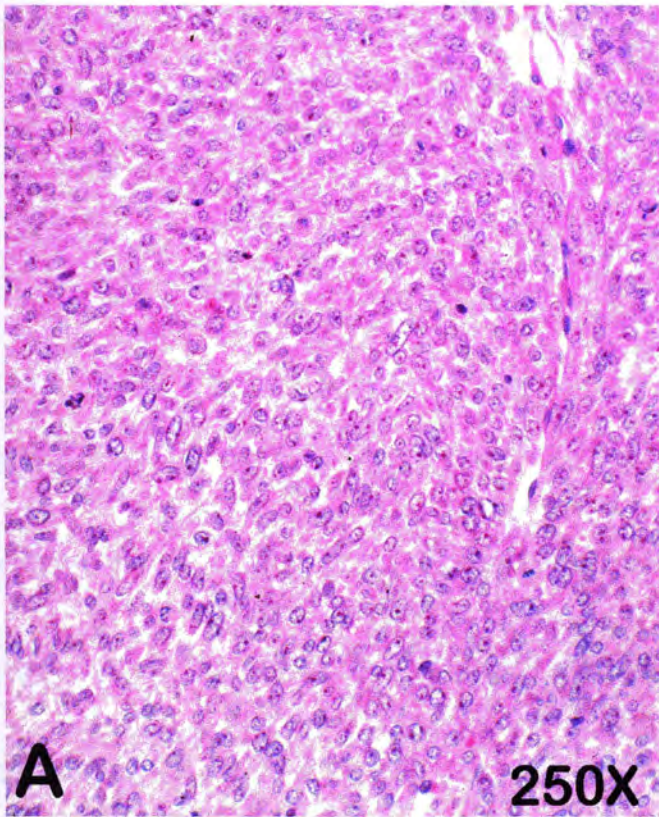


**Figure 2.** Histological comparison of fetal kidney tissue and Wilms' tumor. **A**, fetal kidney at approximately 10 weeks of development; **B**, Classical Triphasic Wilms' tumor. Three histologic components are noted in each specimen ( white asterisks = blastema, large arrows = immature tubuli, and small arrows = stromal tissue).

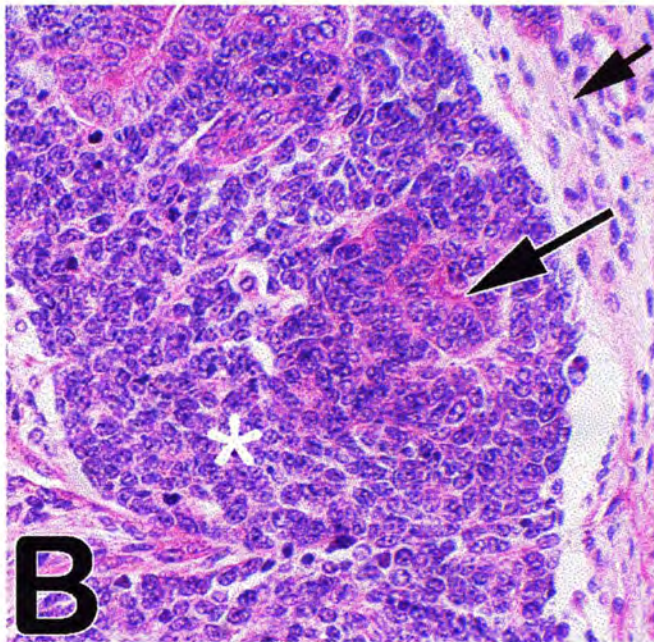
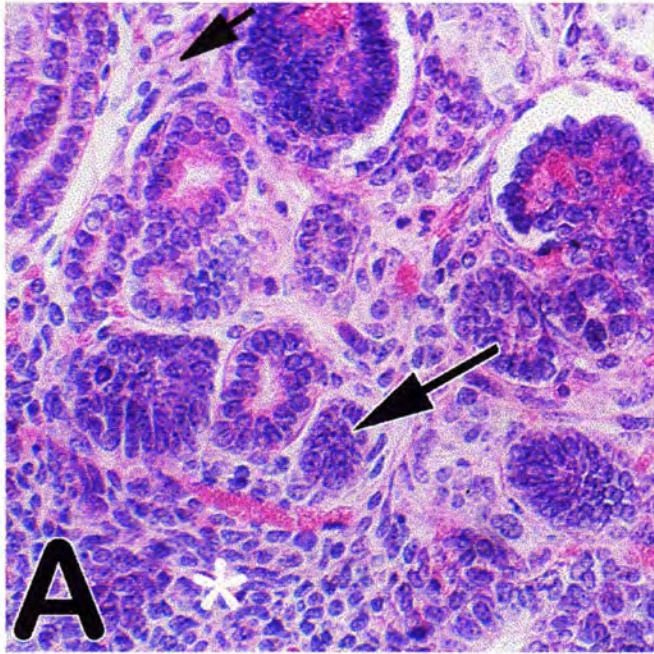


**Figure 3.** Model for Wilms' tumorigenesis and progression indicating the proposed sequence of WT-1 and p53 mutations ( WT = Wilms' tumor; AWT = anaplastic Wilms' tumor).

Adapted from Re GG *et al.*, *Seminars in Diagnostic Pathology* 11(2): 126-135, 1994.



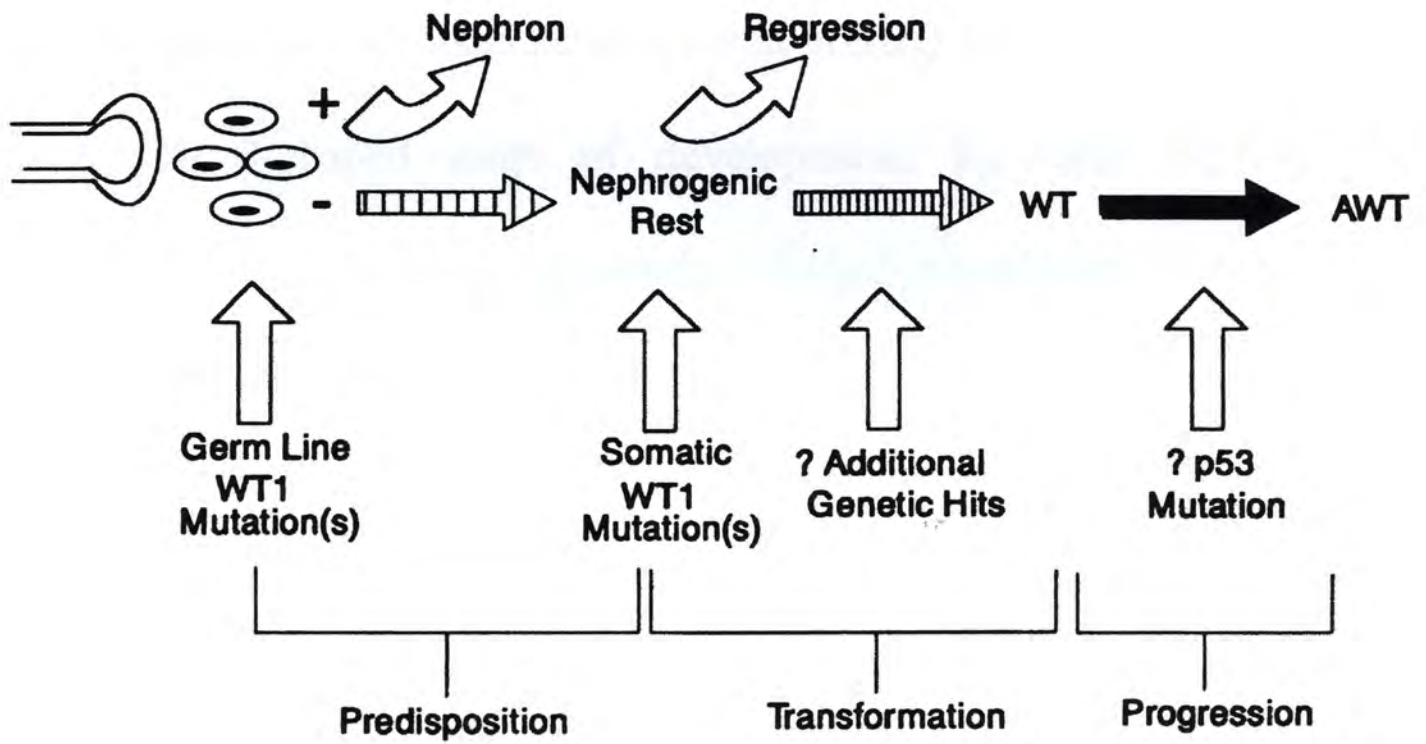


**Figure 4.** Normal development of the kidney. **A**, loose mesenchyme with the beginning of mesenchymal condensation; **B**, condensation around ureteric bud; **C**, comma shaped stage of development; **D**, S-shaped stage of development; **E**, early tubulogenesis; **F**, glomerulogenesis with invasion by blood vessels. Adapted from Saxen L, *Organogenesis of the Kidney*, 1987.

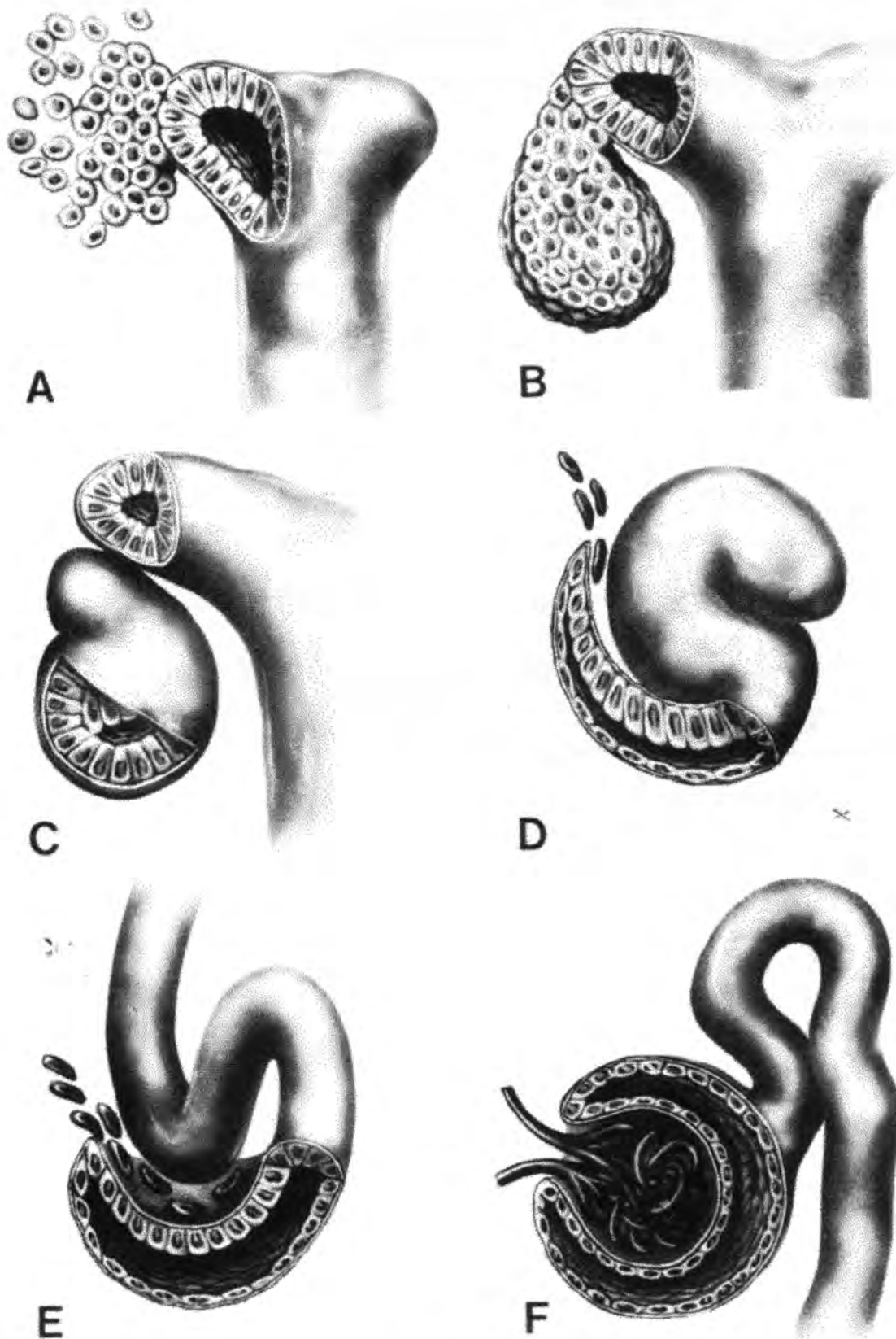


Fig. 1.20. A to F. Semi-schematic illustration of the early development of the nephron from condensation to the S-shaped body (after Saxén, 1984a).

**Table 1A. WT-1 Transcriptional Modulation of Target Genes with Proposed Biologic Effects**

WT-1 transcriptional target	transcriptional modulation of gene expression	proposed biological effects of gene expression regulation
<i>IGF-2</i>	negative	decreased cell proliferation
<i>IGF-1R</i>	negative	decreased cell proliferation
<i>PDGF-A</i>	negative	decreased cell proliferation
<i>TGF-<math>\beta</math></i>	negative	decreased cell growth
<i>Bcl-2</i>	negative	apoptosis
<i>c-myc</i>	negative	apoptosis
<i>p21<sup>waf-1</sup></i>	positive	apoptosis

**Table 1B. p53 Transcriptional Modification of Target Genes with Proposed Biologic Effects**

p53 transcriptional target	transcriptional modulation of gene expression	biological effects of gene expression modulation
<i>p21<sup>waf-1</sup></i>	positive	cell cycle arrest, apoptosis
<i>Bax</i>	positive	apoptosis
<i>MDM-2</i>	positive	negative regulator of p53
<i>GADD-45</i>	positive	DNA repair
<i>IGF-BP3</i>	positive	decreased cell proliferation
<i>thrombospondin-1</i>	positive	angiogenesis inhibited

**Table 2. Summary of Gene Expression Analysis of Developing Kidney Tissue and Pediatric Renal Tumors**

<b>Condition</b>	<b>WT-1 mRNA</b>	<b>Pax-2 mRNA</b>	<b>Pax-8 mRNA</b>	<b>Tenascin -C mRNA</b>
loose (uninduced) renal mesenchyme	negative	negative	negative	negative
condensed (induced) renal mesenchyme	positive	positive	positive	negative
Wilms' tumors	positive	positive	positive	stromal containing Wilms' tumors are positive
CCSK	negative	some positive	negative	some positive
CMN	some positive	some positive	negative	positive

## **Chapter 2**

### **Materials and Methods**

## **I. Tumor Specimens**

Two cases of CCSK and two cases of cellular CMN were obtained from the Surgical Pathology division at the Medical University of South Carolina (MUSC). These tumors were designated CCSK-2 and CCSK-4. CMN from MUSC are referred to as CMN-1 and CMN-2. Both CMN-1 and CMN-2 are cellular (atypical) forms of the disease. One case of CCSK was obtained fresh from the Department of Pathology at Wake Forest University School of Medicine (WFUSM) and was designated CCSK-BG1. Two other cases of CCSK were provided from Timothy Triche, M.D., Ph.D. of the Children's Hospital Los Angeles and were designated CCSK-1 and CCSK-3.

Snap frozen tissues of two classical and three cellular CMN, five CCSK, and the matching adjacent normal kidney for each of the latter tumor types were obtained through application to the National Wilms' Tumor Study repository. CCSK cases are designated CC209, CC236, CC462, CC50057, and CC50113. CMN cases are designated CMN357, CMN458, CMN482, CMN50044, and CMN50524. CMN 357, CMN50524, and CMN50044 are all cellular forms of the disease designated by the prefix ce-. CMN458 and CMN482 are classical forms of the disease designated by the prefix cl-.

## **II. Chemicals**

Unless otherwise specified, routine chemicals for use in this study were obtained from either Fisher Scientific (Atlanta, Georgia) or Sigma Chemical Company (St. Louis, Missouri). Chemical reagents used for electron microscopic studies were purchased from Electron

Microscopy Sciences (Fort Washington, Pennsylvania).

### **III. Nude Mouse Heterotransplantation**

Primary CCSK and CMN tumors were removed surgically and maintained in either saline or Dulbecco's modified Eagle's medium (DMEM) (Gibco BRL, Grand Island, New York) supplemented with penicillin-streptomycin and 15% fetal calf serum (Gibco BRL) before injection into mice as previously described (Garvin *et al.*, 1988). Tumor specimens were minced finely and injected subcutaneously using a 16-gauge needle into 6-10 week old Balb/c nude mice (National Cancer Institute, Bethesda, Maryland). Mice bearing tumors of the appropriate size (approximately 8-12 cm<sup>3</sup>) were sacrificed. Tumor nodules were excised aseptically, minced finely, and again injected subcutaneously into additional nude mice. Additionally, excised nude mouse heterotransplant tissue was either snap frozen or used to establish cell cultures. Heterotransplant histology was evaluated at each passage to compare with the primary tumor specimen.

### **IV. Tumor and Heterotransplant Tissue Fixation, Processing, and Hematoxylin and Eosin Staining**

Following removal of the tumor or tumor heterotransplant, tissue was minced into small pieces (approximately 1-2 cm<sup>3</sup>) and fixed for 8-10 hours at room temperature in either 10% neutral buffered formaldehyde (NBF) or Carnoy's solution (60% absolute ethanol, 30% chloroform, 10% glacial acetic acid). Following fixation, tissues were stored in either 70% (NBF fixed tissue) or 100% (Carnoy's fixed tissue) ethanol overnight. On the following day, tissues were dehydrated in a graded ethanol series, cleared in xylene, and embedded into paraffin wax (Fisher Scientific).

Five  $\mu\text{m}$  sections of paraffin embedded tissue were cut using a microtome and placed



onto microscope slides (Fisher Scientific). Sections were de-paraffinized for 10 minutes in three changes of xylene, and hydrated through a graded alcohol series (100%, 95%, 70%) into tap water and stained using hematoxylin and eosin. Briefly, hydrated sections were stained in Mayer's hematoxylin for 5 minutes, rinsed in two changes of tap water, dipped in 0.25% ammonia water until sections were blue, rinsed in tap water again, and stained with Johns Hopkins eosin for 15 seconds. Tissue sections were then dehydrated using successively two changes of 95% ethanol, two changes of 100% ethanol, and three changes of xylene before coverslipping.

#### **V. Transmission Electron Microscopic Evaluation of Tumor Tissue and Cell Cultures**

Either primary CMN or CCSK tumor tissue was removed and cut into 1 mm<sup>3</sup> fragments and fixed in 2.5% sodium cacodylate buffered glutaraldehyde as the primary fixative overnight. On the following day, tissue fragments were rinsed in 0.1M cacodylate buffer and post-fixed in 2% (w/v) osmium tetroxide in 0.1 M PBS for one hour at room temperature. The tissue was then successively dehydrated in a graded ethanol series and placed in two changes of propylene oxide for ten minutes each at room temperature before infiltration in a series of propylene oxide and Epon 812 (50% propylene oxide/50% epon resin for one hour, 25% propylene oxide/75% epon resin for one hour, and 10% propylene oxide/95% resin for one hour, all at room temperature). Finally, tissues were embedded into pure Epon 812 resin. Resin was allowed to polymerize overnight at 70°C before cutting.

Epon blocks containing tissue fragments were cut into 100-150 nm sections using an ultramicrotome. Sections were placed onto copper grids (Electron Microscopy Sciences). For transmission electron microscopic (TEM) analysis, sections were stained with uranyl acetate

(15g uranyl acetate in 25 ml of absolute methanol) and lead citrate (30 ml Milli-Q water, 1.33g lead citrate, 1.76g sodium citrate, and 8.0 ml of 4% sodium hydroxide). TEM micrographs at various magnifications were obtained using a JEOL 100S Transmission Electron Microscope (JEOL, Peabody, Massachusetts).

Cell cultures were fixed *in situ* and treated as described above. Exceptions to the above mentioned protocol include substitution of 100% ethanol instead of propylene oxide in the infiltration steps. Sections of the cell monolayer were also stained with uranyl acetate and lead citrate as above. Electron micrographs were also generated similarly.

## **VI. Scanning Electron Microscopic (SEM) Evaluation of Tumor Cell Cultures**

CCSK and CMN tumor cells were plated directly onto Thermanox sterile coverslips (Electron Microscopy Sciences) and treated for 24, 48, or 72 hours in the presence of 1.0  $\mu$ M all-*trans* retinoic acid. Cells were fixed in 2.5% cacodylate buffered glutaraldehyde for 1 hour at room temperature, rinsed in 0.1M cacodylate buffer, and post-fixed in 2%(w/v) osmium tetroxide. Coverslips were then rinsed briefly in distilled water and dehydrated in an ethanol series before immersion in hexamethyldisilazane for five minutes at room temperature as previously described (Kuhnel *et al.*, 1989). Hexamethyldisilazane treatment was substituted for critical point drying. After air drying at room temperature for 30 minutes, coverslips were mounted onto an SEM stub, sputter coated with carbon using a Polaron Equipment SEM Coating Unit E5150 (Electron Microscopy Sciences) and visualized using a JEOL JSM-5410LV Scanning Electron Microscope (JEOL).

## **VII. Initiation of Tumor Cell Culture**

Primary tumor tissue obtained from the Surgical Pathology division of the MUSC

Department of Pathology and Laboratory Medicine and the Department of Pathology at Wake Forest University School of Medicine or tissue derived from nude mouse heterotransplants was maintained in DMEM supplemented with 15% fetal calf serum until time to initiate a cell culture. Tissue was minced within a few hours into small pieces of about 2-5 mm and placed into a tissue culture flask coated with Type I collagen (Collagen Corporation, Palo Alto, California, USA) and fetal calf serum (Gibco BRL) until tumor fragments were attached to this substrate (approximately thirty minutes). Alternatively, tumor tissue was minced very finely and subjected to tissue dissociation in type I collagenase, 200 units/mg of dry weight and deoxyribonuclease, 400 units/mg of dry weight (both from Sigma Chemical Company). Both collagenase and deoxyribonuclease were solubilized in Hank's Balanced Salt Solution (HBSS) (Gibco BRL) to a final concentration of 1.4 mg/ml of collagenase and 1.0 mg/ml of deoxyribonuclease. Tissue was completely covered with this solution and subjected to dissociation in a trypsinization flask for 15 minutes at 37° C.

The cell suspension was filtered through sterile 90µm-mesh diameter nylon filters. The filter was then rinsed several times in HBSS. The filtrate was subjected to centrifugation at 180 g at 4° C for 8 minutes in a Sorvall RT6000D centrifuge (DuPont, Newton, Connecticut, USA) in order to obtain a cell pellet. The cell pellet was then resuspended in a small volume of media before plating into a Corning tissue culture flask (Fisher Scientific).

Both CMN and CCSK cultures were plated into media with the following

characteristics: a 1:1 combination of DMEM and Ham's F-12 (F12) medium (both from Gibco BRL) prepared using water from a Milli-Q water purification system and subsequently filtered through a 0.2  $\mu\text{m}$  sterile filter unit (both from Millipore Corporation, New Bedford, Massachusetts, USA). Media was stored at 4° C until use. To prevent fungal or bacterial growth, penicillin (final concentration of 100 U/ml), streptomycin ( final concentration of 100U/ml),and amphotericin B (final concentration of 2 mg/ml) was added to media. Penicillin, streptomycin, and amphotericin B were acquired from Gibco.

At the time of use, the latter combination of DME and F12 was supplemented with insulin (5 $\mu\text{g}/\text{ml}$ ), transferrin (5 $\mu\text{g}/\text{ml}$ ), selenium (5 $\mu\text{g}/\text{ml}$ ), hydrocortisone (36 ng/ml), and triiodothyronine (4pg/ml)(Collaborative Research, Lexington, Massachusetts, USA) as previously described (Hazen-Martin *et al.*, 1994) and either 2%, 10%, or 20% fetal calf serum (v/v). Cells maintained in T75 Corning tissue culture flasks received 15 ml and T25 Corning tissue culture flasks received 5 ml of media. Media were replaced every other day during the propagation of these cells. Cells were maintained in a 5% CO<sub>2</sub>/ 95% air incubator.

Confluent cell cultures in T75 Corning tissue culture flasks were sub-cultured by rinsing the cell monolayer with phosphate-buffered saline (PBS), pH 7.3 followed by the addition of 3.0 ml of 0.05% trypsin-0.02% EDTA (Gibco BRL). Cell detachment was monitored using an inverted phase contrast microscope. Once cells were released from the substrate, trypsin was inactivated in an equal volume of fetal calf serum. Cells were centrifuged in a 50.0 ml conical centrifuge tube at 180 *g* at 4° C for eight minutes. The resulting cell pellet was resuspended in 2.0 ml - 5.0 ml of fresh media and plated into additional Corning tissue culture flasks. Photomicrographs of cell cultures were recorded

using a Zeiss IM35 inverted microscope on 35 mm Kodak Panatomic X-film, ASA 32.

Cell cultures were routinely frozen for future use in their respective growth media with 10% dexamethasone (Fisher Scientific). Frozen cell pellets were maintained in a liquid nitrogen dewar until thawed for additional studies.

### **VIII. Cis-Diamminedichloroplatinum (II) (Cisplatin) DNA Damage Response Assay**

CCSK-2, CCSK-BG1, CMN-1, CMN-2, and the anaplastic Wilms' tumor cell lines W4 and W16 were plated at subconfluence in type I collagen coated T25 Corning tissue culture flasks (Fisher Scientific). Cells were subsequently exposed to  $1 \times 10^{-4}$  M cisplatin (Platinol™, Bristol-Meyers-Squibb, Princeton, New Jersey, USA) diluted in their respective growth media for 2, 4, 6, 8, 10, and 20 hours and maintained at 37°C in a 95% air/5% CO<sub>2</sub> incubator. Control groups did not receive cisplatin. Cells from each time point were collected by trypsinization and total cellular RNA and protein was extracted. RNA was electrophoresed and transferred to nitrocellulose before probing with cDNA probes specific for *p21*, *Bax*, *p53*, and *MDM-2* genes. Protein was resolved by sodium dodecyl sulfate-polyacrylamide gel electrophoresis and electroblotted onto nitrocellulose before probing with p53 and p21 monoclonal antibodies. Cells were also collected for flow cytometric determination of G-1 cell cycle arrest and apoptosis.

### **IX. All-trans Retinoic Acid Induced Cell Differentiation Assay**

CCSK-2, CCSK-BG1, CMN-1, CMN-2, and SK-N-SH neuroblastoma cells (American Type Culture Collection, Rockville, Maryland, USA) were plated at subconfluence in type I collagen coated Corning T25 tissue culture flasks (Fisher Scientific). Cells were subsequently exposed to  $1 \times 10^{-6}$  M atRA for 24, 48, and 72 hours in the dark at

37°C in a 95% air/ 5% CO<sub>2</sub> incubator. Control cells were treated similarly excepting atRA treatment. At each time point, cells were photographed using a Zeiss inverted phase contrast microscope, fixed for both transmission and scanning electron microscopy, and lysed for RNA extraction.

## **X. Immunocytochemistry Using Peroxidase Labelled Secondary Antibodies**

Cells were plated very sparsely onto Lab-tek chamber slides (Nunc Incorporated, Naperville, Illinois, USA) coated with type I collagen and fetal calf serum as previously described for Corning tissue culture flasks. Cells were then fixed for 10 minutes at room temperature in 3.7% formaldehyde in PBS, pH 7.3 or Carnoy's solution. Subsequently, cells were rinsed in 70% alcohol, if fixed in formaldehyde, or 100% alcohol, if fixed in Carnoy's solution. Before staining, cells were rinsed several times in PBS, pH 7.3 and permeabilized using 0.1% Triton-X 100. Cells were again rinsed several times in PBS before blocking in 10% normal horse serum (Vector Laboratories, Burlingame, California, USA) for 30 minutes at room temperature. Serum was then drained and cells were incubated in monoclonal antibodies against p53 (clone DO-7, 1:100 dilution), MDM-2 (1:50 dilution), smooth muscle actin (1:75 dilution), desmin (1:50 dilution), AE1/AE3 cytokeratin (1:50 dilution), or vimentin (1:50 dilution) (Novocastra Laboratories Ltd., Newcastle upon Tyne, Great Britain) for one hour at room temperature. Cells were then rinsed three times for five minutes each in PBS, pH 7.3. and incubated in horse anti-mouse antibody heavy and light chain (1:100 dilution) (Vector Laboratories). After rinsing three times for five minutes each in PBS, pH 7.3, cells were treated with avidin-biotin-horseradish peroxidase complex (ABC) provided in a Vectastain Elite kit and stained using 3-3'-diaminobenzidine (Vector Laboratories). Lab-

teks containing the cells were then dehydrated in a graded ethanol series and xylene and coverslipped before microscopic visualization.

Frozen tumor tissue was embedded in OCT frozen tissue embedding media (Lab-Tek, Arlington Heights, Illinois), cut at 5  $\mu$ M in a cryostat, briefly allowed to adhere to a microscope slide, and fixed in neutral buffered formaldehyde for one minute at room temperature. Tissue sections were then rinsed in PBS, and treated in the same manner as cells on Lab-teks.

Paraffin embedded tissue was cut at 5 mM, deparaffinized in three changes of xylene, incubated in PBS, and finally 10% normal horse serum. The remaining protocol is the same as that used for cells.

## **XI. Immunofluorescence Cytochemistry**

Cells were plated very sparsely onto 35 mm dishes coated with type I collagen and fetal calf serum as previously described for Corning tissue culture flasks. Cells were then fixed for 10 minutes at room temperature in 3.7% formaldehyde in PBS, pH 7.3 or Carnoy's solution. Subsequently, cells were rinsed in 70% alcohol, if fixed in formaldehyde, and 100% alcohol, if fixed in Carnoy's solution. Before staining, cells were rinsed several times in PBS, pH 7.3 and permeabilized using 0.1% Triton-X 100. Cells were again rinsed several times in PBS before blocking in 10% normal horse serum (Vector Laboratories) for 30 minutes at room temperature. Serum was then drained and cells were incubated in monoclonal antibodies against p53 (clone DO-7, 1:100 dilution), smooth muscle actin (1:75 dilution), desmin (1:50 dilution), AE1/AE3 cytokeratin (1:50 dilution), and vimentin (1:50 dilution) (Novocastra) for one hour at room temperature. Cells were then rinsed three times

for five minutes each in PBS, pH 7.3. and incubated in rhodamine labelled goat anti-mouse antibody(1:100 dilution)(Jackson ImmunoResearch, West Grove, Pennsylvania) for 30 minutes at room temperature in the dark. Cells were then briefly rinsed in PBS and mounted in 10% glycerol in PBS, pH 7.3 before visualization with a Zeiss epifluorescence microscope.

## **XII. Flow Cytometry Cell Cycle Analysis**

Approximately  $1 \times 10^6$  cells from cultures of CMN-1, CMN-2, CCSK-2, CCSK-BG1, W4, and W16 were plated into collagen and fetal calf serum coated Corning T25 flasks (Fisher Scientific) and incubated overnight at 37°C in a 5% CO<sub>2</sub>/ 95% air incubator. On the following day, cells were treated with 100 µM cis-diamminedichloroplatinum (Bristol-Meyers-Squibb for 4, 8, and 20 hours. At each time point, cells were trypsinized in 0.05 % trypsin, 0.53M Ethylenediaminetetracetic acid (Gibco).Preparation of cells for flow cytometry was performed essentially as previously described (Schandl, *et al.*, 1997). Briefly, cisplatin treated cells were centrifuged after trypsinization at 1000 RPM for 10 minutes at 4°C, rinsed in PBS, pH 7.3, and centrifuged again at 1000 RPM for 10 minutes at 4°C. Cells were then fixed in 1% formaldehyde for 10 minutes on ice and then rinsed and centrifuged as before. Cells were maintained overnight in 80% ethanol at -20°C before staining. On the following day, cells were rinsed and centrifuged two times in PBS, pH 7.3. Cells were finally stained with propidium iodide staining solution (0.01 µg/ml propidium iodide, 0.01 Kunitz units RNase / µl in PBS, pH 7.3) for 30 minutes in a dark location.  $1 \times 10^4$  Cells were then measured in an EPICS XL-MCL Four-Color Analytical Flow Cytometer (Coulter Corporation, Miami, Florida, USA) and analyzed using Phoenix Multicycle Software.



### XIII. Protein Gel Electrophoresis and Western Blotting

Cell cultures of CMN, CCSK, and anaplastic Wilms' tumors treated with *cis*-diamminedichloroplatinum (Bristol-Meyers-Squibb Pharmaceuticals) were extracted in Laemmli buffer (0.0625 M Tris-Cl pH 6.8, 2% sodium dodecyl sulfate, 5%  $\beta$ -mercaptoethanol, 10% glycerol, and 0.002% bromophenol blue)( Laemmli,1970) . Equal amounts of protein were then electrophoresed in a 11% acrylamide (30:0.8 acrylamide: bis-acrylamide) gel at 90 V in Tris-glycine buffer at room temperature for approximately 21/2 hours. Subsequently, the polyacrylamide gel was electroblotted overnight at 4°C at 35V in protein transfer buffer (20% methanol in tris-glycine buffer) onto a Transblot 0.2 $\mu$ m nitrocellulose membrane (BioRad,Hercules, California, USA).

Nitrocellulose membranes were then blocked in 5% Carnation skim milk, 0.05% Tween 20 (Blotto) for 15 minutes at room temperature. Blotto was then removed and the membrane was probed with a p53 mouse monoclonal antibody, clone D0-7 (1:5000 dilution) (Novocastra) or a 1:500 dilution of p21<sup>cip1</sup> mouse monoclonal antibody (Transduction Laboratories, Lexington, Kentucky, USA) in Blotto/0.05% Tween 20 for one hour at room temperature. Membranes were then rinsed three times,each for five minutes in PBS/0.05% Tween 20 and incubated with a1:7500 dilution of horseradish peroxidase conjugated goat anti-mouse antibody (Jackson ImmunoResearch) for 30 minutes at room temperature. Nitrocellulose membranes were finally rinsed three times, for five minutes each time, and developed using enhanced chemiluminescence (ECL reagents) according to manufacturer instructions (Amersham, Buckinghamshire, England). Membranes were then exposed to Kodak X-OMAT film (Sigma Chemical Company) and developed using a automatic

developer (Konica Corporation, Japan).

#### **XIV. RNA Extraction-Agarose Gel Electrophoresis-Northern Blotting**

RNA was extracted from either snap frozen primary tumor (and/or resulting tumor heterotransplants) or cultured cells essentially as previously reported (Chomczynski *et al* , 1987). Fresh frozen tissue was pulverized into a fine powder using a mortar and pestle under liquid nitrogen. After evaporation of liquid nitrogen, the tissue was lysed in 5.0 ml of denaturing solution (4M guanidinium isothiocyanate, 25mM sodium citrate pH 7.0, 0.5% sarcosyl, 0.1%  $\beta$ -mercaptoethanol, 0.02% sodium azide). The resulting solution was then acidified using 500  $\mu$ l 2M sodium acetate, pH 4.0 and extracted in phenol equilibrated with water, 0.1% hydroxyquinoline, and 0.2% mercaptoethanol, and 49:1 chloroform: isoamyl alcohol solution. After mixing into a homogeneous emulsion, the sample was centrifuged at 4000 g for thirty minutes at 4°C. The resulting aqueous phase was then removed and transferred into another tube and re-extracted in a 1:1 solution of phenol and chloroform, mixed into an emulsion, and centrifuged at 4000 g for 30 minutes at 4°C. The aqueous phase was again removed and precipitated in cold absolute ethanol overnight at -20°C. On the following day, the latter sample was centrifuged at 3500 g for thirty minutes at 4°C. The resulting RNA pellet was then rehydrated in 200  $\mu$ l of water followed by the addition of 200  $\mu$ l of Buffer A (0.4 M sodium chloride, 10mM Tris pH 7.4, 5mM ethylenediaminetetracetic acid, 0.1% sodium dodecyl sulfate ) and re-precipitated in cold absolute ethanol for two hours at -80°C or overnight at -20°C in an Eppendorf tube. The sample was the centrifuged at 10000 g for 10 minutes at 4°C. The resulting pellet was then rinsed once in cold 70% ethanol and centrifuged again at 10000 g for 5 minutes, dried, rehydrated in water, and

concentration measured in a spectrophotometer (Beckman Instruments, Fullerton, California, USA).

Aliquots of 5 $\mu$ g of RNA was loaded into each lane of a 1.2% SeaKem agarose (FMC BioProducts, Rockland, Maine, USA)-5 % formaldehyde-1X 3-[N-morpholino] propanesulfonic acid gel and was resolved by electrophoresis at 55 V at room temperature. To visualize the integrity of the 28S and 18S rRNA species along with smaller RNA molecules and determine loading efficiency, the ethidium bromide stained gel was photoed for permanent records. The gel was then transferred to a 0.2 mm nitrocellulose membrane (BioRad Laboratories) overnight in the presence of 10X SSC using a technique previously described (Southern, 1975). After transfer, the nitrocellulose membrane was baked at 88°C for 1 ½ hours in a Napco vacuum oven model 5831 (Precision Scientific, Chicago Illinois) and kept in a 4°C cooler until hybridization.

## **XV. cDNA Probe Labelling and Nucleic Acid Hybridization**

cDNA fragments of WT-1, p53, p21, MDM-2, IGF-2, BP-2, MDR-1, Pax-2, Pax-8, glyceraldehyde phosphate dehydrogenase (GAPD), Bcl-x, Bax, and Tenascin genes were all labelled using a Random Primed DNA Labelling Kit according to manufacturer instructions (Boehringer-Mannheim, Indianapolis, Indiana, USA). p53, p21, IGF-2, and GAPD cDNA probes were acquired from the American Type Culture Collection. The MDM-2 probe was a gift from Dr. Bert Vogelstein (Johns Hopkins University) and the Tenascin cDNA probe was provided by Dr. Maria Trojanowska (Department of Rheumatology, Medical University of South Carolina). The random priming method of DNA labelling has been previously reported (Feinberg *et al.*, 1987) Briefly, 25 ng of DNA was boiled for 3 minutes, quenched

on ice, and incubated for one hour at 37°C with 3 µl of an equimolar nucleotide mixture (A, T, and G), 5 µl of 10µCi/µl 32P-αdCTP (ICN Pharmaceuticals), 2µl of random hexamers, and 1 µl of Klenow enzyme (total reaction volume = 20 µl). Labelled DNA was then purified using Sephadex (fine) G50 Spin columns per manufacturer procedure (Boehringer-Mannheim) and ethanol precipitated for one hour at -20°C in the presence of cold DNA carrier. DNA was then pelleted by centrifugation at 10000 g for 10 minutes at 4°C. The pellet was washed once in 75% ethanol and centrifuged as before. The DNA pellet was then rehydrated in 200 µl of distilled water and 40 µl was counted in a scintillation counter (Beckman Instruments). The specific activities of probes used were between 1.5 and 2.0 x 10<sup>9</sup> cpm/ µg.

A total of 0.8 x 10<sup>6</sup> cpm of labelled probe per milliliter of hybridization solution (40% formamide, 2.0X SSC, 40mM sodium phosphate, pH 8.0, 200 ug ml sheared salmon sperm DNA) was employed in all experiments. Before hybridization, nitrocellulose filters were pre-wetted for approximately 30 minutes in hybridization solution. The volume of hybridization solution used was determined using 0.08 ml/cm<sup>2</sup> of membrane as a reference. Nitrocellulose filters were incubated overnight at 52°C in hybridization solution. Nitrocellulose membranes were then washed twice (5 minutes each) at room temperature in 2.0X SSC/0.1% SDS and twice (15 minutes each) at 54°C in 0.1X SSC/0.1% SDS, dried, and exposed to X-ray film. Autoradiograms were quantified using Adobe Photoshop version 4.0 software.

## XVI. p53 Polymerase Chain Reaction (PCR)- Single-Stranded Conformation Polymorphism (SSCP) and DNA Sequencing

SSCP was performed following methods previously described (Orita *et al* , 1989; Baird *et al.*, 1992). An aliquot of 1.0 µg of total cellular RNA was first reverse transcribed using an RNA PCR Kit (Perkin-Elmer, Norwalk, Connecticut, USA) and further amplified using the following sets of primers specific for exons 2 - 11 of the human p53 gene as previously described (El Bahtimi *et al.*, 1996):

**exons 2-4:** sense: 5' GACGGTGACACGCTTCCCTGGATT ;

antisense: 5' CATCTTGTTGAGGGCAGGGGAGTA;

**exons 5-6:** sense: 5' ACAGCCAAGTCTCTGACTTGCACG;

antisense: 5' GATGGTGGTACAGTCAGAGCCAAC;

**exons 7-9:** sense: 5' GTGGTGCCCTATGAGCCGCCTGAG ;

antisense: 5' CTCGAAGCGCTCACGCCACGGAT;

**exons 10-11:** sense: 5' GATGGAGAATATTTACCCCTTCAG;

antisense: 5' TCAGTGGGGAACAAGAAGTGGAGA.

The PCR mixture contained 10 pmol of each primer set, 2 nmol of each nucleotide (A,G, and T), 0.25 U *Taq* Polymerase, 10 µl of buffer specified in the RNA PCR Kit, and 1.0 µl 10 α-<sup>32</sup>P dCTP ( 10 µCi/µl, ICN Pharmaceuticals). Thirty cycles of amplification were performed using the following settings on a 9600 Perkin-Elmer Thermocycler: 94°C for 0.5 minutes, 55°C for 0.5 minutes, and 72°C for 1 minute. A 1.0 µl aliquot of the reaction mixture was withdrawn and mixed with 100 µl of 0.1% SDS/ 10mM EDTA. Then 2.0 µl of the latter solution was mixed with 2.0 µl of SSCP loading buffer (95% formamide, 20 mM

EDTA, 0.05% bromophenol blue, and 0.05% xylene cyanol). The resulting solution was heated to 80°C before loading 1.0 ml of sample into a 6% polyacrylamide gel (90 mM Tris-borate, pH 8.3, 4mM EDTA, and 10% glycerol). Control samples were not heated at 80°C before loading. Samples were electrophoresed for 3 hours at 30 W with the use of a cooling fan. After electrophoresis, the gel was dried on filter paper and exposed to X-ray film.

PCR products demonstrating a mobility shift by SSCP analysis were subjected to DNA sequencing on both strands using the appropriate primer set using a Sequitherm DNA Cycle Sequencing Kit (Epicentre Technologies, Madison, Wisconsin, USA). The latter is based upon the dideoxy chain termination sequencing method previously described (Sanger *et al.*, 1977). Either <sup>32</sup>P- or <sup>35</sup>S- $\alpha$ -dATP was employed in all sequencing reactions. Sequencing reactions were performed in a Perkin-Elmer 9600 thermocycler using the following settings: 95°C for 5 minutes, 95°C for 30 seconds and 70 °C for 1 minute for 30 cycles and held at 4°C indefinitely. Sequencing reaction products were electrophoresed in a 6% acrylamide denaturing gel (7M Urea, 4.5 ml of 40% acrylamide, 3.0 ml 10X TBE, 0.248 ml 10% ammonium persulfate to a final volume of 30.0 ml with distilled water , and 19  $\mu$ l TEMED) at 1200 V, constant wattage. Gel was then fixed in for 30 minutes in 5% acetic acid/ 15% methanol, affixed to Whatman filter paper, dried for 30 minutes in a Gel dryer (BioRad Laboratories), and exposed to X-ray film.

## **Chapter 3**

### **Morphological and Molecular Characterization of an *In vitro* and *In vivo* Model for the Study of Clear Cell Sarcoma of the Kidney and Cellular Congenital Mesoblastic Nephroma**

## I. Introduction

Clear cell sarcoma of the kidney (CCSK) and congenital mesoblastic nephroma (CMN) together comprise 10% of all pediatric renal neoplasms (Murphy et al., 1994). CCSK and CMN differ from the more common Wilms' tumor, or nephroblastoma, in histology and clinical behavior. CCSK was first delineated from Wilms' tumor in 1970 as a potentially aggressive tumor which has a propensity for metastasizing to bone in some patients (Kidd, 1970). Thus, some have stressed the diagnostic distinction of this tumor from the relatively benign classical, or triphasic Wilms' tumor (Beckwith *et al.*, 1978; Marsden *et al.*, 1978; Morgan *et al.*, 1978). Contrasting with the clinicopathological features of CCSK, CMN is generally a benign tumor of neonates primarily occurring within the first three months of life (Bolande *et al.*, 1967). CMN may be subdivided into the classical and cellular variants. Cellular CMN has a tendency to recur and metastasize in some instances if not completely resected (Joshi *et al.*, 1986). Because both of these tumors demonstrate signs of stromal differentiation, some have suggested that CMN, particularly cellular CMN, may represent the benign counterpart of CCSK (Beckwith *et al.*, 1978). The latter suggests a relationship similar to that suggested for classical and anaplastic Wilms' tumors (Re *et al.*, 1994; Bardeesy *et al.*, 1994). Nevertheless, the histogenetic origins of these two tumor types, their molecular genetic relationships with each other, and relationships with Wilms' tumor still remain largely unknown.

The vast majority of the available literature on CMN and CCSK has been limited to



morphological studies. CCSK is histologically characterized by the presence of empty appearing nuclei, abundant collagenous extracellular matrix material, and a fine arborizing pattern of blood vessels easily recognized using *Ulex Europeaus* agglutinin staining (Mierau *et al.*, 1989). In some forms, CCSK may be confused with other pediatric renal tumors. For example, CCSK may mimic the blastemal predominant Wilms' tumors, congenital mesoblastic nephroma, and osteosarcoma. Immunohistochemistry has provided little information regarding the origins of CCSK. One report has indicated no reactivity for fibronectin, laminin, and epithelial membrane antigen in all tumors examined (Kumar *et al.*, 1986). Another study indicated that CCSK was positive for vimentin, a marker for mesenchymal cells, but non-immunoreactive for epithelial membrane antigen, von Willebrand factor, desmin, S-100 protein, and Mac387 in eight cases examined (Looi *et al.*, 1993). In contrast, Wilms' tumor cases in the same report were positive for epithelial membrane antigen (in areas of tubular differentiation) and vimentin (in the glomeruloid bodies and stromal cells). Ultrastructural studies of CCSK indicate the near absence of heterochromatin in tumor cell nuclei, few intracellular organelles, and collagen deposition in the extracellular matrix (Haas *et al.*, 1984). Molecular studies of CCSK are extremely limited. One report examined the mRNA expression of the Wilms' tumor suppressor, *WT-1*, and the insulin-like growth factor II (*IGF-2*) in CCSK. In contrast to Wilms' tumors, CCSK did not express *WT-1* while *IGF-2* mRNA levels were high in the same cases in a report of two cases (Yun, 1993).

Two histologically distinct forms of CMN exist: classical and cellular (or atypical). Classical CMN is composed of interlacing bundles of spindled mesenchymal cells with

moderate cellularity and mitotic activity. Cellular CMN, in contrast, is typically composed of larger cells with hyperchromatic nuclei and greater mitotic activity in a denser cellular array (Murphy, 1994). The diagnosis of cellular CMN is sometimes problematic due to its resemblance to other renal neoplasms including monophasic blastemal Wilms' tumor, CCSK, and the RTK. Immunohistochemical studies of both CMN variants have exhibited staining for vimentin, desmin, and actin. No reactivity was reported for S-100, cytokeratin, epithelial membrane antigen, and Leu7 proteins in these tumor types (Pettinato *et al.*, 1989). Ultrastructurally, cellular CMN is characterized by the presence of prominent rough endoplasmic reticulum and bands of peripheral cytoplasmic filaments. Ultrastructural analysis has not, however, provided a clear definition of the cellular derivation of these tumors.

The biological relationships between CCSK, CMN, and Wilms' tumors are enigmatic. The study of CCSK, CMN, and their relationship with Wilms' tumor has been particularly hindered by the relative rarity of both of these tumor types. In this study, we report the development of both a cell culture and nude mouse xenograft model system for the study of CMN and CCSK. Both cultures and xenografts have been surveyed for their light and electron microscopic features and gene expression profile at the immunohistochemical and mRNA level. We report that nude mouse xenografts and cell cultures maintain cellular and molecular characteristics of the corresponding primary tumors in most instances. In some CCSK cell cultures, immunocytochemical changes were noted, however, which may have implications for tumor histogenesis.

## **II. Results**

### **1. *In vitro* Characteristics of CCSK and CMN**

Cell cultures of CMN and CCSK were successfully established from nude mouse xenograft tissue and primary tumor tissue, respectively. Tumor tissue was minced into fragments and placed into a type I collagen and fetal calf serum coated tissue culture flask with approximately 5 milliliters of fetal calf serum-containing growth medium. Cellular outgrowth from fragments was noted in cultures within one week. Phase microscopic analysis revealed spindle-shaped cells in all cultures examined (Figures 1&2). Cellular CMN-2 often demonstrated round to oval cells in addition to the presence of spindle shaped cells (Figure 2B). In addition to the presence of cells with fibroblastic appearance, CCSK cell cultures also contained focal areas of close cellular opposition (Figure 1). Table 1 summarizes this laboratory's experience with development of CCSK and CMN cell cultures.

### **2. Light and Electron Microscopic Analysis of CCSK and CMN Nude Mouse Xenografts**

Primary tumor tissue from two cellular CMN and four CCSK were successfully heterotransplanted into BALB/c athymic (nude) mice. After tumor volume reaches approximately 8-12 cm<sup>3</sup>, mice were sacrificed before removal of tumor and re-injection into subsequent mice. At each passage, tumors were monitored for morphological changes using hematoxylin and eosin (H&E) staining and transmission electron microscopic analysis. Figure 3 summarizes the light microscopic findings of primary and xenografted CCSK and CMN tumors. Figure 3A/A' and Figure 3B/B' correspond to H&E micrographs of cellular CMN-1 and CMN-2 xenografts, respectively. No CMN primary tumor tissue was available

for comparison for either tumor. Figure 3A shows the close cellular opposition of tumor cells in an early CMN-1 mouse xenograft. Figure 3A' is an H&E micrograph of CMN-1 at nude mouse passage 73. Figure 3B is from nude mouse passage 5 and Figure 3B' is from passage 56. Round to spindle cells with a slightly eosinophilic cytoplasm is a feature of both tumors and remains consistent with the histology of cellular CMN tumors. Figure 3C/C' and Figure 3D/D' represent primary tumor specimens and xenografts of CCSK-2 and CCSK-BG1, respectively. Hallmark cells with clear nuclei embedded within eosinophilic collagenous matrix material were characteristic of CCSK-2 and CCSK-BG1 primary and xenografted tumors. Both CCSK-BG1 primary tumor and xenograft contained rosette formation as well. In all cases, tumor histology between primary tumor and xenograft was maintained. Tumor xenograft growth characteristics are summarized in Table 1.

Representative transmission electron microscopic analysis of CCSK-2 and cellular CMN-1 xenograft was also conducted. Ultrastructurally, both CCSK-2 primary tumor and xenograft were characterized by cell nuclei nearly devoid of heterochromatin with a small, single nucleolus present in most cells. A few, small mitochondria with rough endoplasmic reticulum comprise features of the cytoplasm (Figure 4 A&B). Desmosomal junctions were noted in CCSK-2 primary tumor. CCSK-2 xenograft also demonstrated deposition of collagenous matrix material between cells, a characteristic finding of primary CCSK tumors (Figure 4B). CMN-1 early xenograft demonstrated cells with nuclei containing a single nucleolus with moderate amounts of heterochromatin. Tumor cell cytoplasm was characterized by the presence of few mitochondria and sparse rough endoplasmic reticulum (Figure 5A).

CCSK-2 and cellular CMN-1 cell cultures were also examined ultrastructurally. CMN-1 cells grew in sheets while maintained on a type I collagen growth surface and maintained the same bland nuclear and cytoplasmic features of its corresponding xenografted tumor. A single desmosomal junction is noted in Figure 5B. CCSK-2 cells also grew in sheets while maintained on a collagen growth surface. Tumor cells were characterized by empty nuclei, prominent rough endoplasmic reticulum, close interdigitation, and the presence of intermediate filaments. There was no evidence for collagenous matrix production by CCSK-2 cells (Figure 4C). CCSK-BG1 cells were characteristically similar.

### **3. Immunofluorescent Cytochemical Analysis of Intermediate Filament Proteins in CCSK and CMN Cells**

To gain a better understanding of the cellular derivation of both CCSK and CMN, tumor cells were evaluated using mouse monoclonal antibodies to desmin, smooth muscle actin (SMA), vimentin, and cytokeratin intermediate filaments. Both cell cultures derived from CCSK-2 and CCSK-BG1 did not reveal any desmin or cytokeratin filament staining (Figure 6). However, both of these cultures were positive for both vimentin and SMA. OVCAR ovarian carcinoma cells were included as a positive control for cytokeratins and negative control for muscle specific desmin and actin.

CMN cells derived from xenograft material (primary tumor tissue was unavailable) demonstrated a variable immunochemical profile. CMN-1 cells were positive for desmin, vimentin, but only focally positive for SMA (Figure 7). In contrast, CMN-2 cells reacted only with the vimentin monoclonal antibody. TB208 cells derived from an extrarenal malignant rhabdoid tumor were included as a positive control for vimentin protein. OVCAR cells were

again included as a negative control for muscle cell markers.

#### 4. WT-1 and IGF-2 Northern Analysis

To further evaluate the retention of primary tumor features in our *in vivo* and *in vitro* models, we evaluated their gene expression profile. *WT-1* and *IGF-2* are both genes which are highly expressed during fetal kidney development and in Wilms' tumor. Comparative mRNA expression analysis of these two genes was performed in CMN-1, CMN-2, CCSK-2, and CCSK-BG1 primary tumors, xenografts, and cell cultures alongside primary Wilms' tumors and normal kidney cells (Figure 8A). IGF-2 mRNA levels were similar in both CMN-1 and CMN-2 primary tumors and xenografts. However, IGF-2 message was strongly increased in their corresponding cell cultures. In contrast, CCSK-2 and CCSK-BG1 mRNA levels were higher in nude mouse xenografts compared to the corresponding primary tumor. Few copies of IGF-2 message was detected in CCSK-BG1 cultured cells, although expression was unchanged in CCSK-2 cells. All primary Wilms' tumors, but not normal kidney cell cultures, demonstrated IGF-2 mRNA.

*WT-1* mRNA was detected in both cellular CMN cases (Figure 8B). In CMN-1, only the primary tumor and cultured cells expressed detectable *WT-1* message. In contrast, WT-1 was expressed in CMN-2 primary tumor, xenograft, and cultured cells. All four classical Wilms' tumors examined contained abundant WT-1 transcripts. Normal kidney cell lines lacked detectable WT-1 mRNA.

### III. Discussion

Study of the cellular and molecular biology of CCSK and CMN has been hindered by the lack of a useful experimental model system. In addition to our lack of understanding of the inherent genetic defects in CCSK and CMN, the relationship, if any, they share with the more common classical Wilms' tumor remains unknown. In the present study, we have demonstrated the successful establishment and characterization of cellular CMN and CCSK tumor cell cultures and nude mouse xenografts that will be helpful in beginning to understand the pathobiology of both tumors.

The histogenetic origin of both CCSK and CMN has been a debated topic for many years. Previous reports have suggested that CCSK has a latent epithelial nature (Ishii *et al.*, 1989). This hypothesis derived from the observation of mucin production, cytokeratin immunoreactivity, and the development of intracellular canaliculi in a series of xenografted and cultured CCSK tumors. That observation contrasts with the histological and ultrastructural analysis of xenografted and cultured CCSK tumors in this study as none of the CCSK cases examined exhibited signs of epithelial differentiation as reported by Ishii. However, our cultured CCSK tumor cells did exhibit focal areas of close cellular opposition possibly indicative of their epithelial potential. Nevertheless, immunocytochemical analysis of CCSK cell cultures in this study demonstrated reactivity with both SMA and vimentin but not cytokeratin monoclonal antibodies. Vimentin, but not SMA, desmin, or cytokeratin protein was detected in primary fixed tissue of CCSK consistent with prior reports (Looi *et al.*, 1993). Immunohistochemical data of CCSK cell lines and primary tumor tissue and CMN cell lines are summarized in Table 2.

The expression of SMA in our two CCSK cell lines suggests one of two possible explanations. Firstly, the collagen matrix or plastic surface of tissue culture flasks may have a differentiating effect on CCSK tumor cells. Contamination of CCSK cultures with normal smooth muscle cells is unlikely. CCSK-2 and CCSK-BG1 cell cultures demonstrate cells growing in sheets that are relatively undifferentiated, a characteristic feature of tumor cells only. In addition, lack of SMA immunoreactivity in CCSK primary tumors is not likely to be due to fixation problems as arterial smooth muscle was stained. In any case, SMA positivity in CCSK cells has not been reported in immunohistochemical analyses of these tumors. Previous studies have reported no reactivity with epithelial membrane antigen, fibronectin, laminin, desmin, and neural cell markers (Kumar *et al.*, 1986; Looi *et al.*, 1993). CCSK cells were only reactive with vimentin monoclonal antibodies suggesting their primitive mesenchymal nature. The hypothesis that CCSK cells are derived from pluripotential stem cells has been further supported molecularly with the observation that CCSK tumors lack WT-1 expression, a marker for induced renal mesenchymal tissue (Yun, 1993). In the present study, IGF-2 but not WT-1 mRNA transcripts were detected in CCSK.. SMA positivity in CCSK cells may suggest that these cells have potential for differentiating towards glomerular mesangial cells or arterial smooth muscle cells. Given the abundant extracellular matrix deposition of CCSK and glomerular mesangial cells in pathologic conditions, future studies evaluating CCSK cells with mesangial cell markers may be useful.

The histogenesis and pathobiology of cellular, or atypical CMN also remains unresolved. The development of nude mouse xenografts that maintained the histologic and ultrastructural appearance of their primary tumors made the development of cellular CMN



cultures possible. Immunochemical characterization of resulting CMN tumor cell cultures revealed desmin, vimentin, and SMA reactivity. These same cells did not react with cytokeratin specific antibodies.. The latter findings are consistent with previous reports which have documented immunoreactivity for these intermediate filament proteins (Pettinato *et al.*, 1989). These data are further suggestive of a smooth muscle derivation of CMN tumors. Even though there is some overlap in the immunohistochemical profile of CCSK and CMN, Thy-1 immunoreactivity has been reported in CMN, but not CCSK tissue which further suggests that CCSK is derived from a more undifferentiated cell type (Hazen-Martin *et al.*, 1993). Northern analysis of primary tumors, xenografts, and cell cultures demonstrated the retention of gene expression characteristics between and among the two cellular CMN examined. WT-1 and IGF-2 were generally expressed in CMN primary tumors, xenografts, and cell cultures. WT-1 expression was absent in two cases of CMN in a previous report (Tomlison *et al.*, 1992). The latter report did not identify the histologic category of CMN. The observation of WT-1 in primary and xenografted cellular CMN in this study is a novel finding. These data suggest that cellular CMN are relatively undifferentiated tumors that may arise from cellular areas adjacent to the condensing renal mesenchyme. Evaluation of the extracellular matrix protein tenascin, a marker of uninduced mesenchymal cells surrounding condensed mesenchyme may be useful in testing this hypothesis (Truong *et al.*, 1996).

Recent experiments in mice have reported expression of the BF-2 winged-helix transcription factor in cells of the stromal lineage during fetal kidney development (Hatini *et al.*, 1996). In the same study, gene knockout studies of BF-2 revealed that mesenchyme

failed to differentiate into tubular epithelium. In light of these findings, it would be interesting to evaluate both CCSK and cellular CMN xenografts for possible expression or genetic alteration of BF-2 as a means of further comparing these tumors with different stages of renal development. In addition, the CCSK xenograft and cell culture model system will be useful in evaluating the role of p53 in the genetic etiology of this tumor as previous immunohistochemical analyses of CCSK has suggested the presence of mutations in these tumors (Cheah *et al.*, 1996). Finally, additional characterization of both CCSK and CMN using the *in vivo* and *in vitro* model system reported here will not only provide a better understanding of pediatric renal tumors, but also of the normal development of the stromal cell lineage.

**Figure 1.** Phase micrographs of CCSK primary cultures plated on a type I collagen/fetal calf serum substrate. **A**, CCSK-2 cells at 100X; **A'**, CCSK-2 cells at 200X; **B**, CCSK-BG1 cells at 100X; **B'**, CCSK-BG1 cells at 200X. Black arrows indicate the stromal, or fibroblastic appearance of some of the tumor cells. White arrows indicate a single nucleolus which is characteristic of CCSK cells.

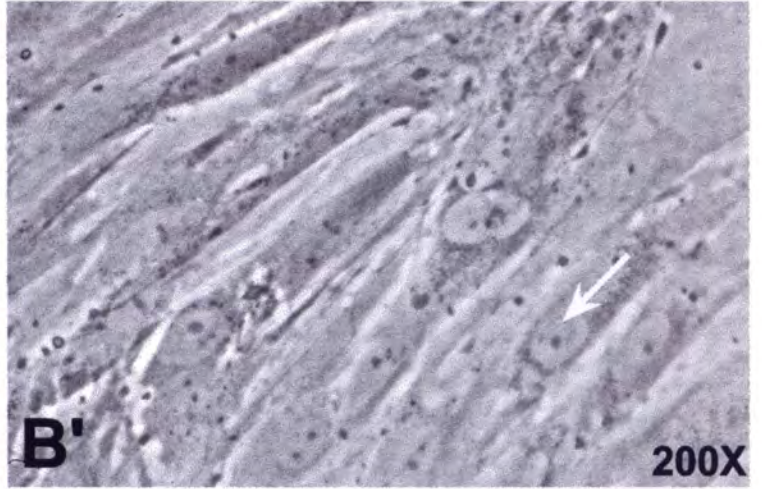
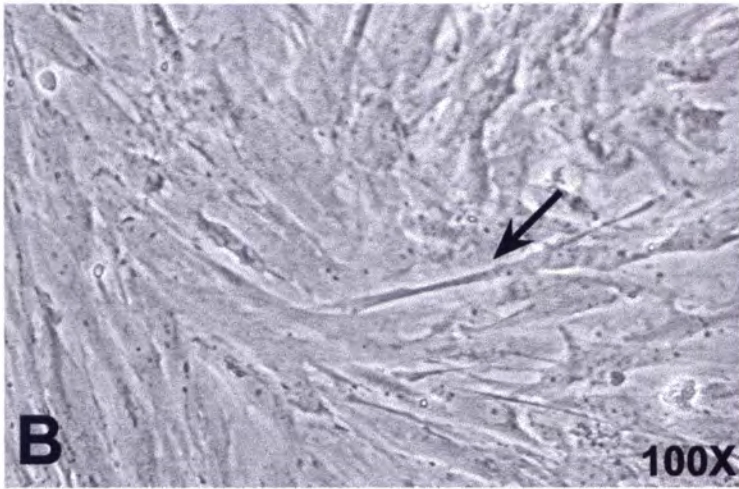
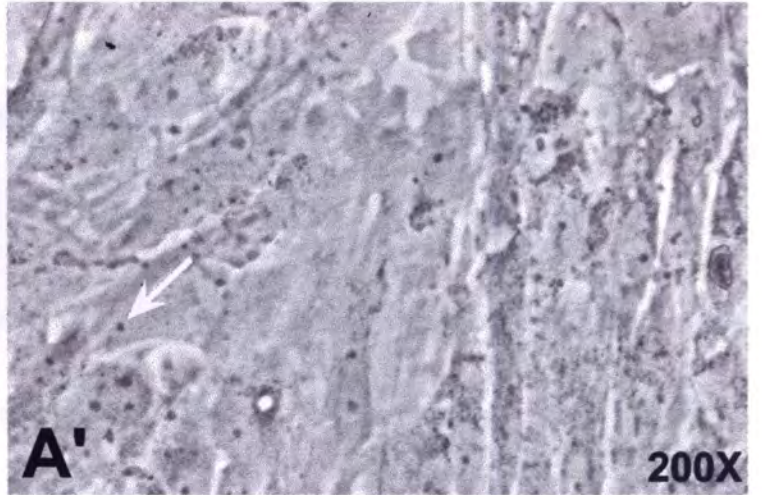


**Figure 2.** Phase micrographs of CMN primary cultures plated on a type I collagen/ fetal calf serum substrate. A, CMN-1 cells at 100X; A', CMN-1 cells at 200X; B, CMN-2 cells at 100X; B', CMN-2 cells at 200X. The black arrow in A indicates one of the many mitotic cells in this photomicrograph. The white arrow in B' indicates the round to elliptical cell shape of CMN-2 cells.

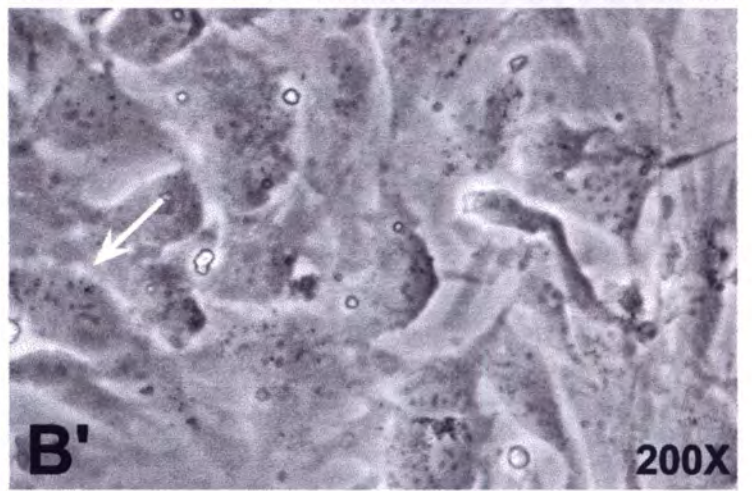
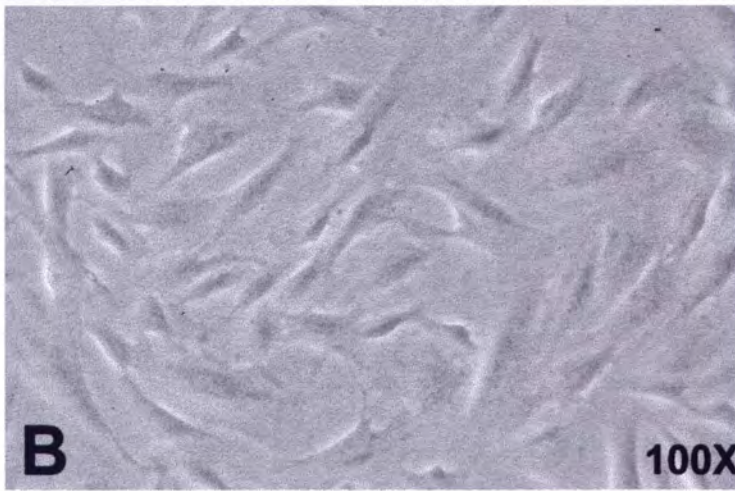
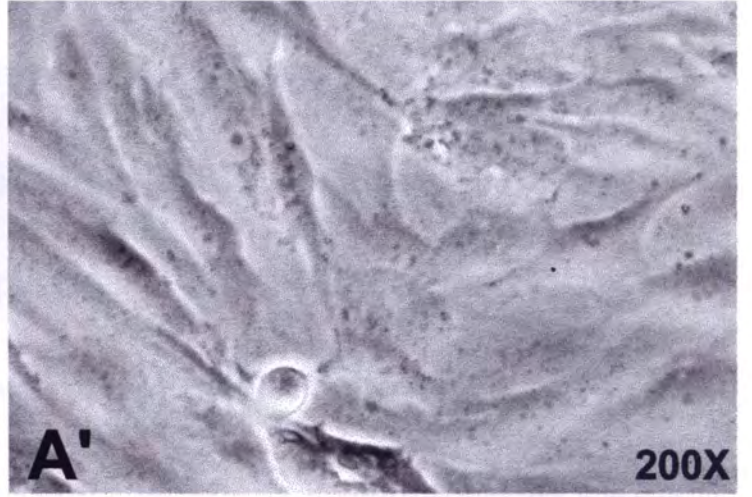
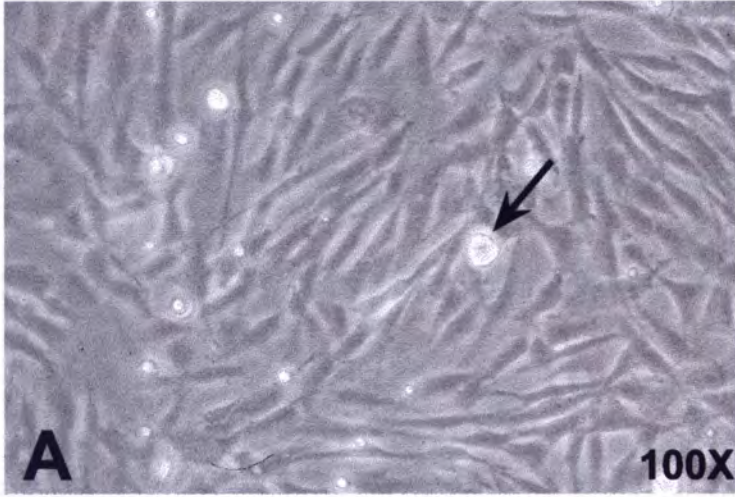


**Figure 3.** Hematoxylin and eosin stained sections of CCSK and cellular CMN primary tumor tissue and nude mouse tumor xenografts. **A**, passage 1 of CMN-1 xenograft; **A'**, passage 73 of CMN-1 xenograft; **B**, passage 1 of CMN-2 xenograft; **B'**, passage 50 of CMN-2 xenograft; **C**, CCSK-2 primary tumor; **C'** passage 2 of CCSK-2 xenograft; **D**, CCSK-BG1 primary tumor; **D'**, passage 2 of CCSK-BG1 xenograft. All micrographs at 250X.

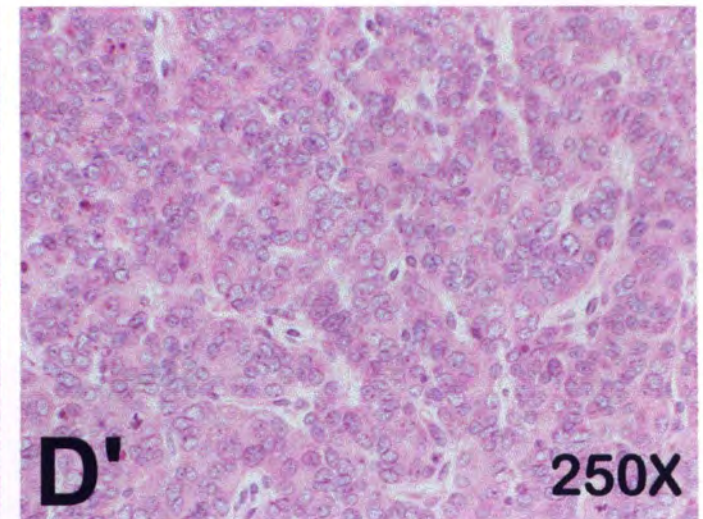
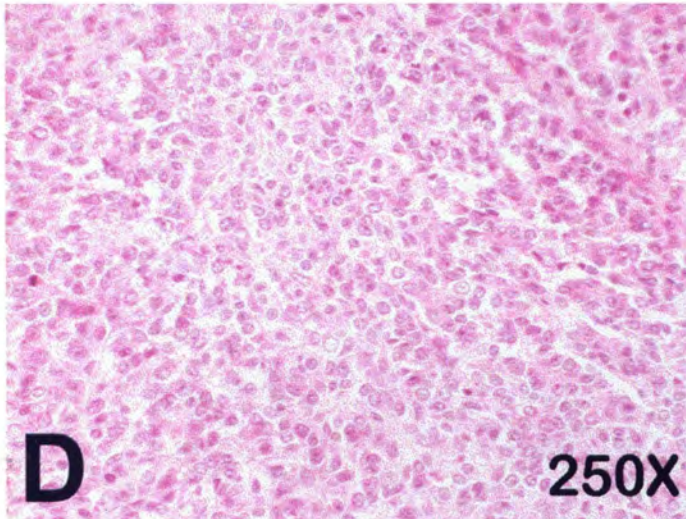
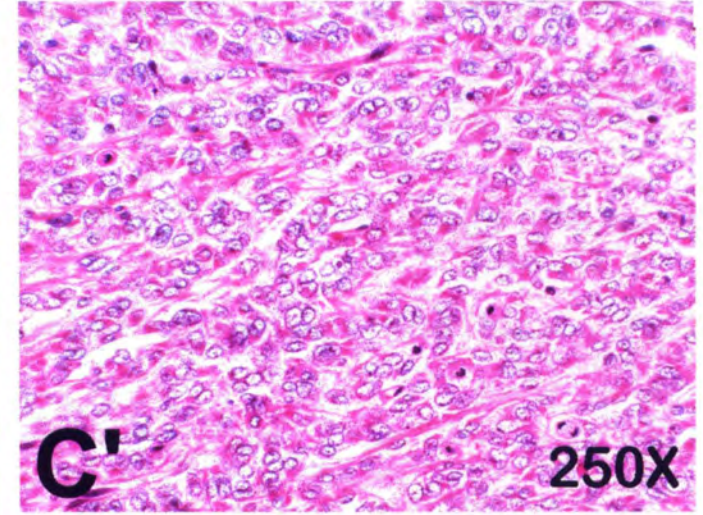
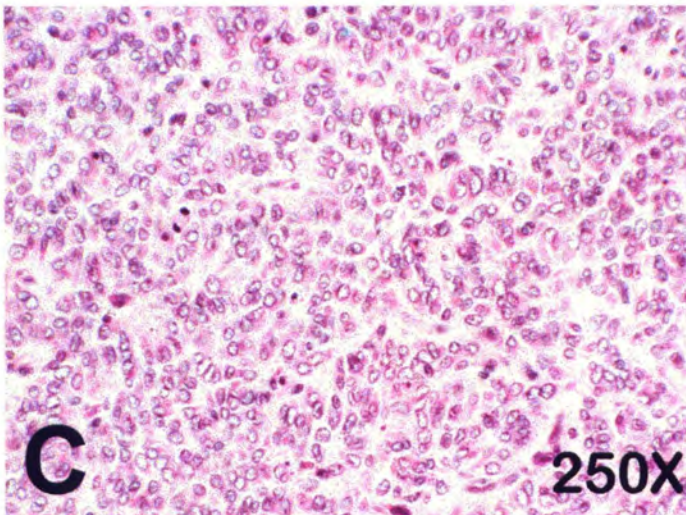
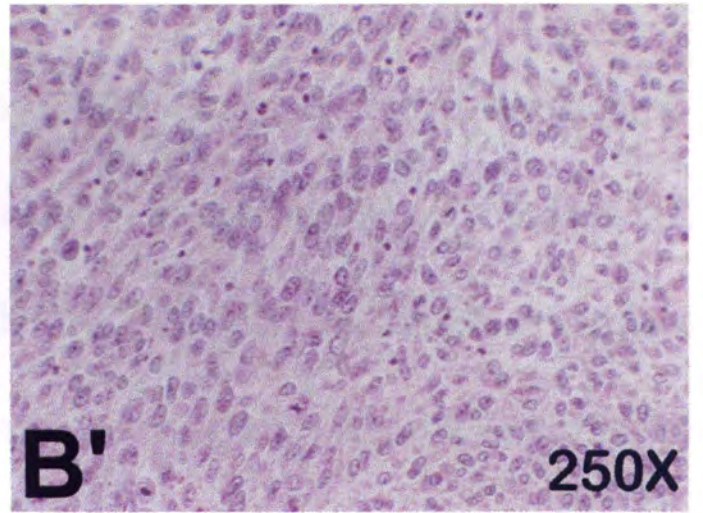
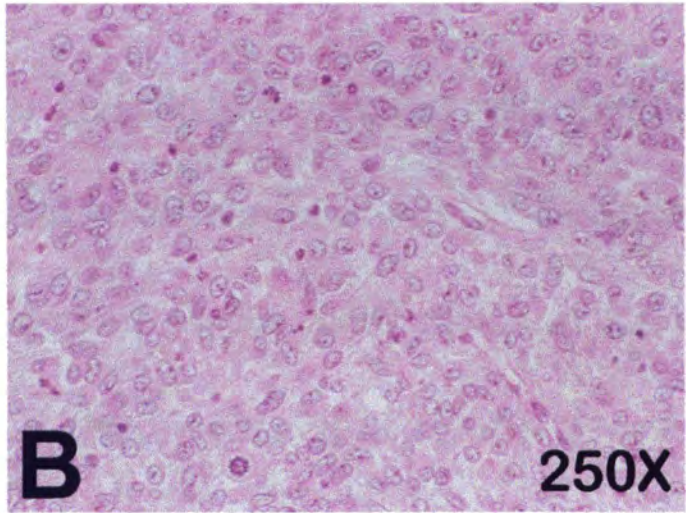
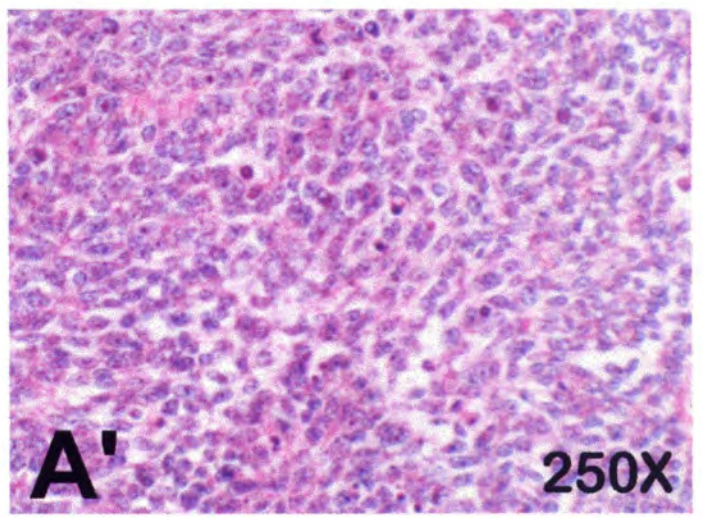
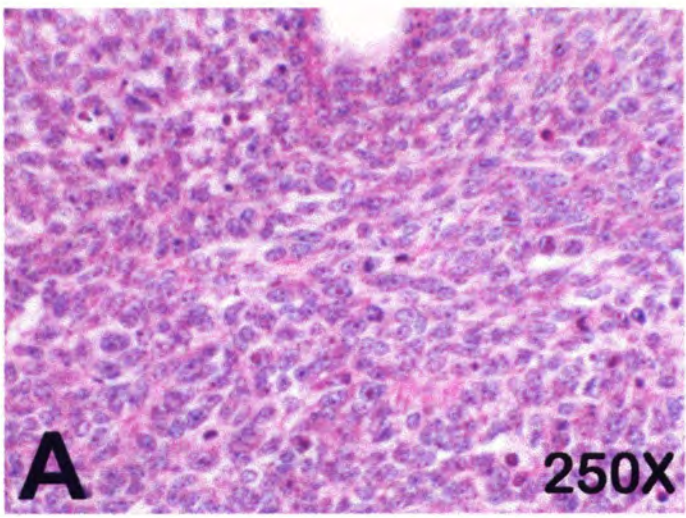
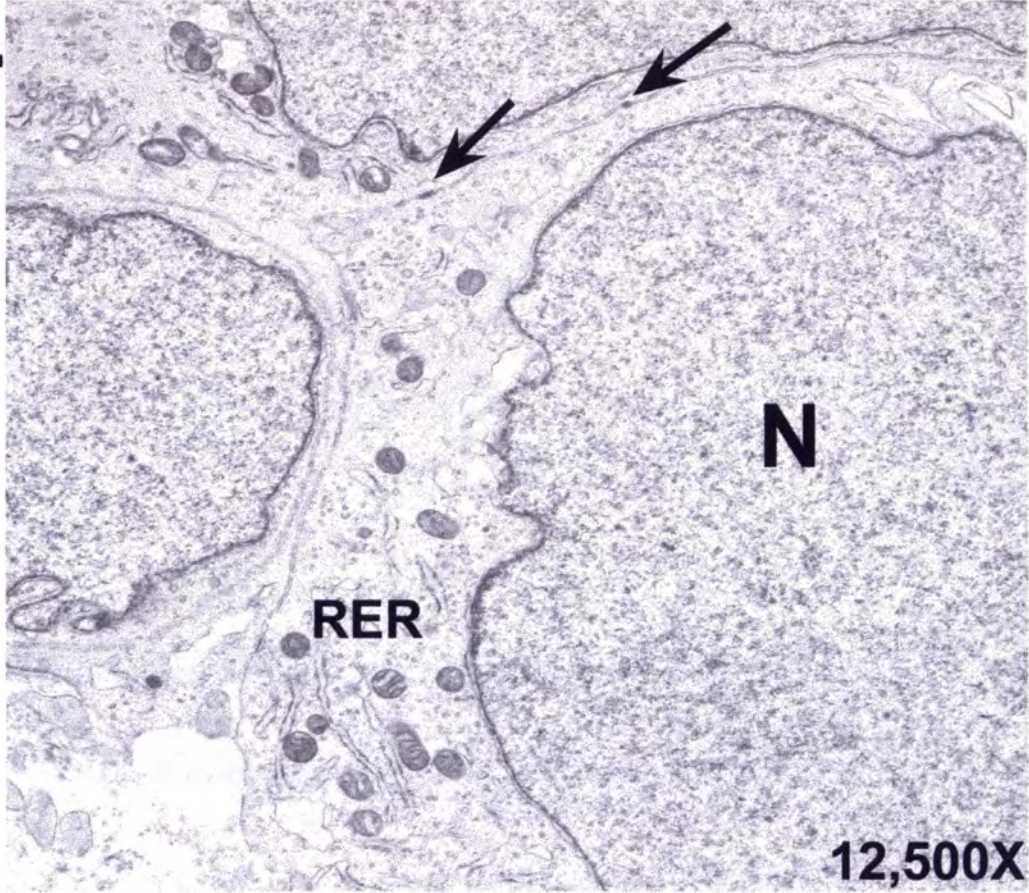


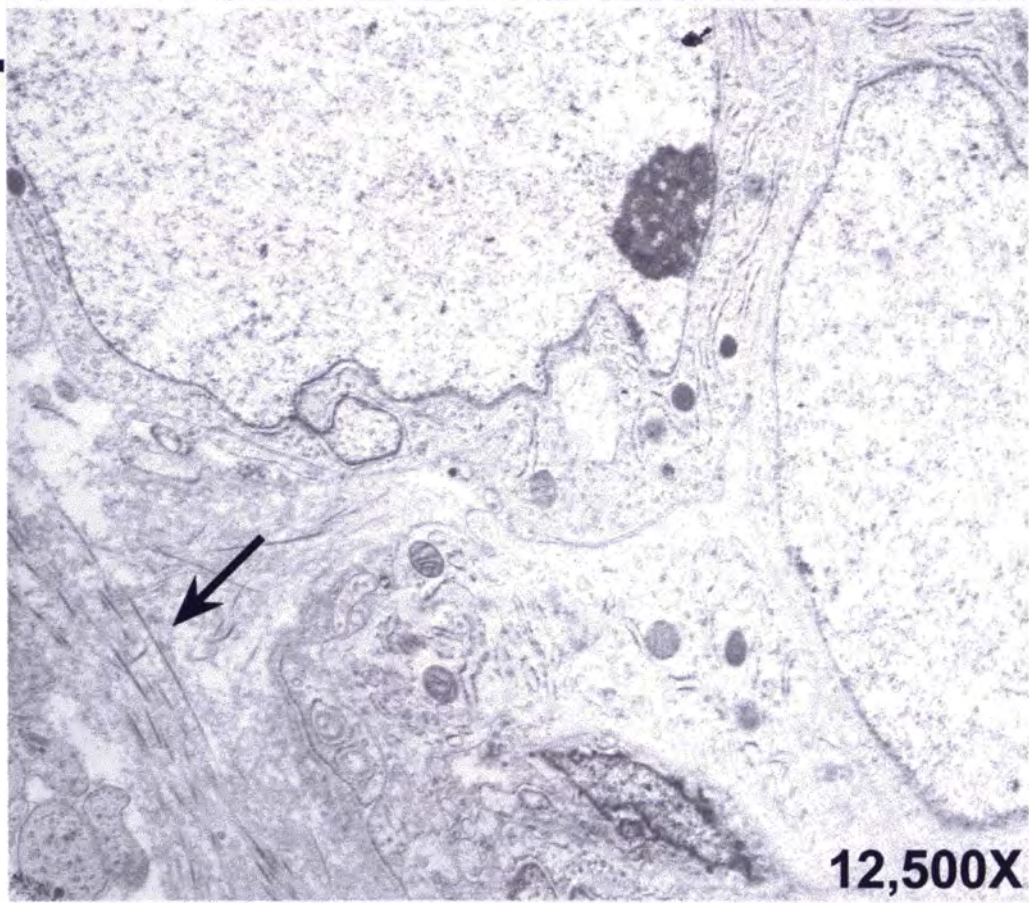


**Figure 4. A,** Transmission electron micrograph of CCSK-2 primary tumor tissue. Arrows indicate primitive cellular junctions between two cells. N designates the cell nucleus which is usually devoid of heterochromatin in CCSK. RER labels the rough endoplasmic reticulum. **B,** Second passage of a CCSK-2 nude mouse xenograft with a nucleus containing a single, prominent nucleolus. The arrow indicates collagenous matrix material which is characteristic ultrastructural feature of CCSK. **C,** Early passage of a CCSK-2 cell culture demonstrating the spindle shaped cells growing in layers. The arrow indicates intermediate filaments within the cell cytoplasm. RER again marks the location of rough endoplasmic reticulum. All micrographs at 12,500X.

**A.**



**B.**

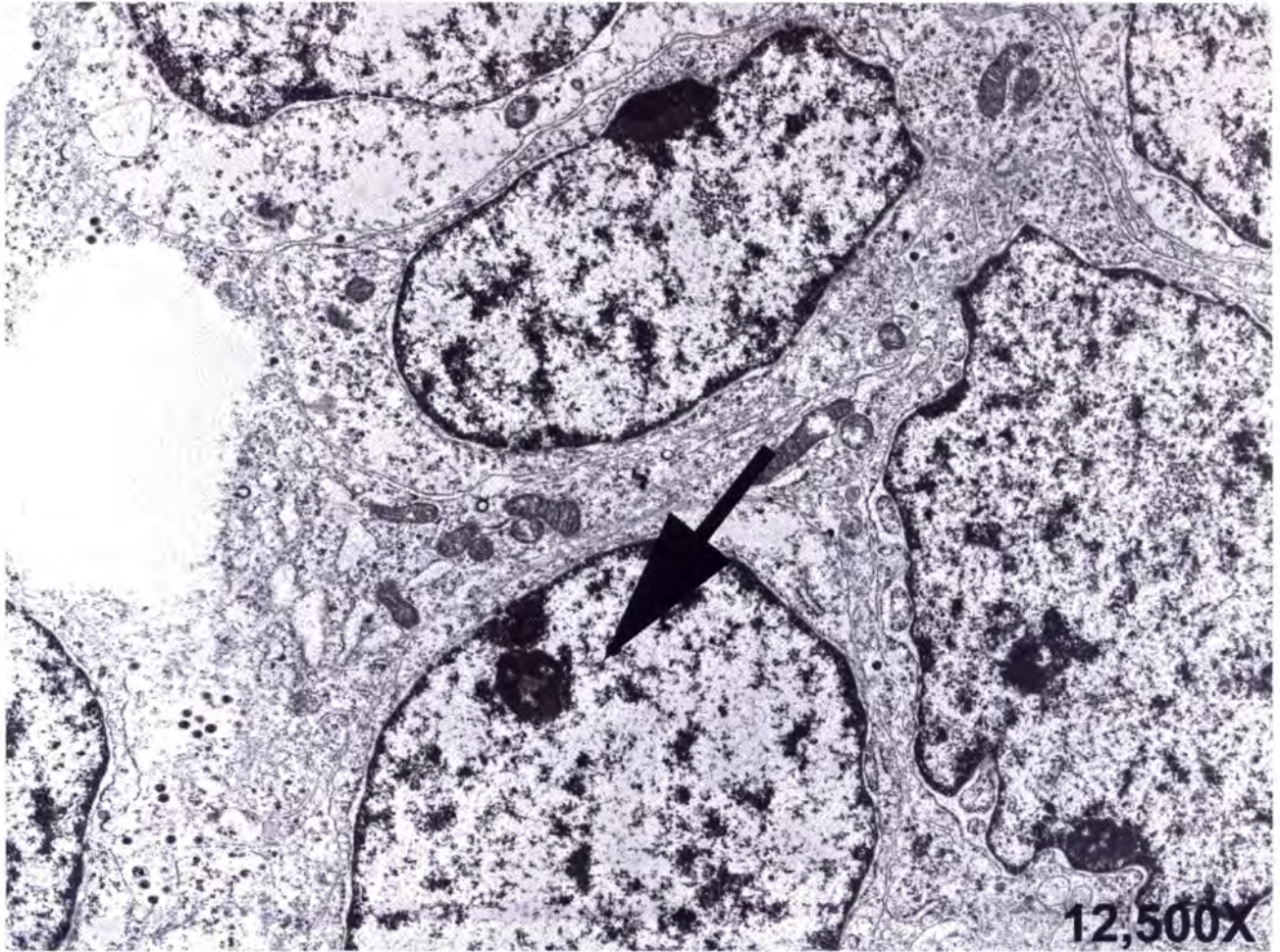


**C.**



**Figure 5.** **A**, Transmission electron micrograph of a CMN-1 nude mouse xenograft. Cells are round to elliptical and contain cell nuclei with heterochromatin and nucleoli (indicated by large arrow). The cytoplasm is rather devoid of other organelles. **B**, Cell culture of a CMN-1 xenografted tumor demonstrating multilayers of cells. Nuclei of cells generally contain a single, prominent nucleolus. The small arrow marks a cell junction between two CMN cells.

**A.**



**B.**

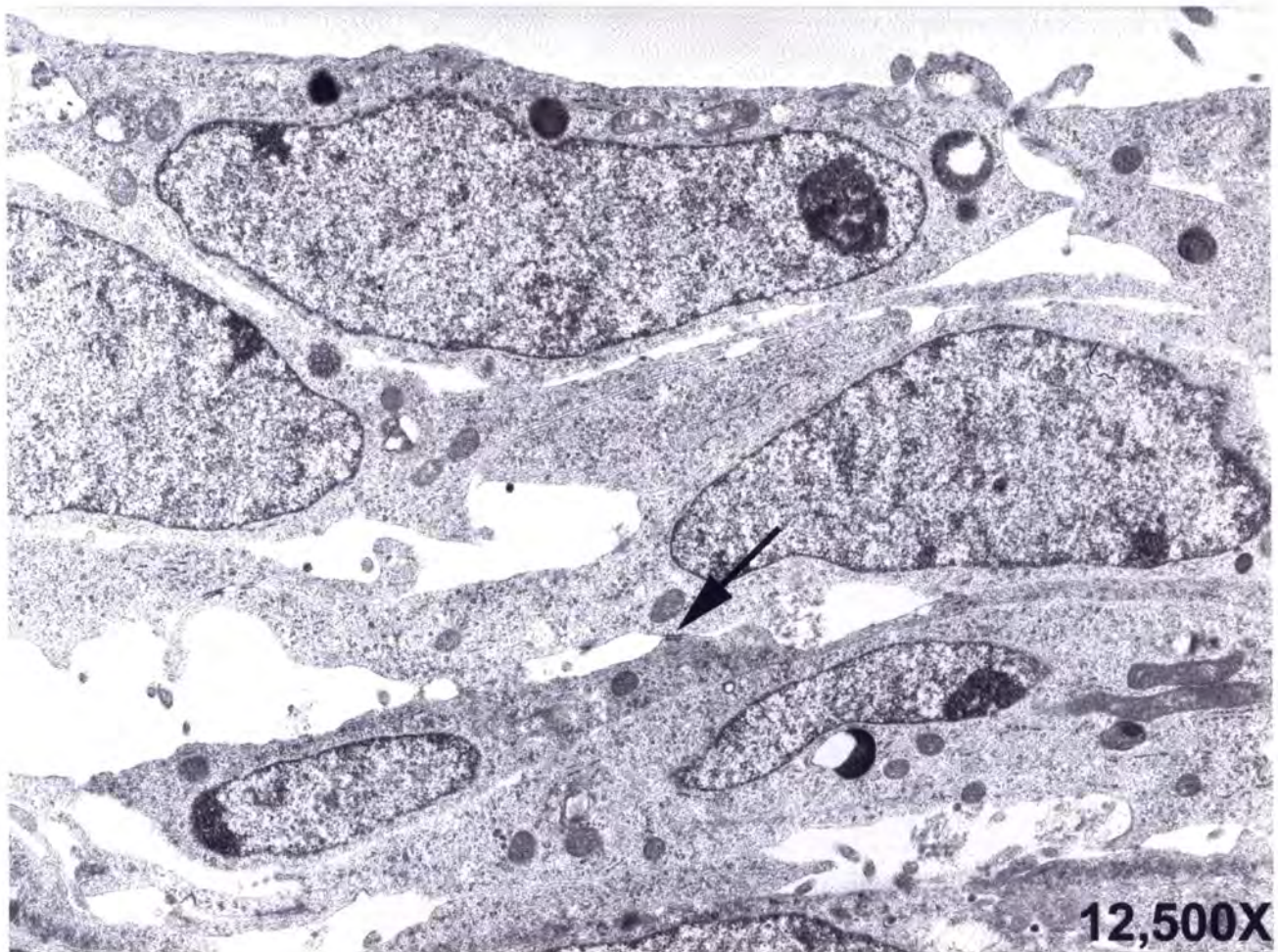


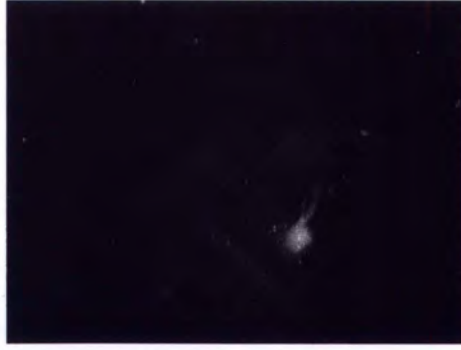
**Figure 6.** Immunocytochemical analysis of CCSK primary cultures using mouse monoclonal antibodies to desmin, smooth muscle actin (SMA), vimentin, and AE1/AE3 cytokeratin intermediate filament proteins. OVCAR ovarian carcinoma cells are included as a positive control for AE1/AE3 cytokeratin staining and a negative control for desmin and SMA staining. Cells receiving no monoclonal antibody but incubated in secondary goat anti-mouse antibody are indicated by omit.

**CCSK-2**

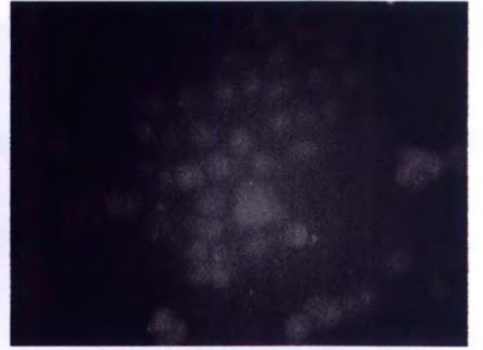
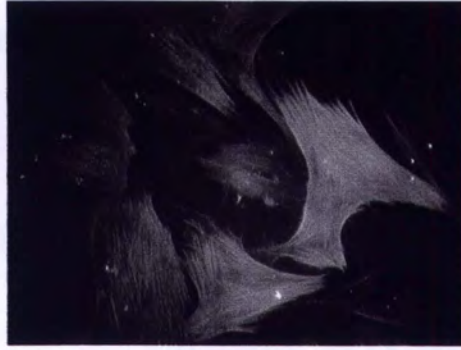
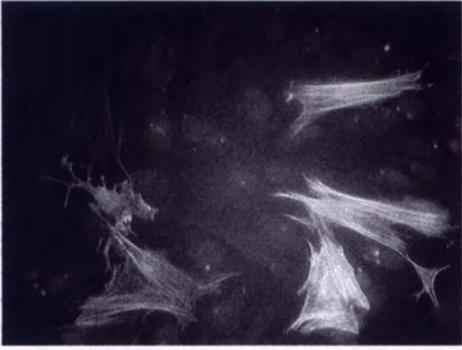
**CCSK-BG1**

**OVCAR**

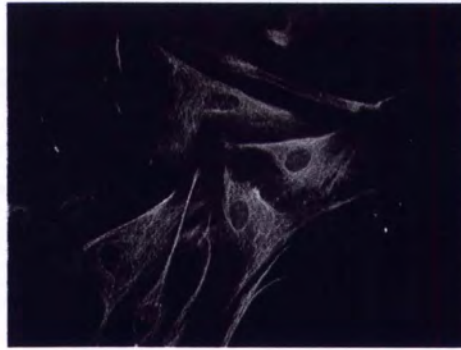
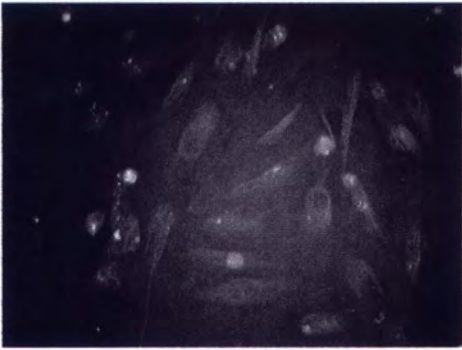
**Desmin**



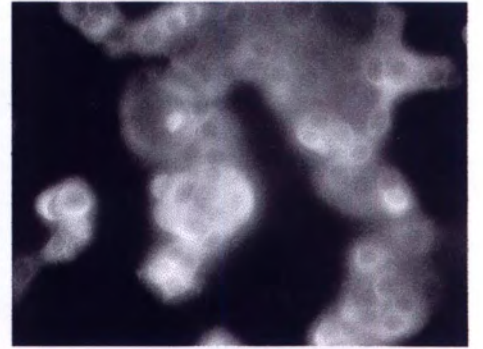
**SMA**



**Vimentin**



**AE1/AE3**



**Omit**



**Figure7.** Immunocytochemical analysis of CMN-1 and CMN-2 cell cultures derived from xenograft tissue using mouse monoclonal antibodies against desmin, SMA, and vimentin intermediate filament proteins. TB208 cells were derived from an extrarenal malignant rhabdoid tumor, a positive control for vimentin. OVCAR ovarian carcinoma cells are negative controls for desmin and SMA. Cells that received no monoclonal antibody but were incubated in secondary goat anti-mouse antibody are designated by omit.

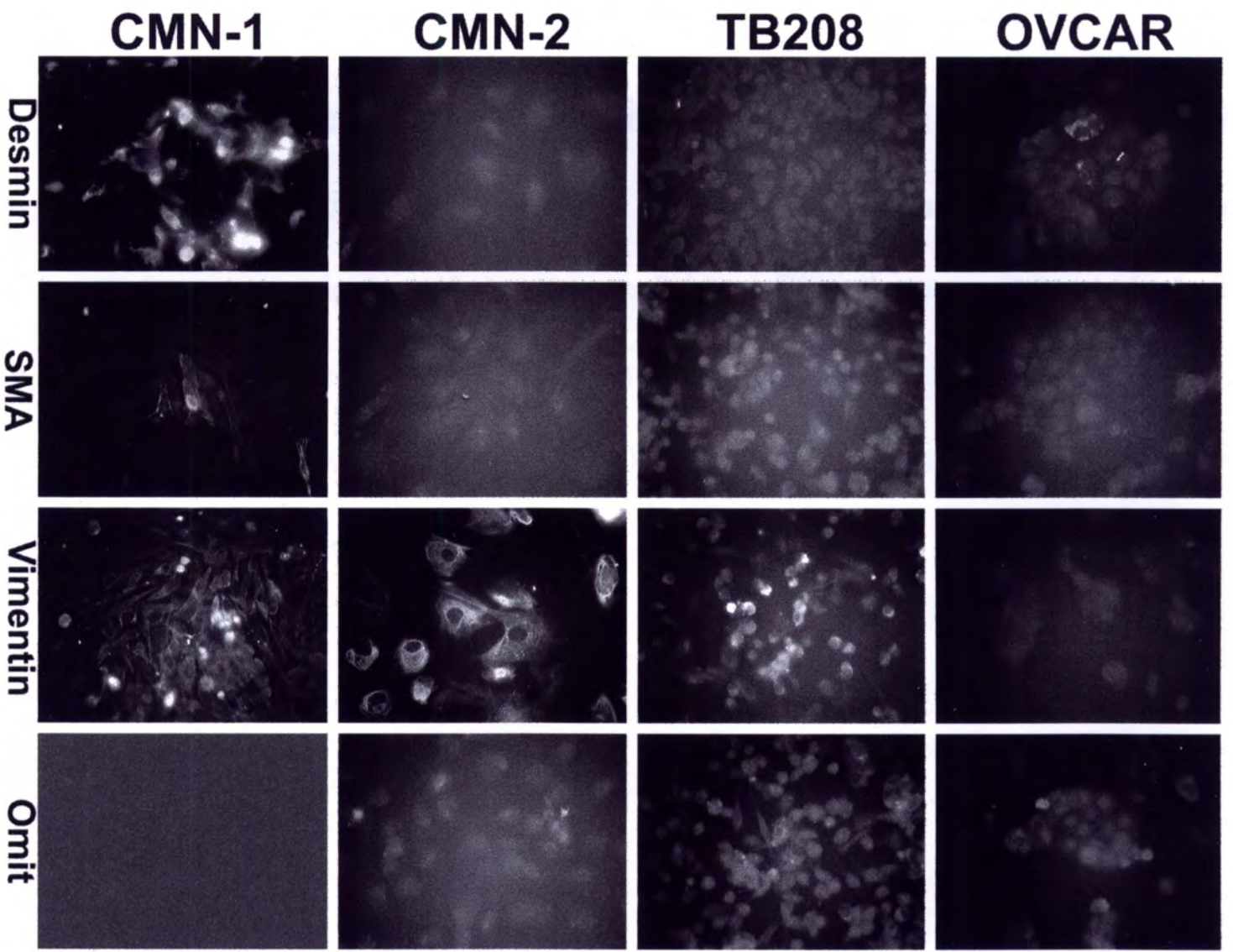




**Figure 8.** Northern analysis of primary tumor (P), xenograft (X), and cell culture (C) mRNA using cDNA probes specific for: **A**, the WT-1 tumor suppressor and **B**, the fetal mitogen IGF-2. WT-1 expression is absent in most cases. Primary Wilms' tumors (W) were included as a positive control for WT-1 mRNA. Normal renal interstitial (RMIC), glomerular mesangial (HMC), and kidney epithelial (PTC) cells were included as negative controls for WT-1 and IGF-2 mRNA expression.

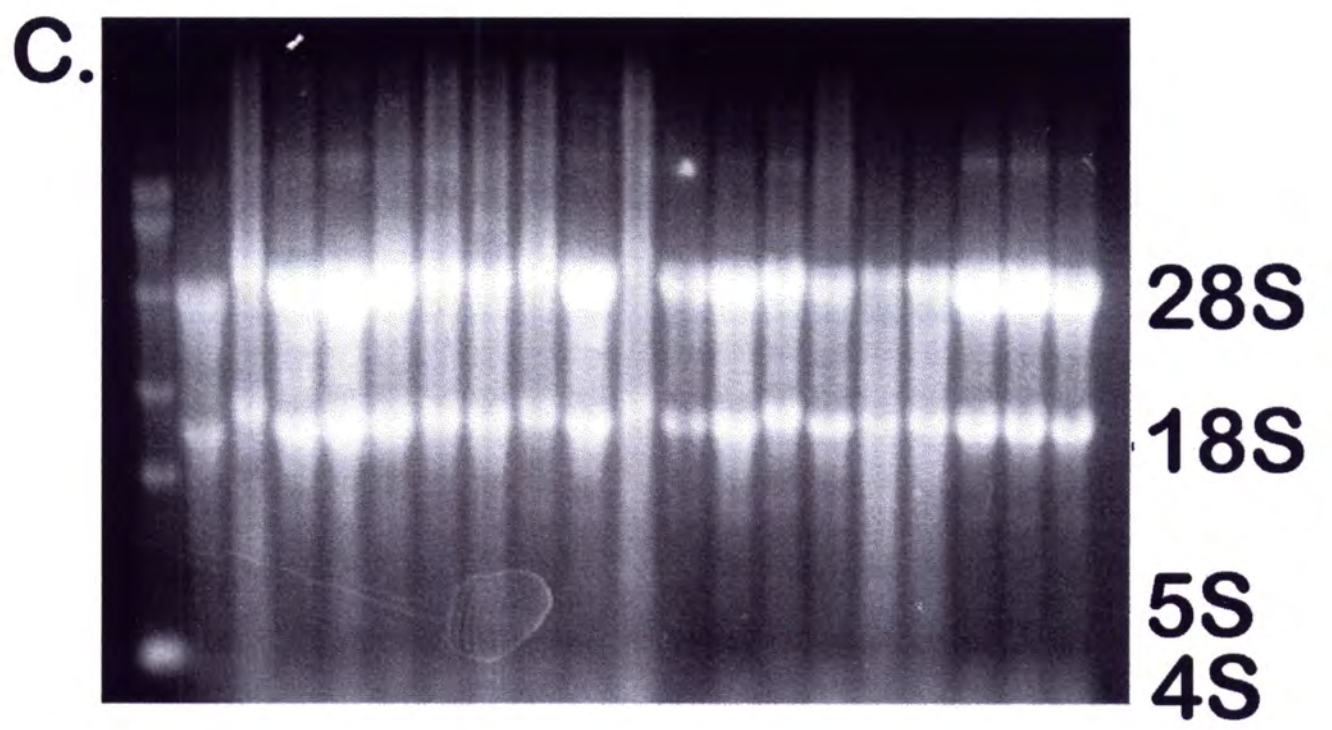
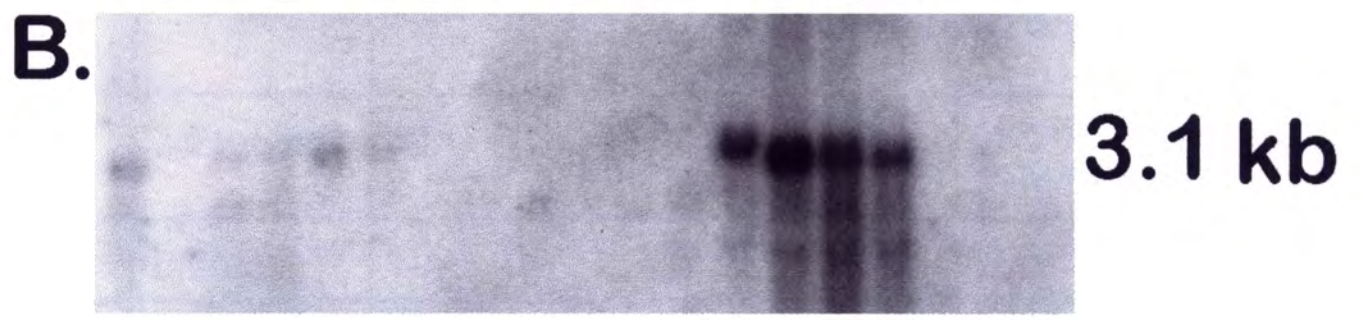
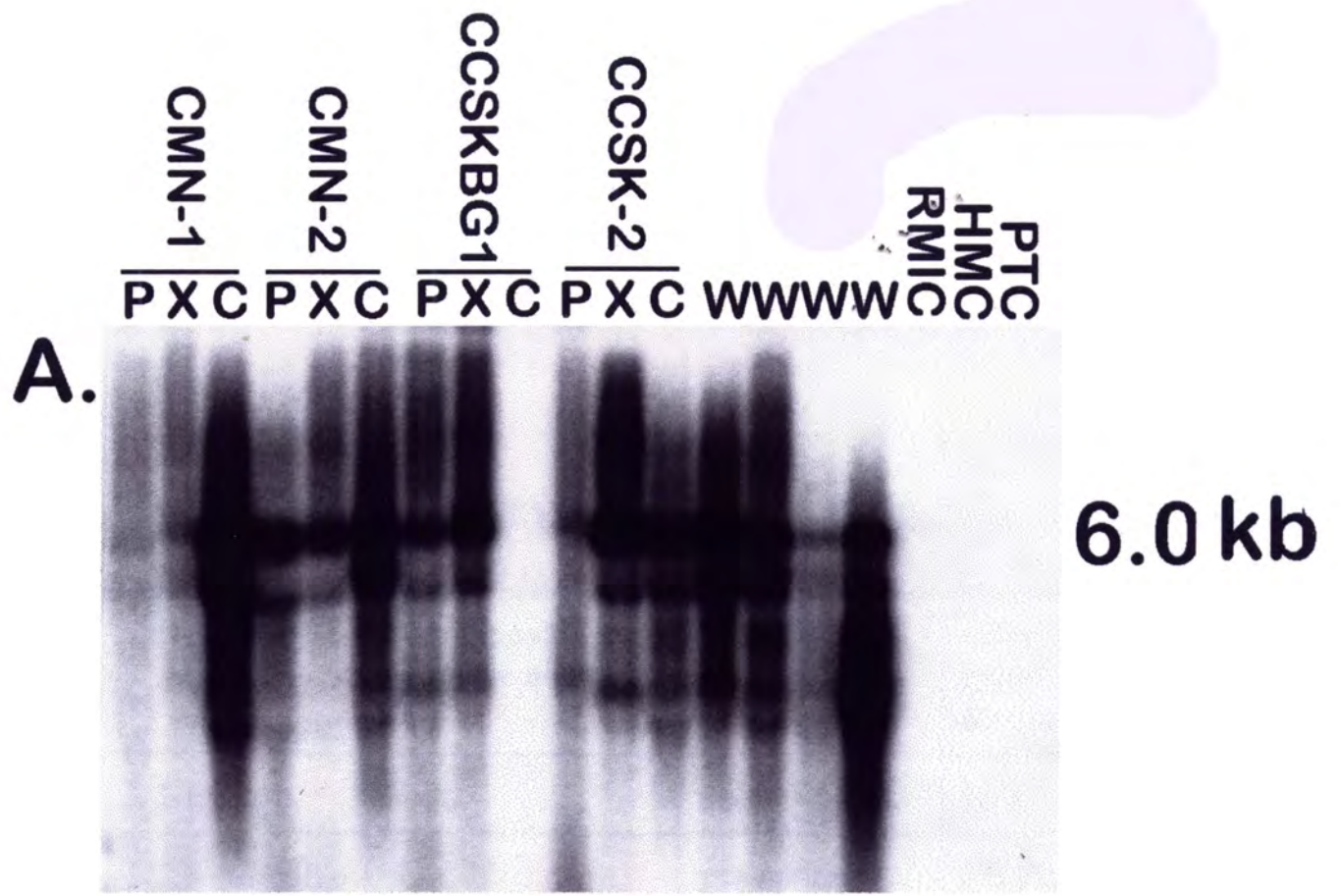


**Table 1. Summary of CCSK and CMN Xenograft and Cell Culture Characteristics**

<b>Tumor Specimen</b>	<b>xenograft turnover time</b>	<b>current xenograft passage number</b>	<b>cell cultures derived</b>	<b>culture growth medium</b>	<b>subculture frequency</b>
CCSK-1	1 month	> 90	no	N/A	N/A
CCSK-2	2.5 months	5	yes (primary tumor and xenograft)	2% FCS in DME/F12	2 weeks
CCSK-3	2.5 months	12	yes (xenograft only)	2% FCS in DME/F12	1 month
CCSK-4	failure	N/A	N/A	N/A	N/A
CCSK-BG1	2.5 months	2	yes (primary tumor and xenograft)	20% FCS in DME/F12	2 weeks
CMN-1	1 month	> 80	yes (xenograft only)	2% FCS in DME/F12	1 week
CMN-2	1 month	> 60	yes (xenograft only)	2% FCS in DME/F12	2 weeks

## **Chapter 4**

**Characterization of the p53 Signal Transduction Pathway in Clear Cell Sarcoma of the Kidney, Congenital Mesoblastic Nephroma, and Anaplastic Wilms' Tumor**

## I. Introduction

Clear cell sarcoma of the kidney (CCSK) is a potentially aggressive renal neoplasm of childhood with a proclivity for the development of bony metastases (Parham *et al.*, 1996). CCSK, first delineated from the more common Wilms' tumor in the 1970s (Kidd, 1970). This tumor is distinguished from other renal tumors of childhood based on its more aggressive clinical behavior and distinct histological characteristics including clear, empty appearing nuclei and abundant extracellular matrix production (Kidd, 1970; Beckwith *et al.*, 1978). CCSK is classified by the National Wilms' Tumor Study in the same category as other childhood renal tumors with poor prognosis including anaplastic Wilms' tumors and the malignant rhabdoid tumor (Murphy *et al.*, 1994). In contrast to CCSK, the congenital mesoblastic nephroma (CMN) is a benign tumor which primarily affects neonates, usually being diagnosed within the first three months of life. First described in the late 1960s, CMN is a relatively benign tumor of the kidney which is usually cured with surgical resection (Bolande *et al.*, 1967; Wigger, 1969). CMNs may be further classified into the classical and cellular (atypical) CMN based on histopathology and clinical behavior (Joshi *et al.*, 1986). In contrast to the wealth of molecular genetic knowledge concerning Wilms' tumorigenesis, few reports exist describing the molecular basis for disease in CCSK and CMN. Some have speculated, however, that CMN may represent the benign counterpart to the more malignant CCSK (Beckwith, 1974).

Anaplastic Wilms' tumor (aWT) is another renal tumor affecting young children which bears a poor prognosis. aWT is thought to develop as a result of a progression event from the more common classical, or triphasic Wilms' tumor (Re *et al.*, 1994; Bardeesy, *et*

*al.*, 1994). Several studies have implicated mutations in the p53 tumor suppressor gene in the development of anaplasia. In a comprehensive study of 140 Wilms' tumors, p53 mutations were documented in 73% of tumors with anaplastic histology. The remaining 129 tumors which did not exhibit morphological anaplasia lacked p53 mutations (Bardeesy *et al.*, 1994). Other reports have indicated that p53 mutations were associated with anaplastic tumors which were invasive and metastatic (Lahoti *et al.*, 1996). Additionally, El-Bahtimi reported p53 mutations in 67% of anaplastic tumors and no mutations in a series of classical tumors examined (El Bahtimi *et al.*, 1996). Others have associated the presence of p53 mutations in anaplastic Wilms' tumors with the development of the multidrug resistance phenotype. One Wilms' tumor cell line, W4, bearing a homozygous p53 mutation overexpressed the multidrug resistance (*MDR-1*) gene which codes for the P-glycoprotein, or multidrug resistance transporter, an integral membrane ATP-dependent pump which prevents accumulation of chemotherapeutic agents in the cytoplasm (Re *et al.*, 1997). Therefore, circumstantial evidence appears to support a role for p53 in the development of anaplasia and resistance mechanisms in these tumors. Because CCSK is a potentially aggressive renal tumor of childhood like aWT, it was hypothesized that abnormalities involving p53 are implicated in CCSK tumorigenesis. One report has indicated possible p53 mutation in a series of CCSK based on immunohistochemical p53 reactivity in a series of formalin fixed paraffin embedded tumor specimens (Cheah *et al.*, 1996). Neither cellular nor classical CMNs have been evaluated for p53 immunoreactivity to date.

The p53 tumor suppressor is located on chromosome 17 and encodes a nuclear phosphoprotein which acts via several signal transduction pathways to elicit either G1 or

G2/M cell cycle arrest, or apoptosis (Levine *et al.*, 1991). Normally, p53 is induced following exposure to ionizing or ultraviolet irradiation and chemotherapeutic agents (Ko *et al.*, 1996). The p53 protein mediates cell growth control by transcriptional modulation of a number of effector genes which contain a consensus p53 binding site within their respective promoters. The *p21<sup>waf1/cip1</sup>* (p21) protein is a cyclin-dependent kinase inhibitor which is transactivated by wild-type p53 protein to elicit cell cycle arrest (El-Diery *et al.*, 1994). This kinase inhibitor is induced in cells that have sustained DNA damage by irradiation or exposure to chemical agents (El-Diery, *et al.*, 1993). The p21 protein mediates cell cycle arrest by binding to and inhibiting the kinase function of cyclin- cyclin dependent kinase complexes and preventing phosphorylation of downstream proteins including the transcription factor Rb, an event which frees the E2F transcription factor to positively regulate the transcription of cyclins. In addition, p21 binds and inhibits the function of the proliferating cell nuclear antigen, a protein controlling S-phase entry (Waga *et al.*, 1994). In other reports, p53 mediates apoptosis by transactivating the pro-apoptotic gene *Bax*, a gene encoding a protein with homology to *Bcl-2* (Miyashita *et al.*, 1995). Furthermore, studies have indicated that wild-type, but not mutant, p53 molecules induced *Bax* expression (Zhan *et al.*, 1994). Transcriptional targets of p53 also include MDM-2, a gene which is amplified in some sarcomas and is involved in negative regulation of p53 (Oliner *et al.*, 1992; Momand *et al.*, 1992). The induction of MDM-2 by p53 after repair of DNA damage establishes an auto-regulatory feedback loop (Wu *et al.*, 1993; Burak *et al.*, 1993). The status of these signal transduction pathways controlled by p53 has not been investigated in CMN and CCSK largely because cell lines derived from these tumors have not been established. This

laboratory, however, has been successful in establishing both CMN and CCSK cell lines which will be useful in evaluating the genetic mechanism(s) of disease in these two renal tumors of childhood.

To evaluate the gene status and functional integrity of the p53 signal transduction pathway in CCSK and CMN, we have evaluated both primary tumors and cell lines for immunohistochemical expression of p53 protein in conjunction with gene structure analysis. Furthermore, using cell lines, we have evaluated the functional state of p53 by the transactivation of *p21*, *Bax*, and *MDM-2* in response to DNA damage following exposure to cis-diamminedichloroplatinum (cisplatin), a chemotherapeutic agent known to generate single and double strand breaks in DNA. Using Northern analysis, we also examined these tumors for evidence of *MDM-2* or *MDR-1* overexpression. We report that p53 protein is detectable immunohistochemically in our CMN, but not our CCSK cell lines. However, immunohistochemical analysis of primary CCSK and CMN tumors failed to demonstrate p53 protein immunoreactivity. Functional analysis of p53 in both CCSK and CMN cisplatin exposed cell lines demonstrated transactivation of p53 target genes including p21, Bax, and MDM-2. In addition, MDM-2 was not overexpressed in any of the CCSK or CMN primary tumors demonstrating that amplification or overexpression of this gene is not relevant to the pathogenesis of these two stromal renal tumors of childhood.



## II. Results

### 1. p53 Immunocytochemistry, SSCP, and DNA Sequencing Analysis

Immunocytochemical staining of p53 is routinely used to screen for mutations of p53 (Esrig *et al.*, 1993). Immunofluorescent staining of p53 was evaluated in two CMN and two CCSK cell lines developed in this laboratory using the mouse monoclonal antibody DO-7, an antibody that recognizes both wild-type and mutant forms of the protein. Immunoreactive p53 was detected in both CMN cultures, but in neither of the CCSK cultures examined (Figure 1). OVCAR ovarian carcinoma cells and the anaplastic Wilms' tumor cell line W16 harboring a previously described p53 hotspot mutation were included as positive controls for p53 protein. W4 anaplastic Wilms' tumor cells harboring a homozygous p53 mutation were not immunoreactive with the DO-7 mouse monoclonal antibody.

To reconcile nuclear p53 staining in the CMN cell lines and its absence from CCSK cells, a panel of CCSK and CMN primary tissues were examined using immunoperoxidase methodology. Five fresh frozen tumors and four paraffin embedded tumors of CCSK examined did not reveal nuclear p53 protein regardless of tumor stage (Table 1A). Further, examination of 3 cellular and 2 classical CMN failed to demonstrate nuclear reactivity. Paraffin embedded tissue matching the immunoreactive cell lines also lacked demonstrable p53 protein expression. An esophageal squamous cell carcinoma containing a previously documented p53 mutation demonstrated nuclear activity and was used as a positive control. CMN-1 and CMN-2 cells, both demonstrating nuclear immunoreactivity for p53 protein, and CCSK-2 cells were subjected to SSCP analysis to screen and direct DNA sequencing to

confirm the identity of p53 mutations (Table 1B). No mutations were detected using primers specific for exons 2-11 of the p53 gene in either of the two CMN cell lines.

## **2. mRNA Induction of Cisplatin Treated Tumor Cells**

Both p53 immunochemistry and DNA sequencing fail to evaluate the function of the p53 protein. In order to assess whether or not the function of this tumor suppressor was impaired in the p53 immunoreactive CMN cell lines, we treated our cell lines with a DNA damaging agent using an approach similar to previous experiments (O'Connor *et al.*, 1997). CCSK cells which were not reactive with the p53 protein were included as a comparison. CMN-1, CMN-2, CCSK-2, CCSK-BG1, anaplastic W4, and anaplastic W16 cell cultures were treated for four and eight hours with 100  $\mu$ M cisplatin and evaluated for their induction of p21 and p53 using Northern analysis (Figure 2). Hybridization with a GAPD cDNA probe was included as a control (Figure 2C). Both CMN and CCSK cell cultures demonstrated induction of p21 mRNA, compared to an untreated control (0 hours), over an eight hour period (Figure 2A). Anaplastic W4 cells which are homozygously mutant for p53 failed to show p21 induction. Anaplastic W16 cells containing a point mutation at codon 273 in the p53 gene revealed a slight p21 induction over the same time period. In contrast to p21 induction, p53 mRNA levels remained unchanged in cisplatin treated CMN cells and declined in both CCSK cell cultures (Figure 2B). p53 mRNA was undetectable in the W4 cell line and declined over eight hours in W16 cells treated with cisplatin.

CMN-1, CCSK-2, and CCSK-BG1 cells were further analyzed for the ability of p53 to transactivate other target genes including Bax and MDM-2 over 20 hours exposure to cisplatin using northern blot analysis (Figure 3 A&B). Hybridization of filters with p21 and

p53 cDNA probes revealed, again, the upregulation of p21 mRNA in all cell lines examined. Whereas p21 induction begins at 2 hours in CMN-1 cells, increased levels of p21 mRNA are not seen in CCSK-2 and CCSK-BG1 cells until 4 and 6 hours. p53 mRNA levels remain stable early and decline late in all cell cultures examined (Figure 3 A&B). Induction of the 1.0 kb Bax- $\alpha$  mRNA was seen in CMN-1 and CCSK-2 cells. In contrast, Bax- $\alpha$  mRNA levels declined in CCSK-BG1 cells. Additionally, Bcl-X mRNA expression diminished with time after cisplatin exposure (Figure 3C). MDM-2 expression was variable in both CCSK cell cultures. CMN-1 cells revealed an initial increase of MDM-2 mRNA at 2 hours exposure before subsequently declining.

Quantification of p21, p53, MDM-2, Bax, and Bcl-X mRNA was performed to establish the extent of gene expression modulation in CMN-1, CCSK-2, and CCSK-BG1 cells after exposure to cisplatin (Figures 4-7). In both CMN-1 and CCSK-2 cells, p21 mRNA levels increased three times after exposure to cisplatin. The strongest induction of p21 occurred at 4 hours in CMN-1 cells and at 10 hours in CCSK-2 cells (Figure 4). Expression of p21 in CCSK-BG1 cells increased between four and six hours even though the extent of induction was less than that demonstrated by CMN-1 and CCSK-2 cells. In all cell lines, p53 mRNA levels remained relatively stable or declined (Figure 5). Uniquely, CCSK-2 cells demonstrated fluctuations in p53 gene expression over twenty hours of exposure to cisplatin even though its expression did not exceed that of the control, or untreated cell culture. MDM-2 expression was induced between two and four hours in CMN-1 cells and between four and six hours in CCSK-2 cells (Figure 6). MDM-2 expression declined in CCSK-BG1 cells between two and four hours before recovering at six hours. Measurement of Bax and Bcl-x was performed to

determine the integrity of the apoptotic signalling pathway in CMN and CCSK cells. In CMN-1 cells, Bax mRNA levels increased 1.5 times between two and eight hours after exposure to cisplatin (Figure 7). Bax gene expression also increased by 2.5 times in CCSK-2 cells after 10 hours of cisplatin treatment. In both CMN-1 and CCSK-2 cells, expression of the anti-apoptotic gene Bcl-X decreased over twenty hours of treatment.

### **3. Stabilization of p53 Protein in Cisplatin Treated Cells**

In the presence of a DNA damaging agent or irradiation, p53 protein is readily stabilized in cells (Kastan *et al.*, 1991). Due to p53-mediated trans-activation of *p21*, increased amounts of p21 protein also provide evidence for a functioning p53 molecule. To evaluate p53 stabilization and p21 accumulation after exposure to cisplatin, protein extracts were prepared from cisplatin treated CMN-1 and CCSK-BG1 cells over a 20 hour period and analyzed by western blot (Figure 8). CMN-1 and CCSK-BG1 blots probed with p53 monoclonal antibody (clone DO-7) demonstrated increased p53 protein expression (Figure 8A). W4 cells and W16 cells were included as a negative and positive control, respectively, for p53 protein expression (Figure 8B). Increased p21 expression was noted in both CMN-1 and CCSK-BG1 cells. p21 protein levels peaked between 6 and 10 hours in CMN-1 cells and between 2 and 6 hours in CCSK-BG1 cells (Figure 8C).

Comparative quantification of p53 mRNA and protein levels in CMN-1 and CCSK-BG1 cells after exposure to cisplatin was also performed (Figure 9). In CMN-1 cells, p53 protein levels increased over four times over a twenty hour period. In CCSK-BG1 cells, p53 protein expression increased over eight times as compared to the control (untreated) sample. Levels of p53 mRNA steadily declined in both CMN-1 and CCSK-BG1 cells over twenty

hours.

#### **4. Flow Cytometric Evaluation of G1 Cell Cycle Arrest**

Flow cytometric cell cycle analysis using propidium iodide staining was included as a final test to evaluate the ability of the p53 immunoreactive cell lines to arrest in G1 or G2 phase of the cell cycle following DNA damage by cisplatin. CMN-1 and CMN-2 cell lines were evaluated for their ability to arrest in G1 phase of the cell cycle after treatment with cisplatin. CMN cells were compared to the p53 null anaplastic Wilms' tumor cell line W4. Both CMN cultures exposed to cisplatin demonstrated G1 arrest after four hours of cisplatin exposure (Figures 10-12 and Table II). CMN-2 cells demonstrated a marked increase in the percentage of cells at G1 after 2 hours of exposure to cisplatin. CMN-1 cells, in contrast, appeared to arrest more slowly. In contrast, the p53 null W4 cell line exhibited little to no increase of cells in G1 phase over the same time period.

#### **5. Steady State mRNA Expression of p53, p21, MDM-2, and MDR-1 in CCSK and CMN Primary Tumors.**

The use of northern analysis was employed in the evaluation of the steady-state levels of elements of the p53 cell signalling pathway. The presence of p53 mRNA was used to rule out deletion of this gene while steady-state p21 levels suggests the normal functioning of the p53 protein as well. Evaluation for *MDR-1* expression was included as a comparison to Wilms' tumors as some anaplastic tumors overexpress this protein (Re *et al.*, 1997). Total cellular RNA was extracted from CCSK primary tumors and analyzed using northern analysis (Figure 13). RNA was probed with p53, p21, MDM-2, MDR-1, and GAPD cDNA fragments to evaluate the steady-state expression of these genes in CCSK primary tumor specimens. KB-

V1, an epidermoid carcinoma cell line, was included as a positive control for amplification of the MDR-1 gene. SJSA-1 pluripotential sarcoma cells were included as a control for MDM-2 amplification. p53 and p21 mRNA levels were detected in all CCSK tumor specimens examined. There was no evidence for gross gene rearrangement of p53 or MDM-2 overexpression in any CCSK case examined. There was also no evidence for MDR-1 amplification or overexpression in CCSK primary tumors. Hybridization with a GAPD cDNA fragment was included as a marker for constitutive gene expression.

Northern analysis of CMN primary tumors was also conducted using probes specific for p53, p21, MDM-2, and GAPD (Figure 14). All primary tumors expressed detectable levels of both p53 and p21 mRNA with no evidence of a gross p53 gene rearrangement or deletion. MDM-2 expression was detected at low levels in 2 classical CMN cases. There were no differences in gene expression between classical and cellular variants of CMN.

### III. Discussion

Mutations of the p53 tumor suppressor gene appears to constitute at least one mechanism of tumor progression in the potentially aggressive and drug-resistant anaplastic Wilms' tumor. In a study of 11 Wilms' tumors with anaplastic features, p53 mutations were documented in 73% of cases (Bardeesy *et al.*, 1994). Other reports have indicated p53 mutations in 66% of anaplastic tumors (El-Bahtimi *et al.*, 1996). Others have correlated p53 protein immunoreactivity with poor outcome in Wilms' tumor (Lahoti *et al.*, 1996). A p53 mutation was also linked to overexpression of the *MDR-1* gene in an anaplastic Wilms' tumor that led to patient death (Re *et al.*, 1997). Because of the association of p53 mutations with pediatric renal tumors bearing poor prognosis, p53 protein expression was examined by immunohistochemistry in a series of CCSK, another potentially aggressive childhood renal tumor with a propensity for bone metastases (Cheah *et al.*, 1996). This report indicated that nuclear p53 protein was detectable in all eight cases examined leading to speculation that there may be a common genetic mechanism leading to resistance and poor outcome in pediatric renal tumors. This hypothesis was further bolstered a report of a translocation (10;17) breakpoint involving chromosome 17p13, the site of the p53 gene locus (Punnett *et al.*, 1989).

To begin to test such a hypothesis, we examined CCSK and CMN cell cultures, primary tumors for p53 protein and mRNA expression using immunochemistry and northern analysis, respectively. p53 nuclear accumulation is an established marker for p53 mutations so cells which demonstrate immunoreactivity may harbor p53 mutations (Esrig *et al.*, 1993). Both CMN cell cultures and CCSK cell lines were initially evaluated for p53

expression. Surprisingly, p53 nuclear reactivity was exhibited by cells derived from the benign CMN and not in CCSK tumor cells. Subsequent SSCP and DNA sequencing failed to demonstrate the presence of a p53 mutation in these immunoreactive cells. To eliminate the possibility that p53 nuclear reactivity in CMN cells was not a characteristic only found in cell cultures, a series of CCSK and CMN frozen and paraffin embedded tumors were examined. This experiment did not show p53 nuclear reactivity in any of the tumor sections examined. In the absence of p53 mutations, overexpression of the p53 binding protein and oncoprotein MDM-2 constitutes an alternative means of p53 inactivation (Momand *et al.*, 1992). In addition, *MDM-2* is amplified in many bone and soft tissue sarcomas leading to the hypothesis that *MDM-2* amplification or overexpression is a plausible occurrence in the “sarcomatous” renal tumors of childhood. Furthermore, *MDM-2* overexpression stabilized p53 protein in rhabdomyosarcoma cell lines (Keleti *et al.*, 1996). This led to the hypothesis that MDM-2 may provide an explanation for the p53 nuclear reactivity in our CMN cultures. Northern analysis of both CMN and CCSK primary tumor tissue did not reveal any evidence for MDM-2 amplification or overexpression, dismissing the role of this gene in CMN and CCSK tumorigenesis. The lack of MDM-2 overexpression in these tumors is consistent with a previous report which identified MDM-2 amplification as a rare occurrence in pediatric tumors (Waber *et al.*, 1993).

In addition, CCSK tumors did not exhibit MDR-1 overexpression by northern analysis. Lack of MDR-1 expression in these tumors contrasts with that previously reported for an epithelial-predominant anaplastic Wilms’ tumor that led to patient death (Re *et al.*, 1997). These data also suggest that MDR-1 overexpression is limited to cells with epithelial



differentiation, that CCSK tumors are not comprised of epithelial cells, and that this gene is not responsible for the potentially poor outcome in this tumor type.

Since tumors with p53 mutations are not always detected using immunohistochemistry, we subjected both CMN and CCSK cell cultures to the DNA damaging chemotherapeutic drug cisplatin to test the ability of the p53 protein to transactivate its downstream effector genes p21, MDM-2 and Bax. This is a technique which has been used successfully in many cell types to evaluate p53 functional capabilities (O'Connor *et al.*, 1997). Both of the CMN and CCSK cell lines exposed to cisplatin demonstrated p21 induction with varying kinetics over 8 hours of exposure. In contrast, anaplastic Wilms' tumor cells with p53 mutations demonstrated a diminished to absent induction of p21. Flow cytometric cell cycle evaluation revealed G1 cell cycle arrest in all CMN and CCSK cell cultures, but not in p53 null W4 anaplastic Wilms' tumor cells, demonstrating the ability of the p53 protein to mediate a signal transduction cascade, through p21, leading to cell growth arrest. Furthermore, the pro-apoptotic Bax gene was induced in both CMN-1 and CCSK-2 cells over 20 hours. Bax mRNA levels declined, however, in CCSK-BG1 cells. MDM-2 gene expression was also induced in CMN and CCSK cell lines with varying kinetics. p53 mRNA levels was not affected in any of the cisplatin treated cell lines indicating that p53 protein mobilization and not p53 mRNA induction is important in the cellular response to DNA damage. Previous reports have indicated that wild-type p53 protein induction occurs during the cellular response to DNA damage (Kastan *et al.*, 1991). Therefore, CMN-1 and CCSK-BG1 cells were exposed to cisplatin for intervals of two hours for a total of twenty hours. Both cell cultures exhibited protein stabilization over this time period consistent with the normal function of p53.

Taken together, these data indicate that p53 mutations are not present in CCSK and CMN tumors, a finding that contrasts the p53 genotype in anaplastic Wilms' tumor cells. An explanation for the p53 nuclear reactivity in CMN cells is not known. However, the p53 protein may be rendered more stable in cell culture conditions for these cell types. Alternatively, p53 may be stabilized by other p53 binding proteins such as 53BP2 (Gorina *et al.*, 1996). Previous studies have suggested that inactivation of p53 enhances the sensitivity of some cells to chemotherapeutic agents (Hawkins *et al.*, 1996). For example, the p53 null W4 anaplastic Wilms' tumor cells, derived from a patient that died from disease, were more sensitive to cisplatin exposure than the CMN-1 cell line which was derived from a benign tumor with a normal p53 gene. Therefore, this study also demonstrates the utility of evaluating the function of p53 in pediatric renal tumor cells and has implications for the uses of DNA damaging agents as a chemotherapeutic treatment strategy in these tumors.

**Figure 1.** Immunocytochemical evaluation of p53 protein in cultured CCSK and CMN cells. Column **A**, Cells stained with mouse monoclonal antibody to p53 (clone DO-7) and rhodamine-conjugated secondary goat anti-mouse antibody. Column **B**, corresponding phase micrograph to Column A. Column **C**, cells which received only secondary rhodamine-conjugated goat anti-mouse antibody. Column **D**, corresponding phase micrographs to Column C. Rows indicate cell line evaluated. OVCAR (ovarian carcinoma) cells and anaplastic Wilms' tumor cells bear p53 mutations and act as controls for the p53 protein. Anaplastic W4 cells contain no immunochemically detectable p53 protein.

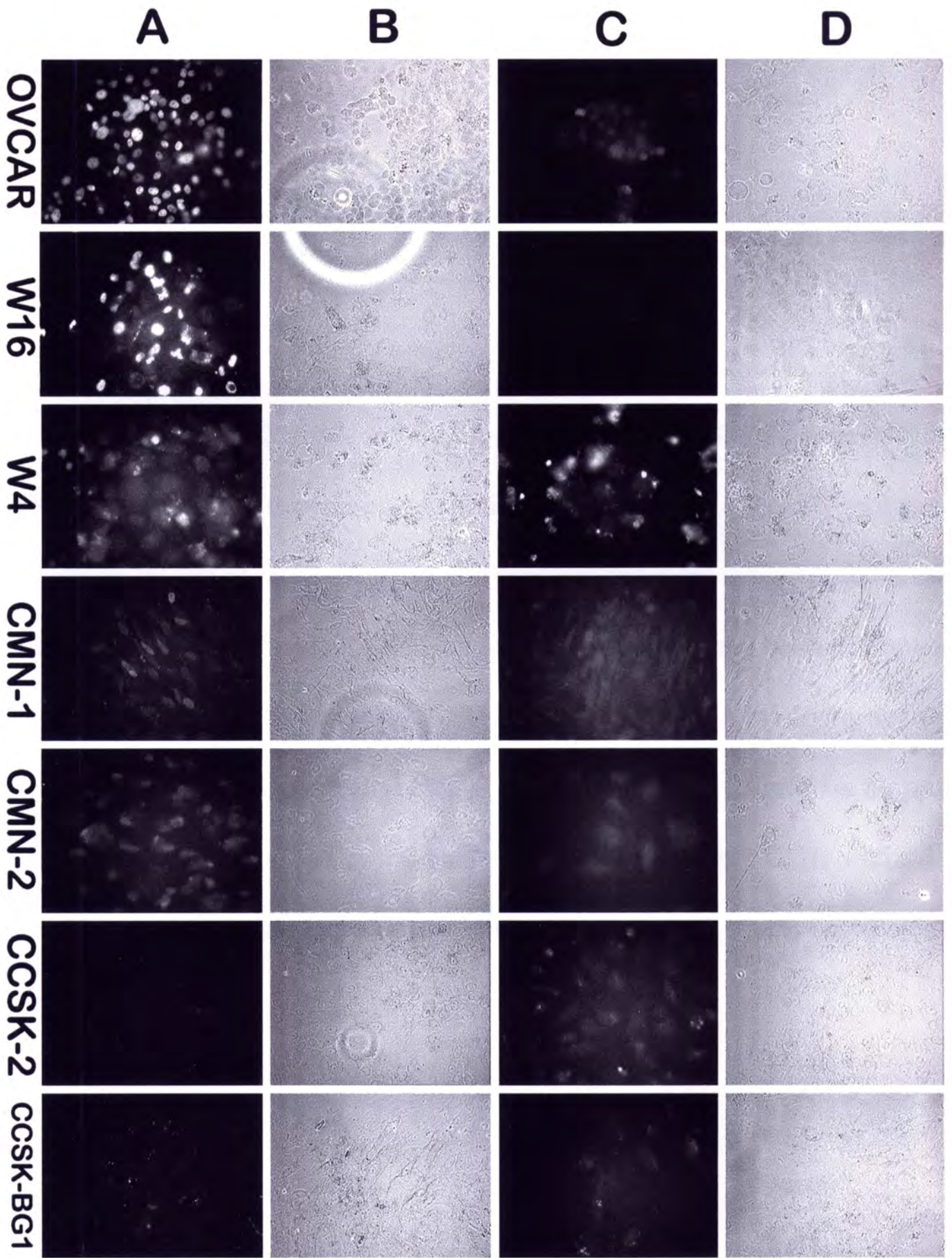


**Figure 2.** Northern analysis of p21, p53, and GAPD in cisplatin treated CCSK and CMN cell cultures. Cell lines employed in experiment are indicated at top of blot. The different genes analyzed are noted at the left of each blot. Cisplatin exposure times are indicated above each lane in hours (0 hours = untreated cells). **A**, Induction of p21 mRNA over 8 hours of cisplatin exposure. CMN-1, CMN-2, CCSK-2 and CCSK-BG1 induced p21 mRNA in varying degrees. W4 and W16 anaplastic Wilms' tumor cells bearing p53 mutations were included as negative controls. **B**, Evaluation of p53 mRNA over 8 hours of cisplatin exposure. **C**, Hybridization with a GAPD cDNA fragment was included as a control for constitutive gene expression.

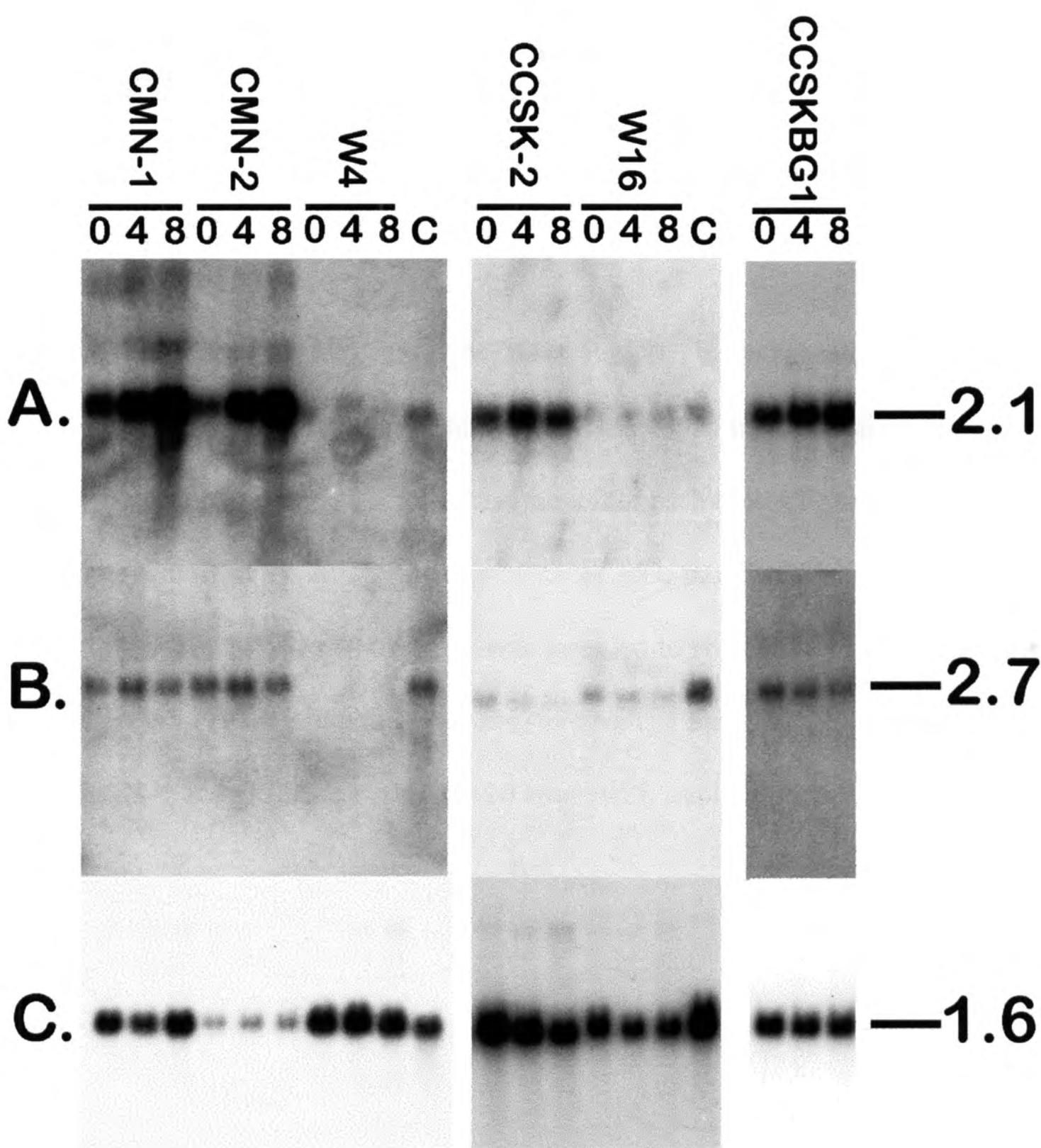
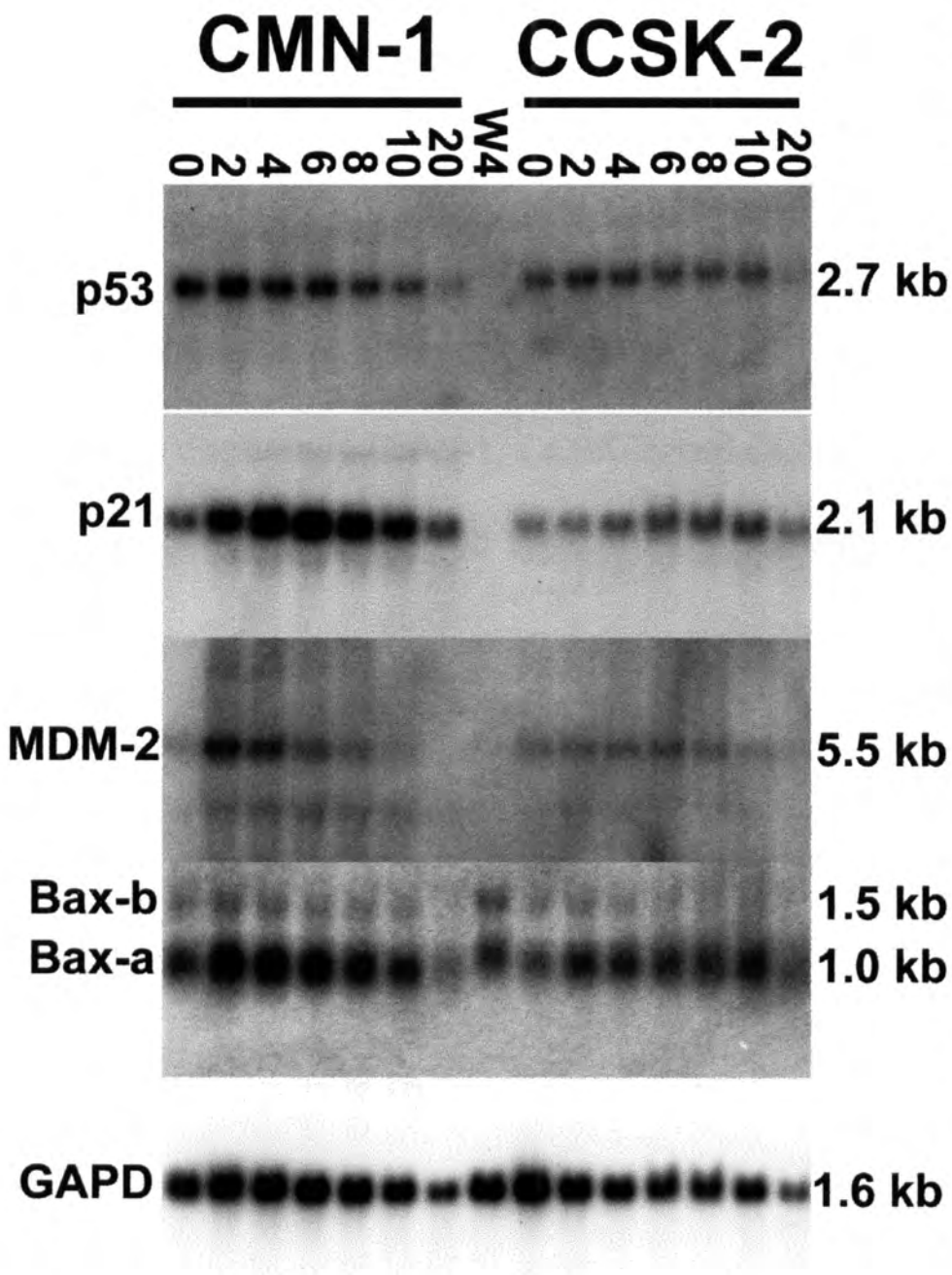
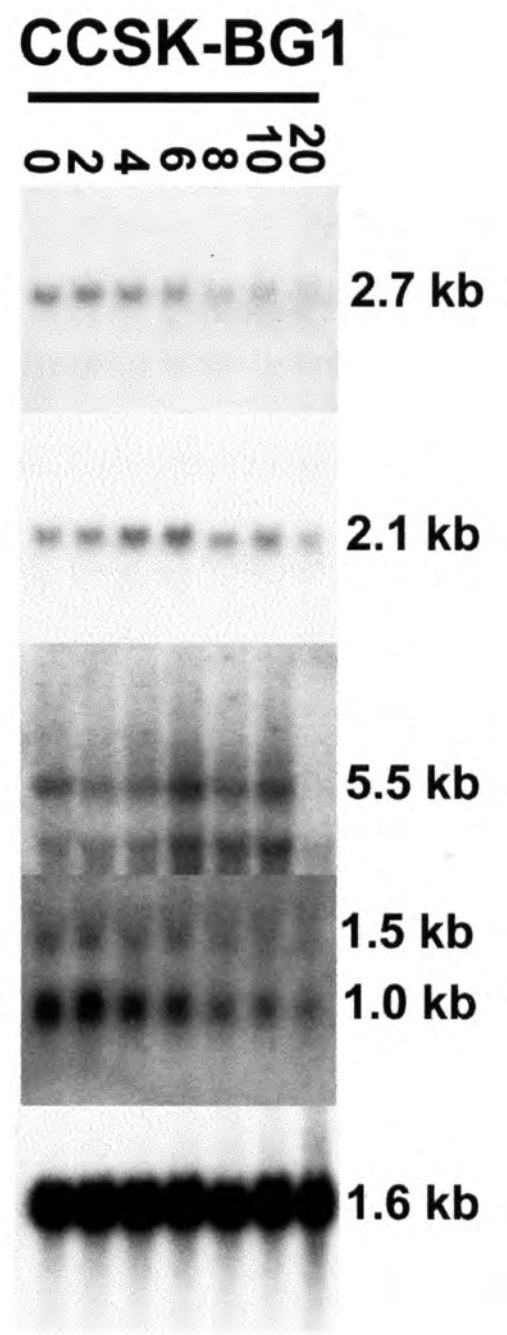


**Figure 3.** Northern analysis of p53, p21, MDM-2, Bax, Bcl-x<sub>L</sub> and GAPD mRNA in CCSK and CMN cell cultures exposed to cisplatin. Cells employed in experiments are indicated above each blot. Genes analyzed are noted at the left of each blot. Cisplatin exposure times are noted above each lane. **A**, Northern analysis of p53, p21, MDM-2, Bax, and GAPD. Hybridization with a GAPD cDNA probe was included to ensure for equal lane loading in both A and B. W4 cells are included as a negative control for p53. **C**, Northern analysis of Bcl-x<sub>L</sub> in CMN-1 and CCSK-2 treated for 20 hours with cisplatin.

**A.**



**B.**



**C.**

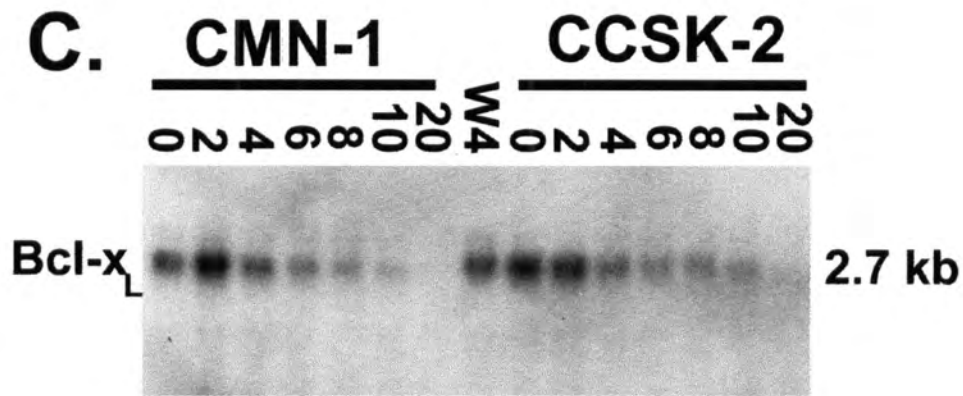




**Figure 4.** Line Graph illustrating p21 waf-1 mRNA quantification over twenty hours of exposure to cisplatin in CMN-1, CCSK-2, and CCSK-BG1 cell cultures. A key to the right of the graph identifies the cell types used in the experiment. mRNA quantification was performed using Adobe Photoshop version 4.0 Software.

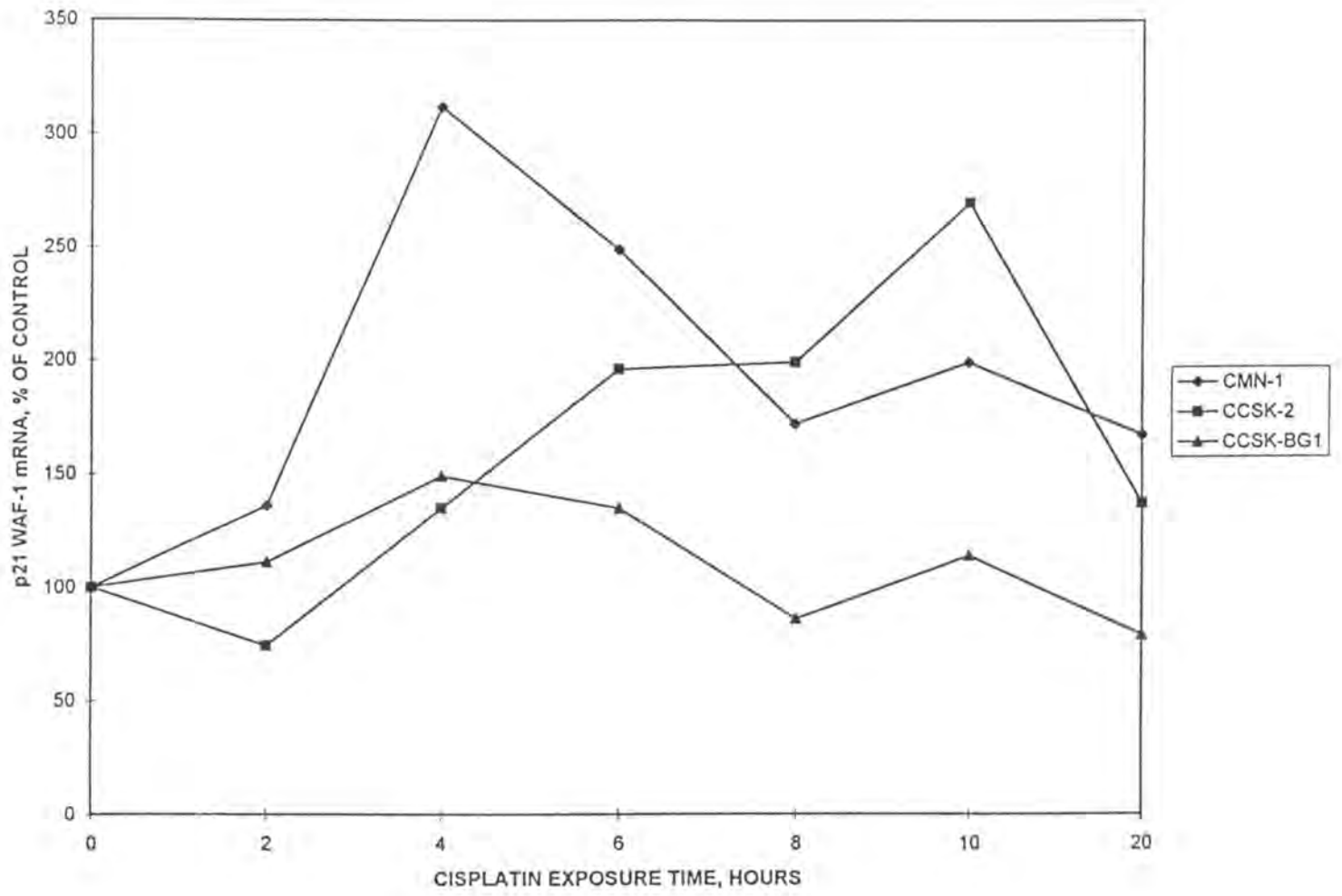


**Figure 5.** Line graph illustrating p53 mRNA quantification over twenty hours of exposure to cisplatin in CMN-1, CCSK-2, and CCSK-BG1 cell cultures. A key to the right of the graph identifies the cell types used in the experiment. mRNA quantification was performed using Adobe Photoshop Version 4.0 software.

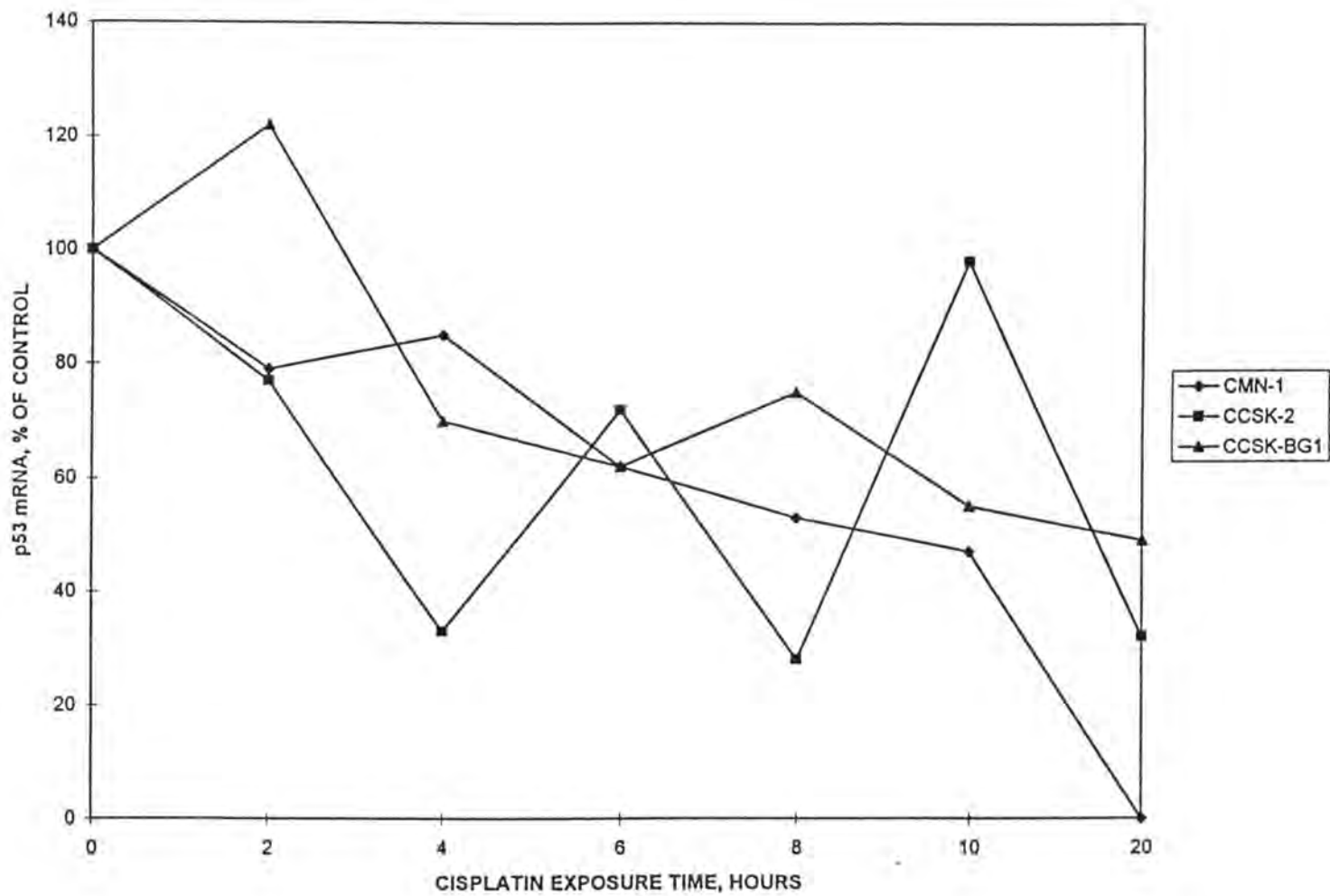


**Figure 6.** Line graph illustrating MDM-2 mRNA quantification over twenty hours of exposure to cisplatin in CMN-1, CCSK-2, and CCSK-BG1 cell cultures. A key to the right of the graph identifies the cell lines used in the experiment. mRNA quantification was performed using Adobe Photoshop Version 4.0 software.

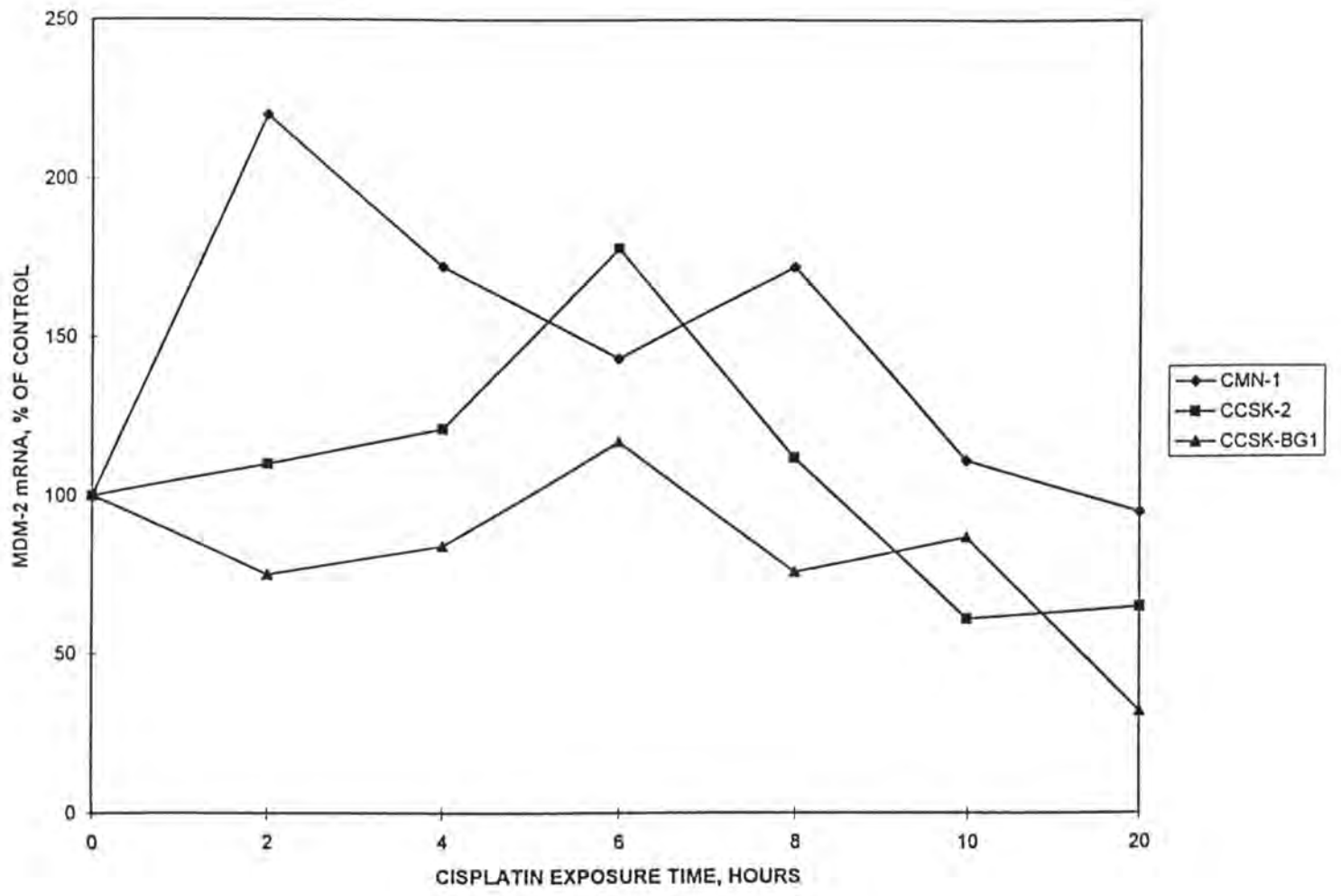
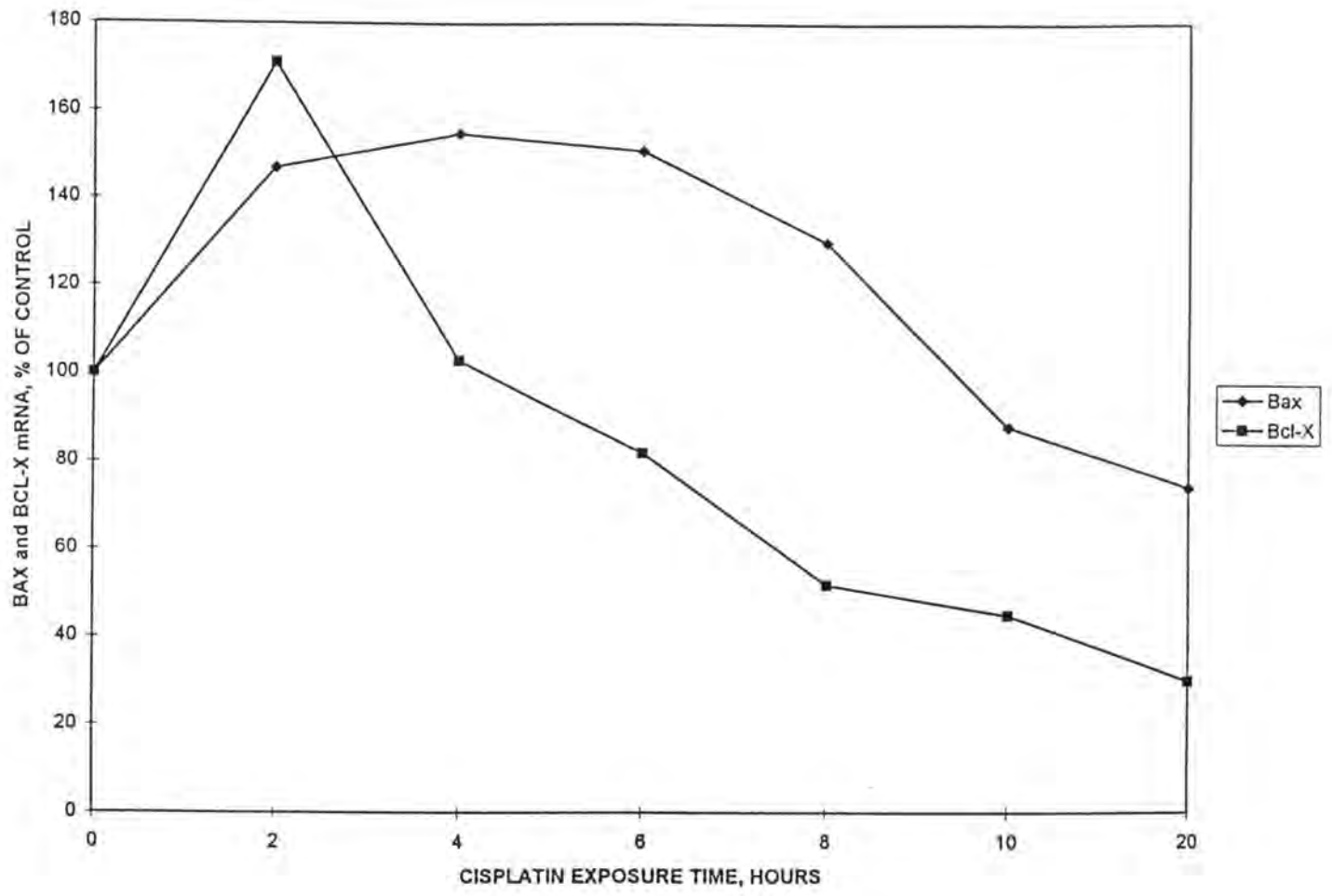


**Figure 7.** Line graph illustrating quantification of Bax and Bcl-X mRNA over twenty hours of exposure to cisplatin. **A**, Bax and Bcl-X mRNA quantification in CMN-1 cells. **B**, Bax and Bcl-X quantification in CCSK-2 cells. Quantification was performed using Adobe Photoshop Version 4.0 software.

**A.**



**B.**

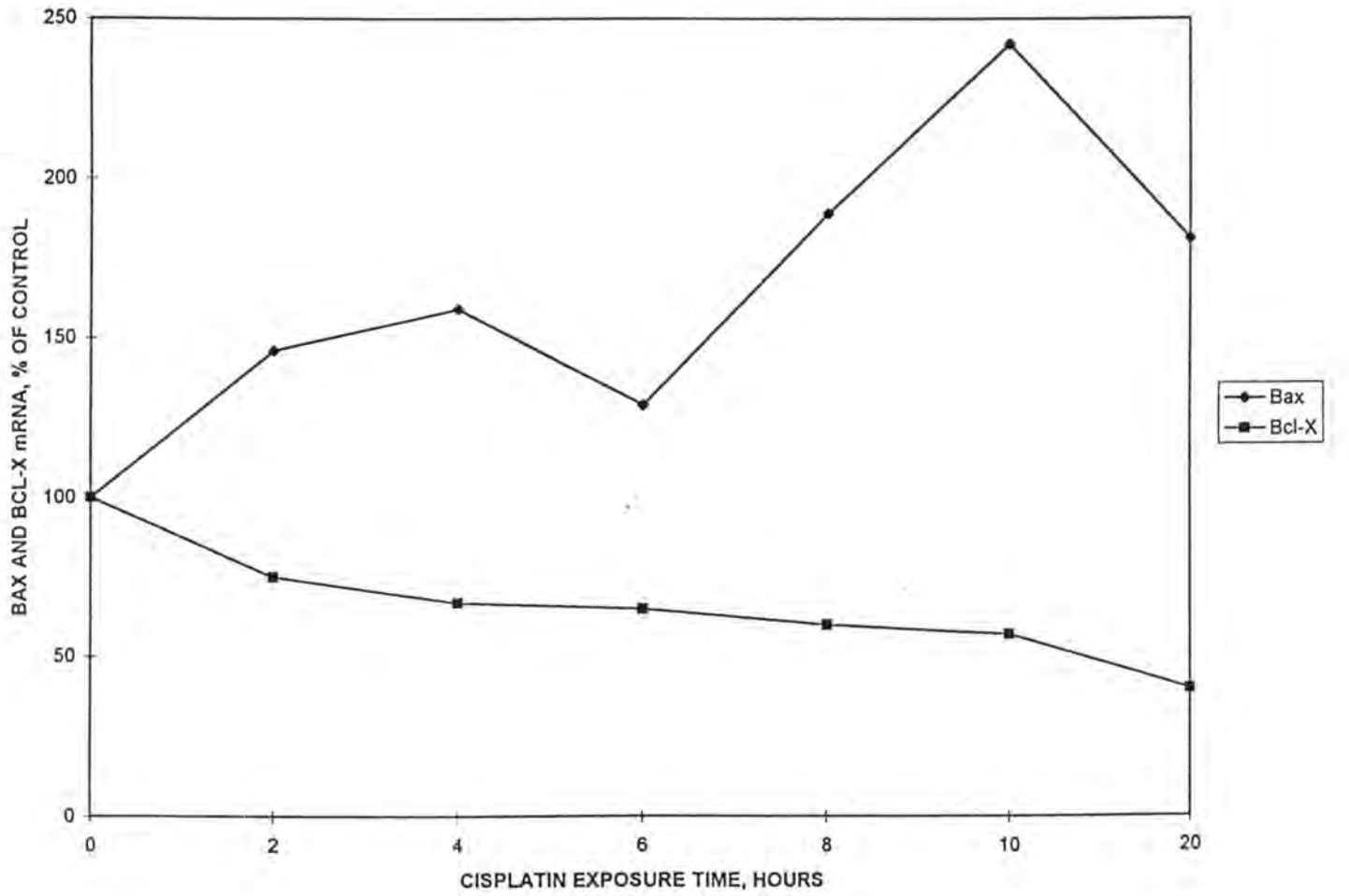




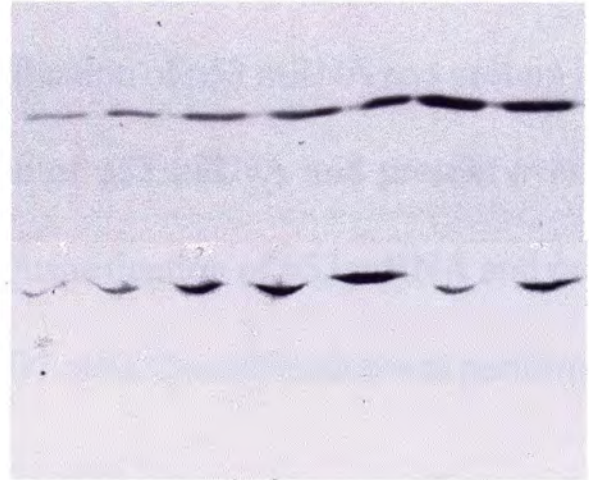
**Figure 8.** Western blot analysis of p53 and p21 protein in CMN-1 and CCSK-BG1 cells after 20 hours of exposure to cisplatin. Exposure time is noted above each lane and cells used are indicated at the left of each blot. **A**, Western analysis of p53 using the mouse monoclonal p53 antibody (clone DO-7) showing p53 accumulation over 20 hours in both CMN-1 and CCSK-BG1. **B**, p53 negative and positive controls. p53 mutant W4 cell extracts lack demonstrable p53 protein. p53 mutant W16 cell line, in contrast, shows abundant p53 protein. **C**, Western analysis of p21 using a mouse monoclonal antibody in cisplatin exposed CMN-1 and CCSK-BG1 cells. p21 protein levels increased over 10 hours in CMN-1 cells. In contrast, p21 protein levels rose between 2 and 6 hours in CCSK-BG1 cells before declining at 8 hours. Equal amounts of protein were loaded into each lane.

**A.**

0 2 4 6 8 10 20

**CMN-1**

**CCSK-BG1**



**B.**

W/4  
W/16



p53+/-  
p53-/-

**C.**

0 2 4 6 8 10 20

**CMN-1**

**CCSK-BG1**

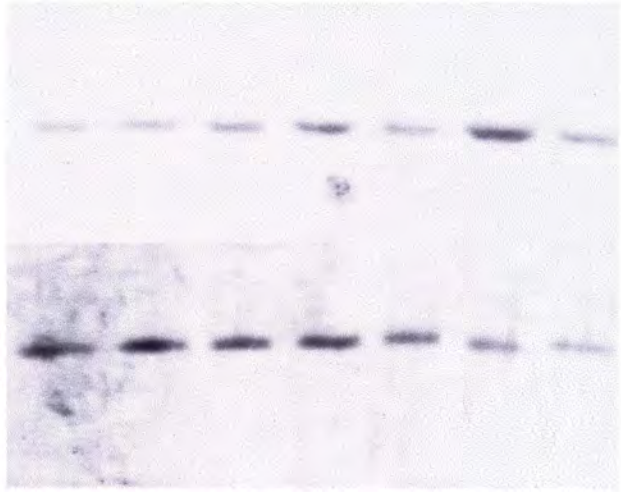
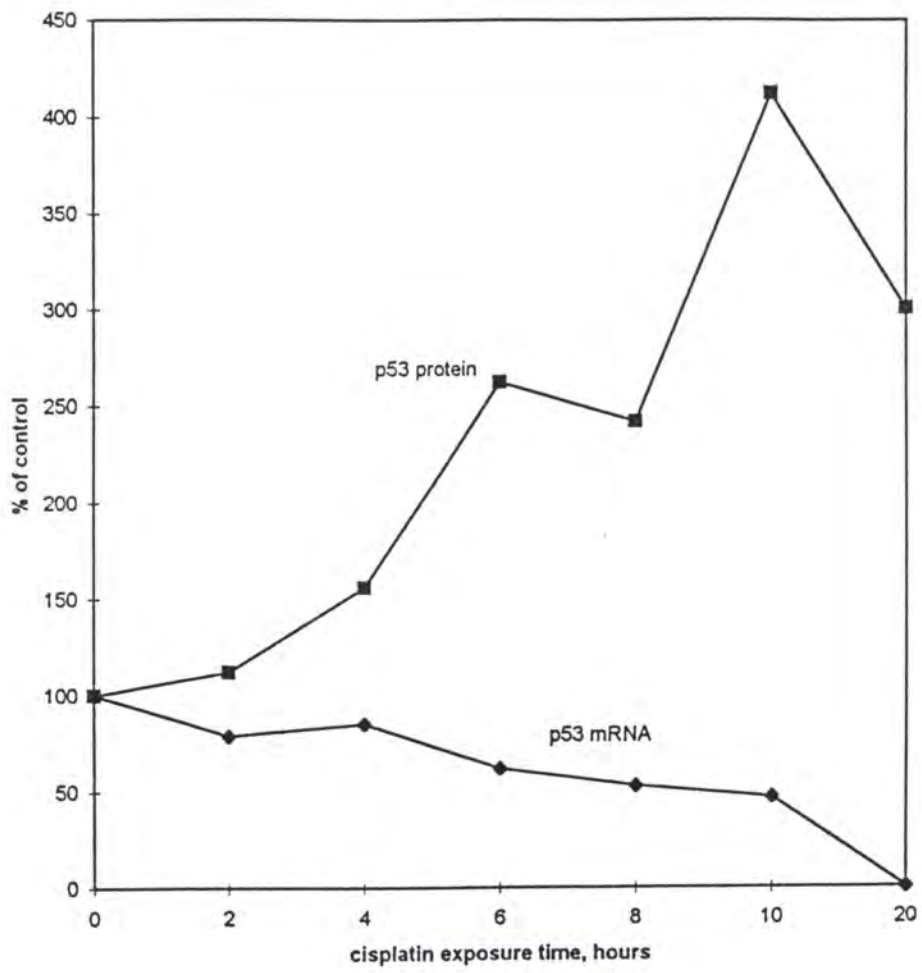


**Figure 9.** Comparative Quantification of p53 mRNA and protein in CMN-1 and CCSK-BG1 cell cultures. **A,** Quantification of p53 mRNA and protein over twenty hours of cisplatin exposure in CMN-1 cells. **B,** Quantification of p53 mRNA and protein over twenty hours of cisplatin exposure in CCSK-BG1 cells. Quantification was performed using Adobe Photoshop Version 4.0 software.

A.



B.

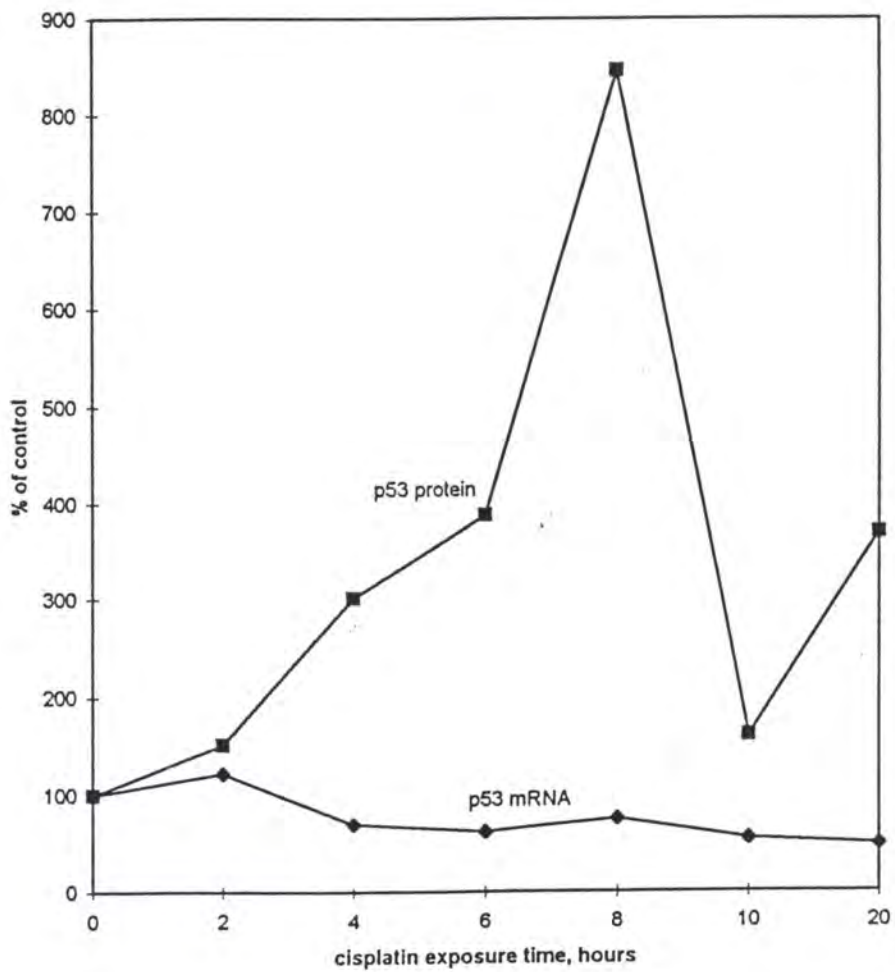
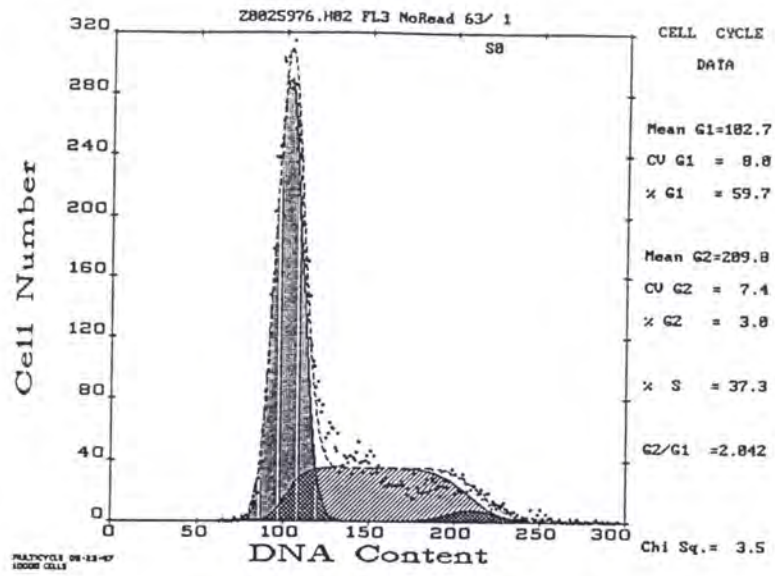
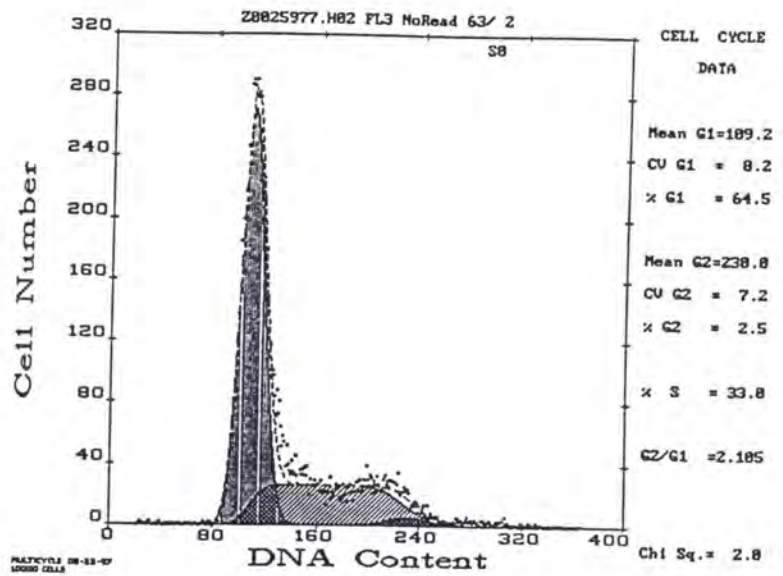


**Figure 10.** Flow cytometric cell cycle analysis of CMN-1 cells exposed to cisplatin over four hours. Relative DNA content and cell number represent the x- and y- axes, respectively. Percentage of cells in each phase of the cell cycle are noted at the right of each histogram. **A**, Control, CMN-1 cells receiving no cisplatin. **B**, CMN-1 cells treated for two hours with cisplatin. **C**, CMN-1 cells treated for four hours with cisplatin.

A.



B.



C.

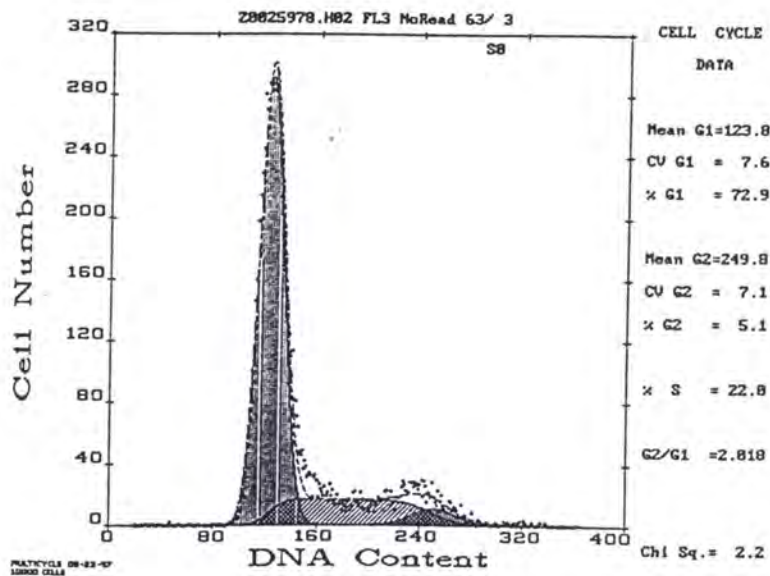
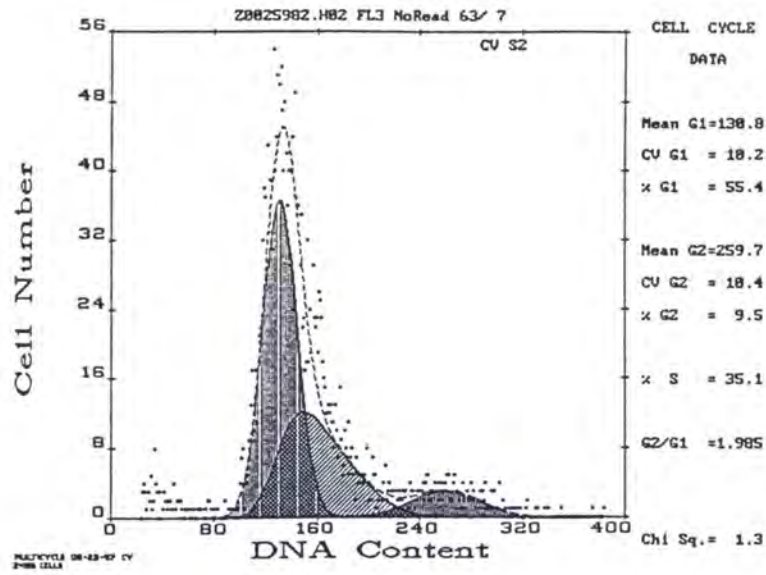
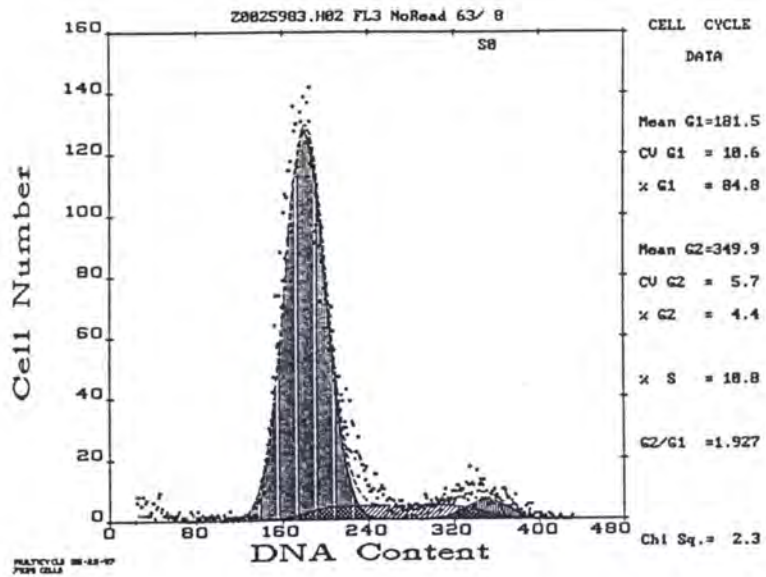


**Figure 11.** Flow cytometric cell cycle analysis of CMN-2 cells exposed to cisplatin over four hours. Relative DNA content and cell number represent the x- and y- axes, respectively. Percentage of cells in each phase of the cell cycle are noted at the right of each histogram. **A**, Control, CMN-2 cells receiving no cisplatin. **B**, CMN-2 cells treated for two hours with cisplatin. **C**, CMN-2 cells treated for four hours with cisplatin.

A.



B.



C.

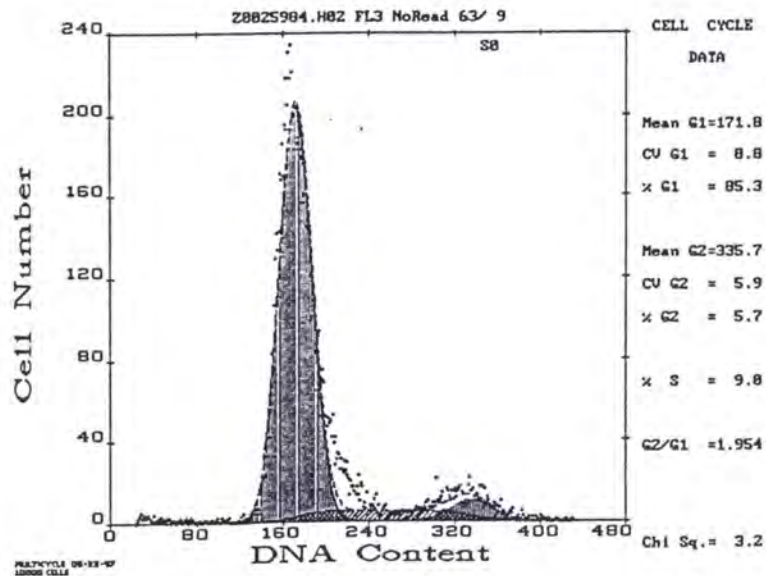
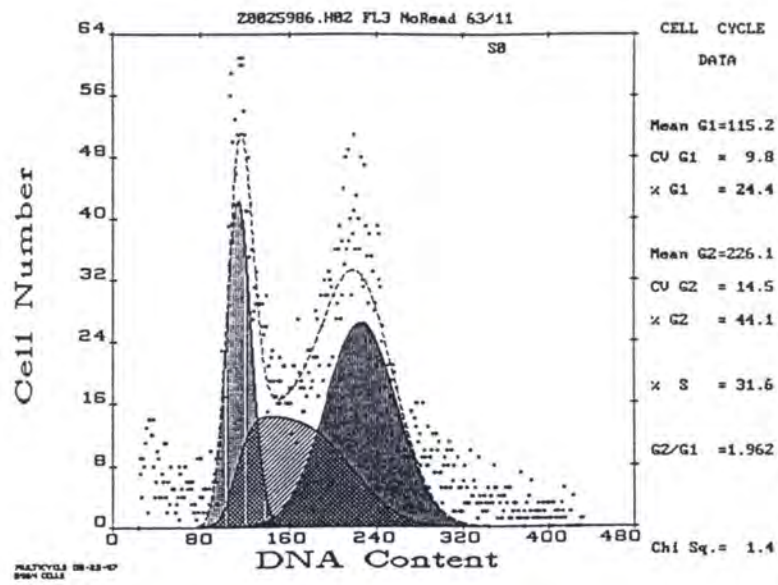


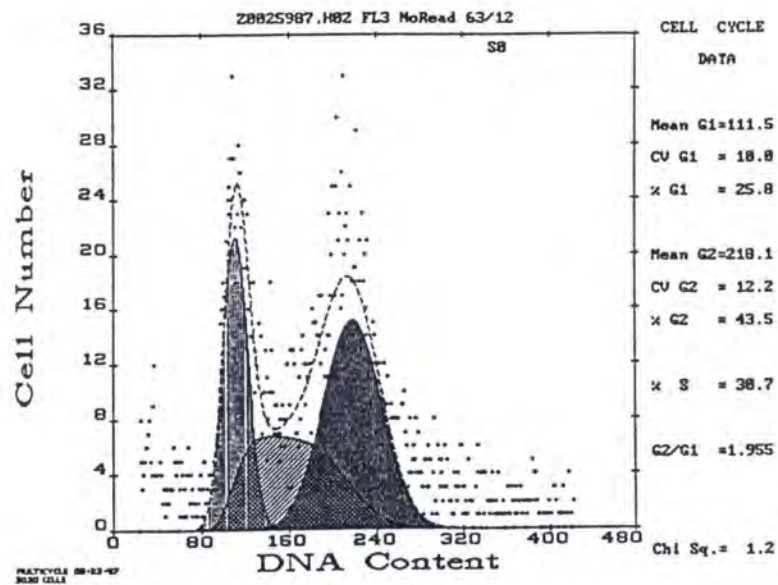


**Figure 12.** Flow cytometric cell cycle analysis of the p53 null, anaplastic Wilms' tumor W4 cells exposed to cisplatin over four hours. Relative DNA content and cell number represent the x- and y- axes, respectively. Percentage of cells in each phase of the cell cycle are noted at the right of each histogram. **A**, Control, W4 cells receiving no cisplatin. **B**, W4 cells treated for two hours with cisplatin. **C**, W4 cells treated for four hours with cisplatin.

A.



B.



C.

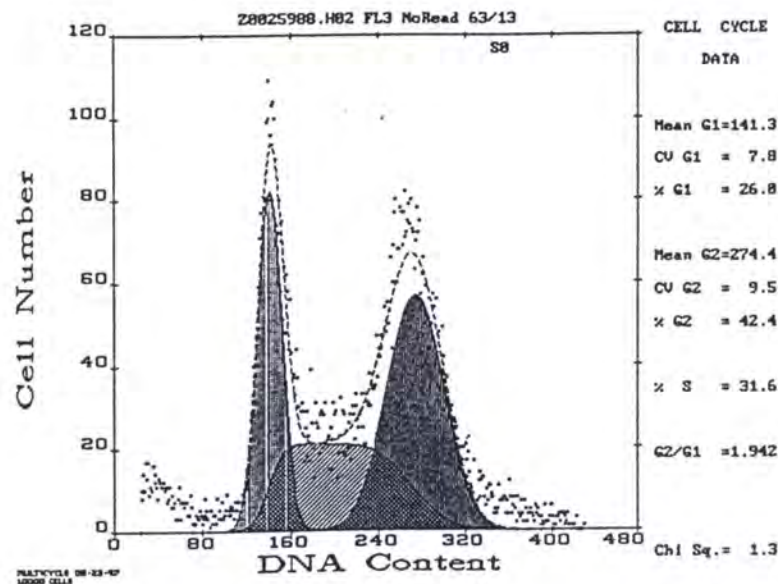


**Figure 13.** Northern analysis of p53, p21, MDM-2, MDR-1, and GAPD mRNA in CCSK primary tumor specimens. Tumor sample identity is noted above each lane. Genes evaluated are noted at the left of each blot. An ethidium bromide stained gel is included to document RNA integrity. KB-V1 is a epidermoid carcinoma cell line known to contain amplified copies of the multidrug resistance gene, MDR-1. SJSA-1 is a pluripotential sarcoma cell line with documented MDM-2 amplification. The presence of p53 and p21 mRNA is noted in all CCSK examples with no evidence of gene rearrangement. CC-50013 (lane 3) contains a degraded RNA sample and is non-informative. There is no evidence of MDM-2 or MDR-1 amplification or overexpression in any CCSK sample evaluated. Hybridization with a cDNA probe specific for GAPD was included to ensure for gel loading efficiency.

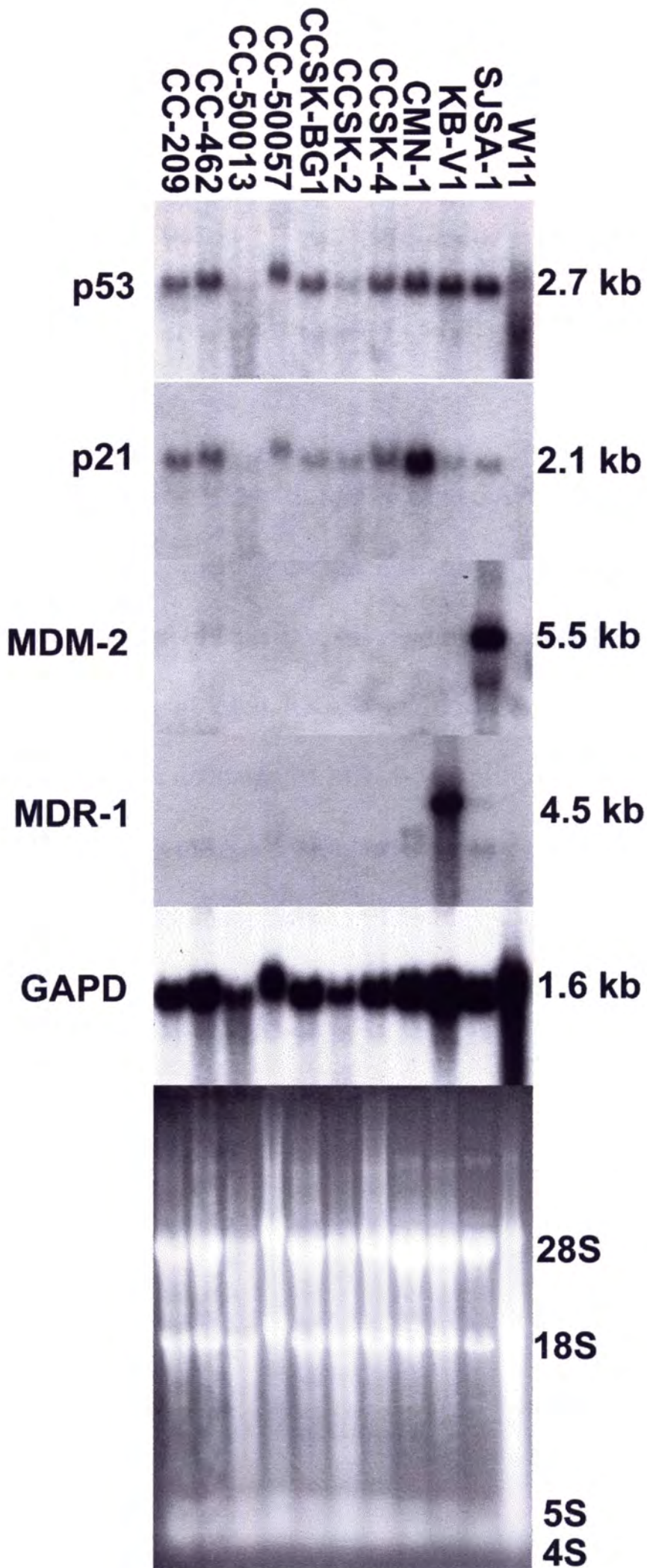


**Figure14.** Northern analysis of p53, p21, MDM-2 and GAPD in cellular (ce) and classical (cl) CMN primary tumor specimens. Tumor specimen identity is noted above each lane. Genes evaluated are listed to the left of each blot. An ethidium bromide gel is included at the bottom to document the integrity of each RNA sample. SJSA-1 mRNA was derived from a pluripotential sarcoma with documented MDM-2 amplification. Both cellular and classical CMN contain p53 and p21 mRNA with no evidence of gene rearrangement. There is no evidence of MDM-2 amplification or overexpression in CMN primary tumors. Hybridization with a GAPD cDNA probe was included to ensure for gel loading efficiency.

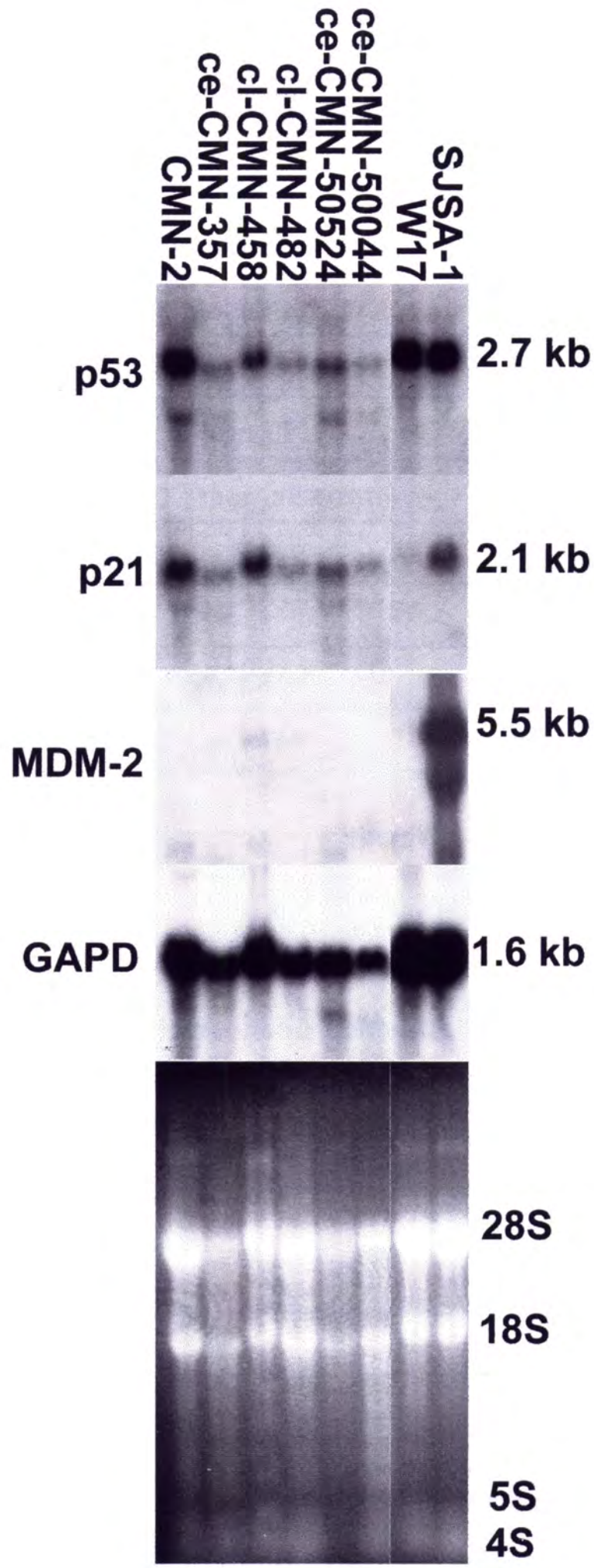


**Table 1A. Immunohistochemical Results on Frozen CCSK Primary Tumor Specimens Stained with p53 monoclonal antibody (DO-7)**

<b>Tumor Specimen Case ID</b>	<b>Tumor Stage</b>	<b>p53 Immunoreactivity</b>
CC-209	Stage I	-
CC-236	Stage II	-
CC-462	Stage III	-
CC-50057	Stage unknown	-
CC-50113	Stage II	-
ceCMN-357	Stage I	-
clCMN-458	Stage I	-
clCMN-482	Stage II	-
ceCMN50044	Stage I	-
ceCMN50524	Stage I	-
esophageal squamous cell carcinoma	Stage unknown	+++

**Table 1B. Summary of p53 Immunohistochemical and Gene Structure Data for CCSK and CMN Cell Cultures, Paraffin Embedded Primary Tumor, and Xenograft Tissue**

<b>Cell Culture</b>	<b>p53 immunochemistry cells</b>	<b>p53 immunochemistry paraffin</b>	<b>p53 gene structure</b>
CCSK-1	+/-	-	N/D
CCSK-2	-	-	wild-type
CCSK-3	-	-	N/D
CCSK-BG1	-	-	N/D
CMN-1	++	-	wild-type
CMN-2	++	+/-	wild-type
W4 anaplastic	-	-	point mutant
W16 anaplastic	++++	++++	point mutant

**Table II. Flow Cytometric Cell Cycle Analysis of Cisplatin Treated CMN and Anaplastic Wilms' Tumor Cells (G1 = G1 phase of the cell cycle)**

<b>Cell Line</b>	<b>p53 Immunoreactivity</b>	<b>p53 gene status</b>	<b>% cells in G1 untreated</b>	<b>% cells in G1 2 hours</b>	<b>% cells in G1 4 hours</b>
<b>CMN-1</b>	positive	wild-type	59.7	64.5	72.0
<b>CMN-2</b>	positive	wild-type	55.4	84.8	85.3
<b>W4(anaplastic)</b>	negative	mutant	24.4	25.8	26.0



## **Chapter 5**

### **Steady State and Retinoic Acid Induced Gene Expression Analysis of Clear Cell Sarcoma of the Kidney and Congenital Mesoblastic Nephroma: A Model For Tumor Histogenesis**

## **I. Introduction**

Pediatric renal tumors represent one of the most common abdominal tumors affecting young children and have long been interpreted as aberrations of normal nephrogenesis (Gonzalez-Crussi, 1984). These neoplasms may be subclassified based upon their clinical behavior, their association with genetic syndromes, cytogenetic lesions, and distinctive histological characteristics (Murphy *et al.*, 1994). By far the most common childhood renal tumor, Wilms' tumor, or nephroblastoma, is most readily recognized as a developmental anomaly. These tumors are often characterized by their classical, triphasic histology which includes disorganized, immature tubular elements, blastema, and stromal tissue, or different combinations of the three latter cell types, structures which are also evident in the developing fetal kidney. Because of the close parallel in the cellular architecture between Wilms' tumor and fetal kidney tissue, it has been suggested that tumorigenic events probably occur during key points in the development of the kidney (Re *et al.*, 1994). In contrast to the relatively straightforward interpretation of Wilms' tumor histogenesis, the origins of other renal tumors of childhood are more subtle. One example is clear cell sarcoma of the kidney (CCSK) which was first delineated from Wilms' tumor in several reports dating to the 1970s (Kidd, 1970; Beckwith *et al.*, 1978). CCSK, which accounts for approximately 5% of all renal tumors of children, has Wilms' tumor distinguishing clinicopathologic features including a delicate chromatin pattern creating empty-appearing nuclei, prominent hyalinization, and a propensity for the development of bone metastases, a characteristic which sharply contrasts the usual

favorable outcome of most Wilms' tumors (Murphy *et al.*, 1994). Although the histogenetic origin of this tumor is unknown, some have suggested that it may arise from renal medullary interstitial, mesangial, endothelial, or blastemal cap cells (Beckwith *et al.*, 1978; Haas *et al.*, 1984). Authors of these same reports also speculated that CCSK may represent the malignant counterpart of the relatively benign, congenital mesoblastic nephroma (CMN) (Beckwith *et al.*, 1978). Compared to CCSK, CMN is a relatively benign tumor first described by Bolande which primarily affects neonates as the vast majority of cases are diagnosed in the first three months of life (Bolande *et al.*, 1967; Wigger, 1969). Like CCSK, CMN accounts for 5% of all childhood renal malignancies and is the most common abdominal tumor of neonates. CMNs may be further subdivided into two categories based upon their histology and clinical behavior: the classical and the more common and potentially more aggressive cellular CMN (Murphy *et al.*, 1994; Joshi *et al.*, 1986). Like CCSK, the developmental origin of CMN is unresolved even though its histological appearance suggests that it is a neoplasm of fibroblasts or myofibroblasts (Parham, 1996). Hypotheses regarding the histogenesis of both CMN and CCSK are primarily based upon electron microscopic studies and immunohistochemistry (Haas *et al.*, 1984; Kumar *et al.*, 1986; Pettinato *et al.*, 1989). To date, the gene expression profile of CMN and CCSK have not been completely evaluated in the context of the genetic basis of normal kidney development.

The development of the metanephros, or functioning adult kidney, occurs via reciprocal inductive events between the metanephric mesenchyme and the ureteric bud (Saxen, 1987). As development proceeds, metanephric mesenchyme differentiates into most structures of the nephron including the glomerulus and tubules. The ureteric bud, instead,

forms elements of the renal collecting duct system and the Columns of Bertin. With the introduction of molecular biological techniques, a large and varied array of genes which control normal kidney development have been identified (Lechner *et al.*, 1997).

WT-1 is a well recognized example. WT-1 is a zinc finger tumor suppressor gene that is deleted or mutated in Wilms' tumors and responsible for proper formation of the urogenital system (Call *et al.*, 1990; Kreidberg *et al.*, 1993). WT-1 expression is induced in metanephric mesenchyme following ureteric bud induction and remains expressed at high levels throughout the comma-shaped and S-shape stages of nephron formation. In the adult, WT-1 is only expressed in glomerular podocytes. WT-1 expression is also highly expressed in many Wilms' tumors, particularly in areas of blastema and tubular differentiation suggesting that Wilms' tumors are derived from areas of induced, condensing renal mesenchymal tissue (Pritchard-Jones *et al.*, 1991). Two previous reports demonstrated the absence of WT-1 transcripts in two cases each of CCSK and CMN (Yun, 1993; Tomlison *et al.*, 1992).

The WT-1 transcription factor mediates the expression of several key genes involved in fetal tissue growth and pediatric neoplasia including *IGF-2*. *IGF-2* is overexpressed in many pediatric tumor types (Reeve *et al.*, 1985). Interference of IGF-2 binding with its cognate receptor, IGF-1R, by the use of a monoclonal antibody specific for the receptor inhibits the growth of Wilms' tumors in vitro and in vivo (Gansler *et al.*, 1989). The latter suggests the importance of an IGF-2 autocrine growth loop in Wilms' tumor cell proliferation. Detection of an IGF-2 binding protein, BP-2, has also been described in Wilms' tumor cells, although the modulatory role that this protein plays in Wilms'

tumorigenesis or its role in IGF-2 mediated autocrine growth is unresolved (Vincent *et al.*, 1994). In other cell systems, BP2 has been reported to both inhibit and potentiate cell growth depending upon the cell system employed (Jones *et al.*, 1995).

Pax-2 and Pax-8 are both paired box class transcription factors that are expressed in two partially overlapping, asynchronous waves during nephrogenesis. Pax-2, like WT-1, is induced following ureteric bud induction and persists throughout the early stages of nephrogenesis (Dressler *et al.*, 1990). In contrast, Pax-8 is expressed at a later stage, as it remains expressed in the S-shaped body (Poleev *et al.*, 1992). Like WT-1, expression of Pax-2 and Pax-8 is a marker of induced metanephric mesenchyme; cells of the stromal lineage, presumably cells not receiving inductive signals, do not express WT-1, Pax-2, or Pax-8. The expression pattern of the normal kidney closely parallels findings in Wilms' tumor. WT-1, Pax-2, and Pax-8 are expressed in both blastema and areas of tubular differentiation in Wilms tumors, but not in stromal areas, as assessed by *in situ* hybridization (Eccles *et al.*, 1995).

WT-1, Pax-2, and Pax-8 are all markers for renal tubules and the non-vascular glomerulus of the developing nephron. Very few markers have been identified for the developing renal stroma, or interstitium (Ekblom *et al.*, 1991). Tenascin, a mesenchymal extracellular matrix protein, is expressed in areas of dense mesenchymal tissue immediately surrounding differentiating epithelium, a pattern which is consistent with that this protein is critical for normal mesenchymal to epithelial transformations in several developing organs, including the kidney (Chiquet-Ehrismann *et al.*, 1986). Tenascin expression was absent from the uninduced mesenchyme and cells undergoing epithelial differentiation in developing

mouse kidney (Aufderheide *et al.*, 1987). The latter study also reported persistence of tenascin expression in the medullary renal interstitial areas with loss of expression in renal cortical areas after nephrogenesis ceased. Others have demonstrated that tenascin immunoreactivity is also detectable in the glomerular mesangium with increased amounts noted in glomerulopathies and interstitial nephritides (Koukoulis *et al.*, 1991). Therefore, these data suggest that tenascin may provide one of the few known markers for a better understanding of pediatric renal tumor histogenesis, particularly those with hypothesized stromal origins.

The newly described marker of renal stroma, the winged-helix transcription factor BF-2, will also aid in the evaluation of both normal stromal development and the formation of pediatric renal tumors (Hatini *et al.*, 1996).

The use of differentiation agents such as all-trans retinoic acid (atRA) has been useful in understanding the pathobiology and histogenesis of a variety of tumor types including neuroblastoma and promyelocytic leukemia (Wada *et al.*, 1992; Brietman *et al.*, 1980). AtRA induces differentiation in cells by binding to nuclear Retinoic Acid Receptors (RAR) which are capable of homo- and heterodimerization with retinoid X-receptors. Among the effects of atRA on gene expression, is its potent induction of several RAR isoforms including RAR- $\alpha$  during differentiation (Leroy *et al.*, 1991) Subsequently, these receptors bind to retinoic acid response elements (RARE) in target genes (Leid *et al.*, 1992). Among other genes, expression of cell cycle regulatory genes p53 and p21 are also affected upon atRA treatment (Dony *et al.*, 1985; Liu *et al.*, 1996). Because Vitamin A derivatives including atRA have previously described utility in inducing differentiation in metanephros organ culture (Vilar

*et al.*, 1996) and in other pediatric tumors including neuroblastoma, this differentiation agent was chosen to test the hypothesis that CCSK, CMN, and Wilms' tumors are each derived from precursor cells at different renal developmental stages.

In this report, we have evaluated the expression profile of WT-1, Pax-2, Pax-8, IGF-2, BP-2, and tenascin using northern analysis in a series of CCSK and CMN primary tumors as a means of beginning to understand the histogenesis of these neoplasms in relation to Wilms' tumor. Furthermore, we have treated CCSK and CMN cell cultures with *all-trans* retinoic acid, evaluated changes in gene expression, and correlated these changes with morphological alterations assessed by transmission and electron microscopy.

## **II. Results**

### **1. Expression of Genes Involved in Normal Nephrogenesis in CCSK and CMN Primary Tumors**

A series of CCSK (Figure 1) and CMN (Figure 2) primary tumors was examined for tenascin, WT-1, Pax-2, Pax-8, IGF-2, and BP-2 gene expression using northern analysis. Tenascin was expressed at low levels in 3/7 CCSK tumors. In contrast, tenascin mRNA was expressed at high levels in both cellular and classical CMN tumors. Tenascin expression was undetectable in an epithelial anaplastic Wilms' tumor (W17) (Figure 2) and in the KB-V1 epidermoid carcinoma cell line. Tenascin was expressed in a triphasic classical Wilms' tumor W11 (Figure 1). SJSA-1 pluripotential sarcoma cells were included as an independent comparison in both panels and expressed low levels of tenascin mRNA (Figure 1&2). Expression of WT-1 was absent in 100% of all CCSK primary tumors examined. In contrast, WT-1 mRNA was detectable in 3/6 CMN tumors (1 classical and 2 cellular tumors). Both W11 and W17 tumors expressed WT-1 message. Pax-2 was variably expressed in 3/7 of CCSK and 1/3 of CMN tumors examined. Both Wilms' tumors W11 and W17 were included as positive controls for Pax-2 expression. Pax-8 mRNA was detected in one CCSK and two CMN tumors. IGF-2 and BP-2 were highly expressed in CCSK, CMN, and WT examined with rare exception. Hybridization with a GAPD cDNA probe was included as an indicator of constitutive gene expression.

### **2. Phase Contrast Microscopy of atRA Treated CCSK and CMN Tumor Cells**

To attempt to understand the cellular origin for these rare renal neoplasms of childhood, cultured tumor cells were treated with the morphogen atRA for three days in a



dark incubator. Figure 3 illustrates the light microscopic characteristics of CCSK-2 and CCSK-BG1 tumor cell cultures treated with 1  $\mu$ M atRA. Both untreated cell cultures demonstrated round to spindle shaped morphology. atRA treated cell cultures exhibited focal areas of close cellular clumping, in some instances forming mounds (Figure 3D). CCSK-2 cultures also formed clusters of closely juxtaposed cells. Untreated CCSK-2 and CCSK-BG1 cell cultures were also noted to contain foci of closely opposed cells upon re-examination, however, indicating that the light microscopic features of these cells were not due to atRA exposure alone.

Concurrent experiments treated SK-N-SH neuroblastoma cells and both CMN-1 and CMN-2 cells with 1  $\mu$ M atRA (Figure 4). SK-N-SH cells exhibited the formation of interlacing neurite structures after 72 hours of atRA treatment indicating that neuroblastoma cells were induced to differentiate. In contrast, there was no light microscopic indication of cellular differentiation in either of the CMN cell cultures examined. Both cell cultures maintained a rounded spindle shaped morphology during the experiment. CMN-2 cells continued to grow in the presence of atRA as indicated by their increased cellular confluency.

### **3. TEM and SEM Analysis of atRA Treated CCSK and CMN Cell Cultures**

The same atRA treated cell cultures of CCSK-2 and CMN-1 photographed using phase contrast microscopy were fixed for TEM and SEM analysis. Untreated CCSK-2 cells demonstrated cells growing in multiple layers by TEM (Figure 5A) whereas those cells exposed to atRA for three days exhibited marked cellular interdigitation (Figure 5B). There was no apparent signs of intracytoplasmic organellar composition or development of intracellular filaments in treated versus untreated tumor cells. Furthermore, indications of

epithelial differentiation including the development of cell polarity was not found. To better visualize the three dimensional affects of atRA on morphology, CCSK-2 tumor cells were examined using SEM. Whereas the untreated cells demonstrated cells with a dome-shaped morphology intermixed with flatter cells, atRA exposed cells were tightly opposed and flattened (Figure 5 C&D).

CMN-1 cells treated with atRA exhibited marked cellular changes by TEM and SEM analysis that were not apparent using phase microscopy alone (Figure 6). CMN-1 cells that were not treated with atRA grew in sheets of cells that were not closely juxtaposed. Upon three days exposure to atRA, CMN-1 cells became closely interdigitated and flattened leaving little intercellular space (Figure 6 B&D). As in CCSK-2 cells, there was no evidence of intracellular organellar change or development of intermediate filaments in CMN-1 cells.

#### **4. atRA Induced Gene Expression Alterations in CCSK and CMN Cells**

Total cellular RNA was extracted from CMN-1, CMN-2, CCSK-2, CCSK-BG1, and SK-N-SH neuroblastoma atRA treated cell lines were evaluated for alterations in mRNA expression for genes that are important for normal nephrogenesis using northern analysis (Figures 7-10). atRA exposed CCSK-2, but not CCSK-BG1 cells exhibited induction of both tenascin and Pax-2 mRNA over a 48 hour time period. W17 and W16 anaplastic Wilms' tumor cells were included as a positive control for Pax-2 mRNA. IGF-2 mRNA levels initially increased in SK-N-SH neuroblastoma cells before declining at 72 hours. Neither CCSK-2 nor CCSK-BG1 cells revealed IGF-2 mRNA differences over 48 and 72 hours of atRA exposure, respectively. RAR- $\alpha$  gene expression was induced in SK-N-SH neuroblastoma cells over 48 hours before declining at 72 hours. CCSK-2 cells demonstrated

no significant RAR- $\alpha$  induction over 48 hours. In contrast, CCSK-BG1 cells revealed induction of the 3.5 kb RAR- $\alpha$  transcript over 72 hours with a concomitant decrease in a transcript migrating at 2.3 kb. There was no apparent change in p53 gene expression in any of the atRA treated cell cultures. Furthermore, there was no significant changes in p21 expression in either CCSK-2 or CCSK-BG1 cells, but a significant increase was noted in SK-N-SH cells at 48 hours of atRA exposure.

CMN-1, but not CMN-2 cells treated with atRA exhibited several gene expression alterations over 72 hours. In contrast to CCSK-2 cells, tenascin mRNA decreased in CMN-1 cells with a concurrent induction of Pax-2 mRNA (Figures 9-10). IGF-2 and BP-2 mRNA levels remained stable in CMN-1 cells through 48 hours before declining at 72 hours. RAR- $\alpha$  mRNA was induced in the first 48 hours in CMN-1 cells before declining at 72 hours. Similar to the findings in CCSK cell cultures, both CMN cultures did not reveal any changes in p53 gene expression. p21 message, in contrast, was induced in SK-N-SH and declined at 72 hours in CMN-1 cells. Hybridization of RNA to a GAPD cDNA fragment was included as a control for constitutive gene expression. A model for the histogenetic origin of Wilms' tumor, CMN, and CCSK is presented in Table 11. This model is based on the steady-state and atRA induced gene expression profile of genes expressed during normal nephrogenesis. The hypothesized origins for these tumors are noted.

### III. Discussion

Current understanding of the histogenesis of pediatric renal tumors has been largely based upon light and electron microscopy and immunohistochemical studies (Haas *et al.*, 1984; Kumar *et al.*, 1986; Pettinato *et al.*, 1989). These reports have supported the distinction of CCSK and CMN from Wilms' tumors and other childhood renal tumors. However, studies have not evaluated a sufficient number of cases to be meaningful due to the relative rarity of both neoplasms. Furthermore, the study of the cellular origin of these tumors has been hindered by the lack of an experimental model to test current CCSK and CMN histogenetic hypotheses. In the present study, we were able to evaluate a large series of CCSK and CMN primary tumors for mRNA expression of genes controlling the normal nephrogenic program, such as WT-1 Pax-2, and tenascin, in an effort to build a working model of the developmental origin of these neoplasms. Furthermore, both tumors were evaluated for morphological and gene expression alterations after treatment with the morphogen atRA in an *in vitro* differentiation assay.

Previous molecular biological analysis of CCSK and CMN has been limited. Two independent studies reported that CCSK and CMN expressed the fetal mitogen IGF-2 and not the Wilms' tumor suppressor gene, WT-1 (Yun, 1993; Tomlison *et al.*, 1992). In the present study, WT-1 was not expressed in 7 CCSK primary tumors examined, although WT-1 message was detected in three CMN tumors. In addition, WT-1 expression was previously detected in two CMN nude mouse xenografts. The latter represents the first reported expression of WT-1 in this tumor type. Unlike WT-1, IGF-2 and the IGF-2 binding protein BP-2 were highly expressed in both CCSK and CMN supporting an embryological origin of

these tumors. Further analysis of CCSK and CMN primary tumors revealed Pax-2 expression in selected tumor specimens. The latter contrasts with previous reports of one CCSK and one CMN which indicated no expression of Pax-2 or Pax-8 and other reports which demonstrated Pax-2 and Pax-8 expression in Wilms' tumors and in induced mesenchyme (Tagge *et al.*, 1994; Dressler *et al.*, 1992; Poleev *et al.*, 1992). The observation of both WT-1 and Pax-2 mRNA in some CMN and Pax-2 mRNA in selected CCSK has two alternative explanations. Firstly, the presence of Pax-2 mRNA may be explained by entrapped normal kidney glomeruli embedded within tumor tissue (glomerular podocytes express WT-1 postnatally). However, this explanation does not explain WT-1 expression in cellular CMN xenografts analyzed previously since normal kidney tissue does not grow in nude mice. Alternatively, this data may indicate that CMN tumors are derived from mesenchymal cells in close juxtaposition with the condensing mesenchyme that receive inductive signals from the ureteric bud. Pax-2 expression in CCSK may be further indicative of the pluripotential nature of CCSK cells (i.e. their ability to differentiate into cells of tubulogenic potential). Previous histological analysis of the three Pax-2 mRNA positive CCSK did not demonstrate evidence of epithelial differentiation, however.

To clarify these results, CCSK and CMN were analyzed for tenascin mRNA expression, a marker of cells surrounding the condensing renal mesenchyme and interstitial cells (Ekblom *et al.*, 1991; Aufderheide *et al.*, 1987; Truong *et al.*, 1996). Tenascin expression was extremely high in all CMN tumors examined and contrasted with the variable and low tenascin mRNA content of CCSK. These data provides molecular evidence for the origin of CMN in the uninduced renal mesenchymal tissue that is destined to become the

interstitium of the kidney. Expression of tenascin in some CCSK further suggests the possibility of its differentiation along multiple differentiation pathways including the stromal lineage. The absence of WT-1, Pax-2, and tenascin expression in the majority of CCSK cases also supports the notion that this tumor arises in primitive, uncondensed renal mesenchyme.

atRA is a well characterized inducer of neural cell differentiation in neuroblastoma cells (Robson *et al.*, 1985) Due to this previously described utility of atRA, CCSK and CMN cell cultures were treated with the differentiation agent atRA to evaluate morphological and gene expression alteration. SK-N-SH neuroblastoma cells exhibited the characteristic formation of neurites by light microscopy in atRA exposed cells. However, phase microscopic analysis of CCSK and CMN failed to demonstrate specific changes in cultures that received retinoic acid similar to previous reports of an atRA treated Wilms' tumor (Vincent *et al.*, 1996). Both treated and untreated CCSK cultures, however, exhibited focal areas of close cellular opposition and cell clumping interspersed with flat stromal cells consistent with multipotential differentiation of CCSK. CMN cells, in contrast, did not reveal any light microscopic evidence of epithelial differentiation. However, TEM and SEM analysis of both cell types treated with retinoic acid demonstrated marked changes in cellular arrangement without any effect on intracytoplasmic ultrastructural features. Both CCSK and CMN cultures exhibited marked cellular flattening and close cell juxtaposition in samples treated for three days with atRA. The latter cultures provided no evidence of epithelial differentiation in either tumor type as cell polarity, tight junctions, and rounded morphology were not identified. These results, then, are consistent with fibroblastic or smooth muscle

differentiation of CMN and CCSK. Previous studies in this laboratory identified smooth muscle actin positivity in both the CCSK-2 and CMN-1 cultures used in this experiment. Future studies will include evaluating atRA induced changes in intermediate filament composition in these cells in order to further characterize the effects of this differentiation agent.

Cells which were evaluated morphologically were also evaluated for changes in gene expression after exposure to atRA. Gene expression alterations varied within and between the cell types, but included induction of tenascin and Pax-2 in CCSK-2 cells. In contrast, CMN-1 cells exhibited downregulation of tenascin mRNA with a concurrent induction of Pax-2 message. Tenascin induction in CCSK-2 cells provides further evidence for the origin of this tumor in the uninduced renal mesenchyme as atRA may have spurred these cells to differentiate into the interstitial lineage. The TEM and SEM and northern analysis data of CCSK-2 supports this hypothesis. In contrast to CCSK, CMN-1 cells exhibited downregulation of tenascin in their differentiated phenotype. atRA has been previously reported to induce tenascin expression in neuroblastoma cells and is consistent with our findings in CCSK-2, but not CMN-1 cells (Linnala *et al.*, 1997). Pax-2 induction in CCSK-2 and CMN-1 cells also suggests the origin of these tumors in the uninduced mesenchyme. In contrast to CCSK-2 and CMN-1, CCSK-BG1 and CMN-2 cells do not exhibit gene expression alterations after atRA exposure. The latter further illustrates the heterogenous and pluripotential characteristics of these tumors.

atRA has also been reported to modulate the expression of IGF-2 and BP-2 in neuroblastoma cell lines (Babajko *et al.*, 1996). For that reason, these genes were evaluated

for changes in our CCSK and CMN cells. No changes in IGF-2 mRNA levels were evident in CCSK cells. However, CMN-1 cells exhibited a downregulation of IGF-2 after 72 hours of treatment. In contrast, SK-N-SH cells included in this experiment induced IGF-2 mRNA at 48 hours supporting a previous report suggesting that IGF-2 induction is necessary for SK-N-SH neuronal differentiation (Ueno *et al.*, 1993). The lack of IGF-2 induction in CCSK and CMN cells of this study discounts the role of increased IGF-2 in the differentiation of these tumor cells. Downregulation of this gene in CMN-1 at 72 hours suggests a resting cellular phenotype that does not require IGF-2 expression. Further, the concurrent downregulation of BP-2 in CMN-1 cells lends support to the notion that BP-2 and IGF-2 function in tandem in these cells and that both are not needed, or are only required at low levels, to maintain the differentiated phenotype of these cells. This data does not discount the possible role of IGF-2 in the process leading to differentiation, however.

Finally, alterations in the expression of modulators of the cell cycle were also evaluated in these tumors. Previous reports have indicated that the cyclin-dependent kinase inhibitor, p21 is induced by retinoic acid exposure in hematopoietic and hepatoma cell lines and that this modulation of expression was mediated through RAR- $\alpha$  (Steinman *et al.*, 1994; Liu *et al.*, 1996). In our studies, p21 mRNA was not induced by atRA treatment in CCSK and CMN cells. However, p21 was induced in our control SK-N-SH cell line. In addition, the steady state level of p53 mRNA remained unchanged in CCSK and CMN cells. Uniquely, p21 mRNA declined at 72 hours in CMN-1 cells, possibly indicative of a resting cellular phenotype. Therefore, upregulation of the p21 and p53 gene in CCSK and CMN cells does not appear to be a requirement for differentiation. Again, this data does not rule out the



possibility of post-transcriptional or post-translational mechanisms leading to increased p53 or p21 stability as a means of atRA mediated differentiation of these tumor cells.

In summary, atRA treatment of CCSK and CMN cells caused dramatic morphological changes in both. These changes did not, however, demonstrate overt signs of epithelial differentiation in either tumor type. The distinct cellular flattening and close opposition of cells is more consistent with fibroblastic or smooth muscle cell differentiation. Gene expression alterations were variable in our tumor cell cultures, however, the changes noted may have implications for investigating the histogenesis and retinoic acid -mediated control of gene expression in these rare renal tumors of childhood in the future. Additionally, steady-state examination of gene expression for Pax-2, WT-1, and tenascin strongly suggest that CMN cells arise from secondary mesenchyme destined to become the renal interstitium due their high expression of tenascin mRNA. In contrast, our data suggests that CCSK cells are derived from more primitive, pluripotent loose mesenchymal tissue. Some may argue that CCSK and CMN arise from cells that have already been induced and lost certain gene expression characteristics (such as WT-1 expression) linked to the condensing mesenchymal phenotype. Previous studies using retroviral markers dismiss this notion, however In studies of the embryological rat kidney, induced mesenchymal cells differentiated into proximal and distal tubular cells and glomerular epithelium, not renal interstitium (Herzlinger *et al.*, 1992). Future study of the expression of the BF-2 transcription factor, a newly described marker of immature renal stroma (Hatini *et al.*, 1996) would be helpful in further discriminating, or linking, these two stromal tumors. Because CCSK and CMN sometimes resemble other renal neoplasms, information gleaned from the further study of the

histogenesis of these tumor types has implications for the proper diagnosis, and therefore, treatment of these tumor types in the future. Further, the biological basis for the development of the normal renal interstitium remains unknown. Therefore, the use of these stromal tumor cultures may be useful in elucidating mechanisms of normal nephrogenesis as well.

**Figure 1. A,** Northern analysis of genes relevant to normal nephrogenesis including tenascin-C, WT-1, Pax-2, Pax-8, IGF-2, BP-2, and GAPD in CCSK primary tumor tissue. Tumor specimens are noted above each lane of blots. A classical WT, W11 was included as a positive control for WT-1, Pax-2 and Pax-8. Hybridization with a GAPD cDNA fragment was included to evaluate gel loading efficiency. **B,** Ethidium bromide stained gel of total cellular RNA.

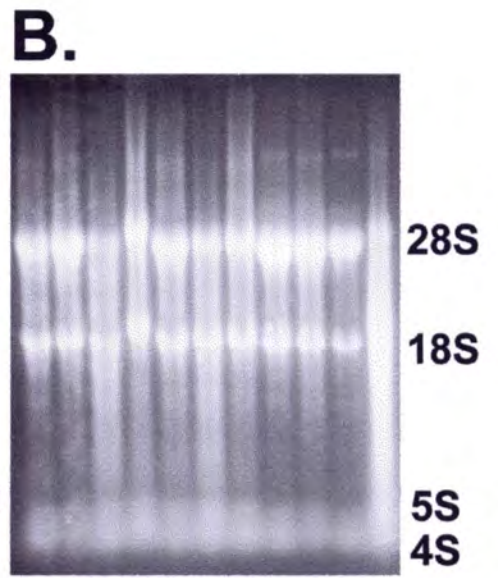
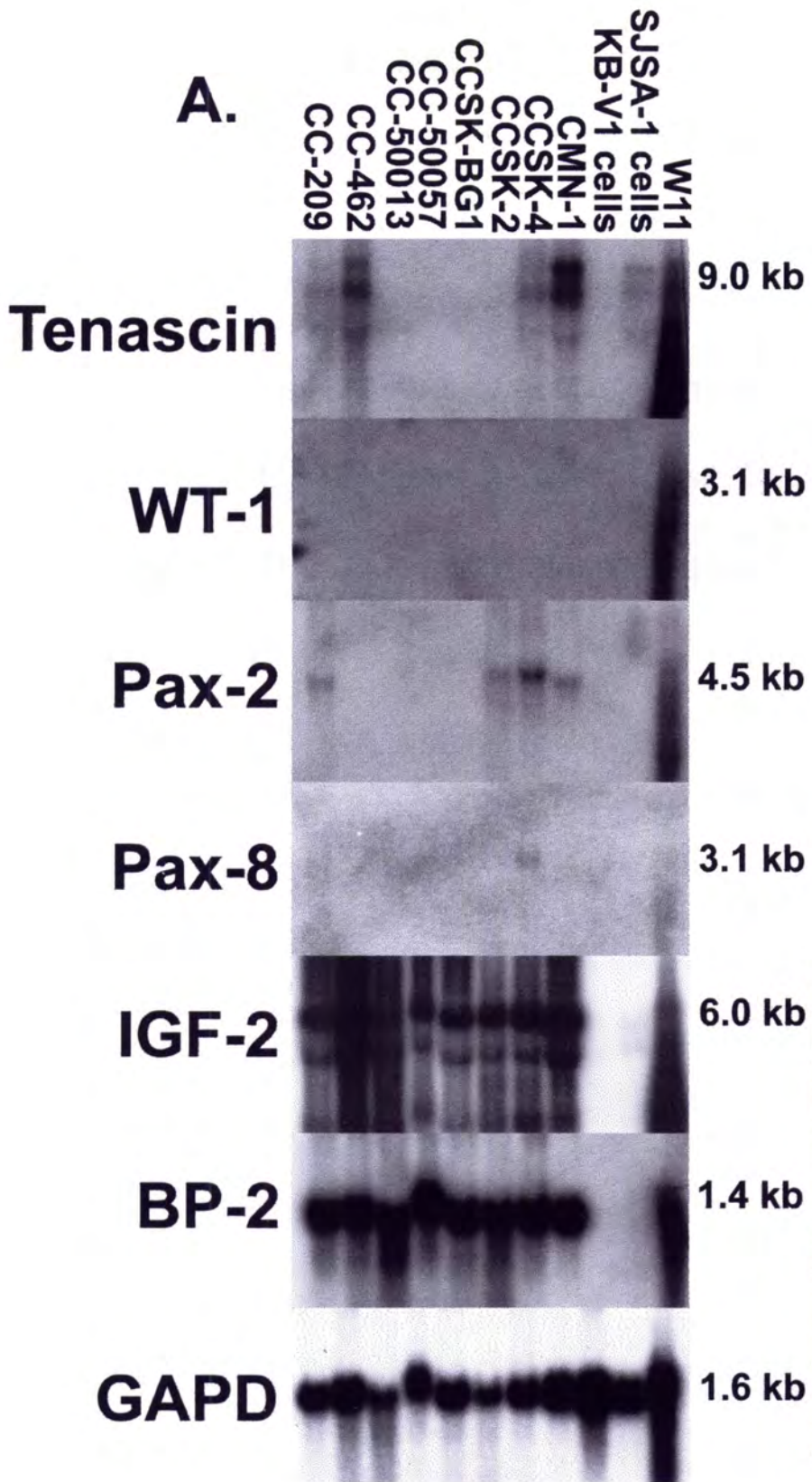


**Figure 2.** **A**, Northern analysis of developmentally coordinated genes of nephrogenesis including tenascin-C, WT-1, Pax-2, Pax-8, IGF-2, BP-2, and GAPD in a series of cellular (ce) and classical (cl) CMN primary tumors. anaplastic Wilms' tumor W17 was included as a positive control for WT-1, Pax-2, and Pax-8 mRNA. Hybridization with a GAPD cDNA fragment was included to ensure for equal loading efficiency. **B**, Ethidium bromide stained gel of total cellular RNA.

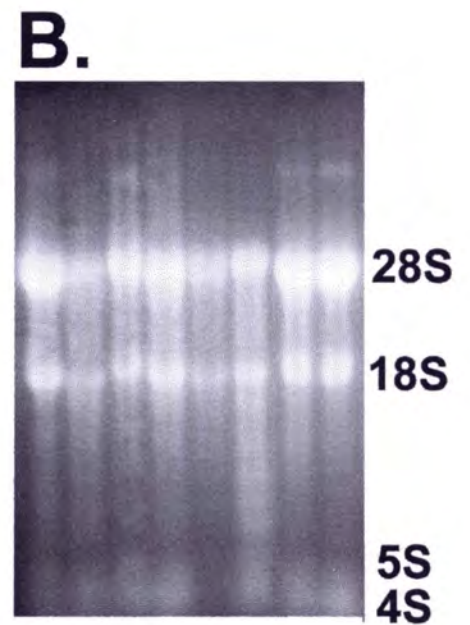
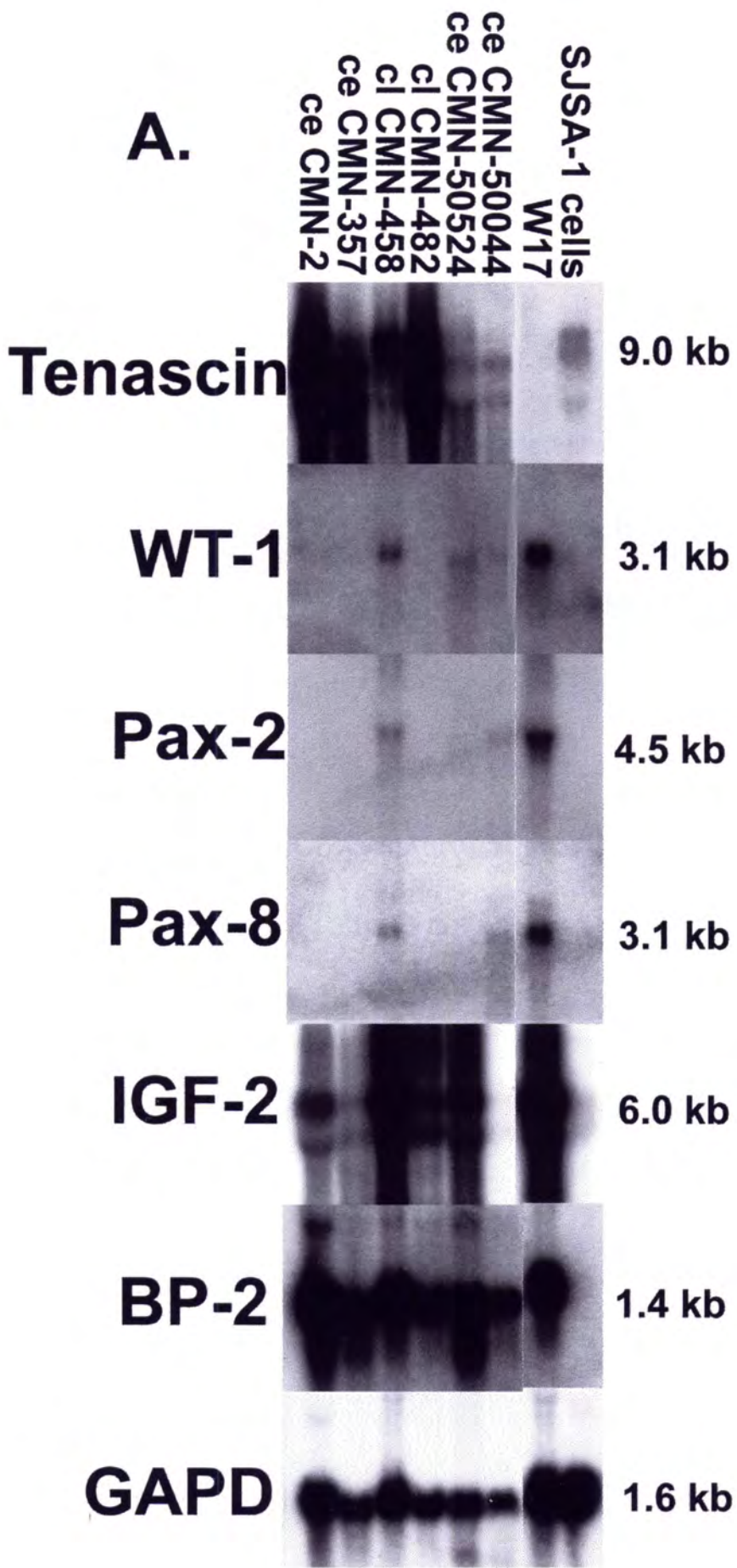


**Figure 3.** Phase micrographs of untreated and atRA treated CCSK primary cell cultures. **A**, phase micrograph of untreated CCSK-2 cells. **B**, CCSK-2 cells treated for 3 days with 1  $\mu$ M atRA. **C**, Untreated CCSK-BG1 cells. **D**, CCSK-BG1 cells treated for 3 days with 1  $\mu$ M atRA. Cells treated with atRA did not demonstrate marked differences at the light microscopic level after 3 days of retinoic acid exposure. Although B and D demonstrate close cell opposition in both CCSK cultures after atRA exposure, these findings were also found focally in primary cell cultures not exposed to atRA. All micrographs at 200X.

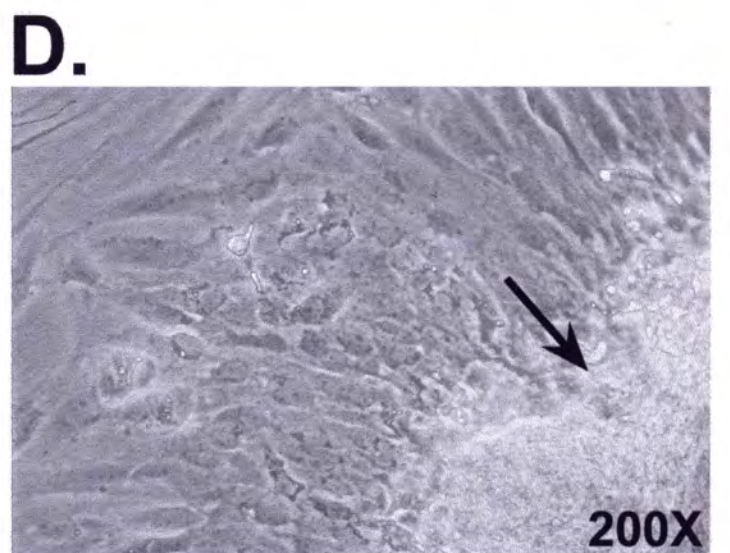
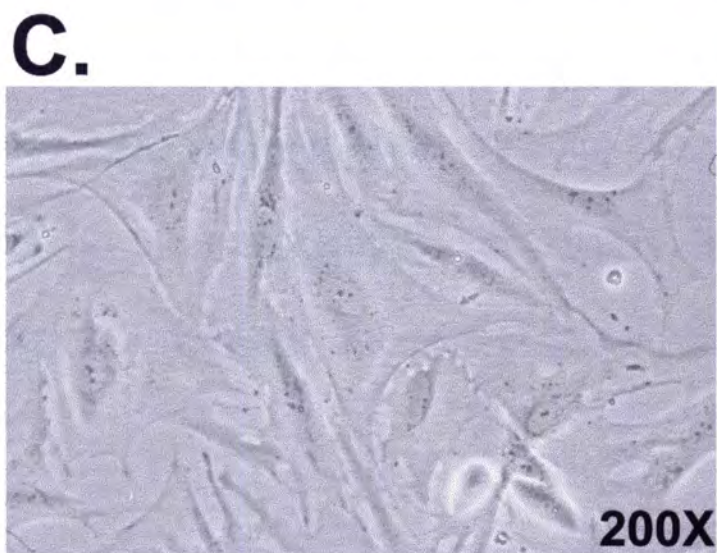
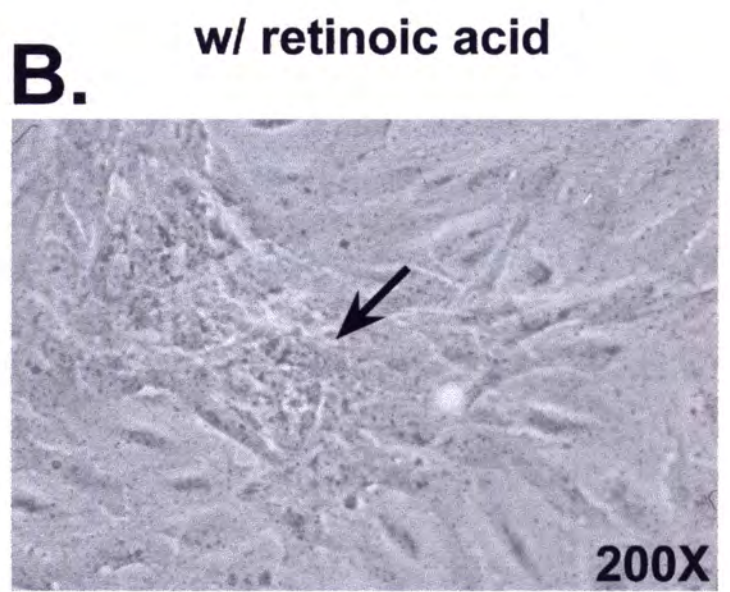
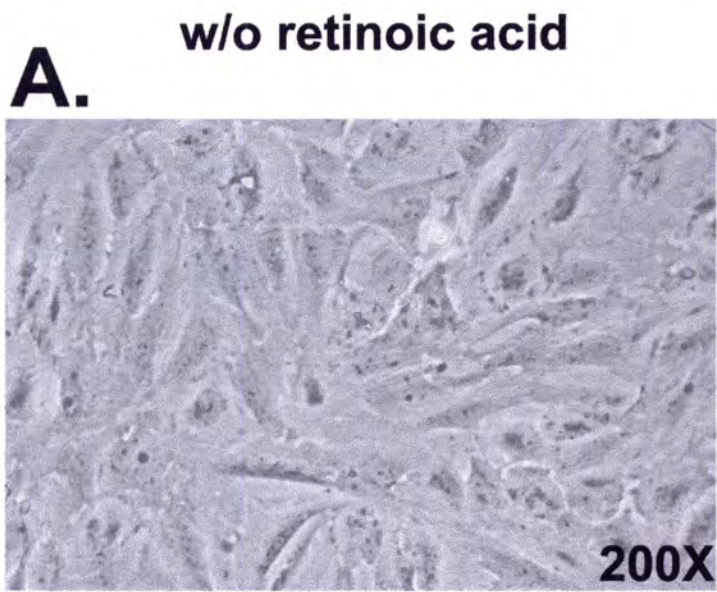




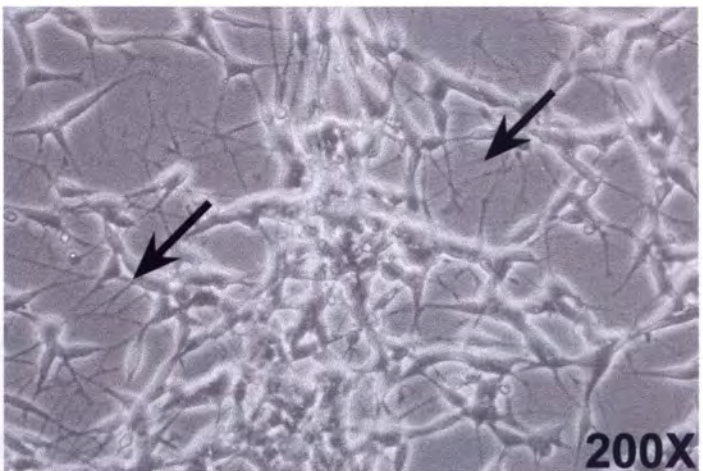
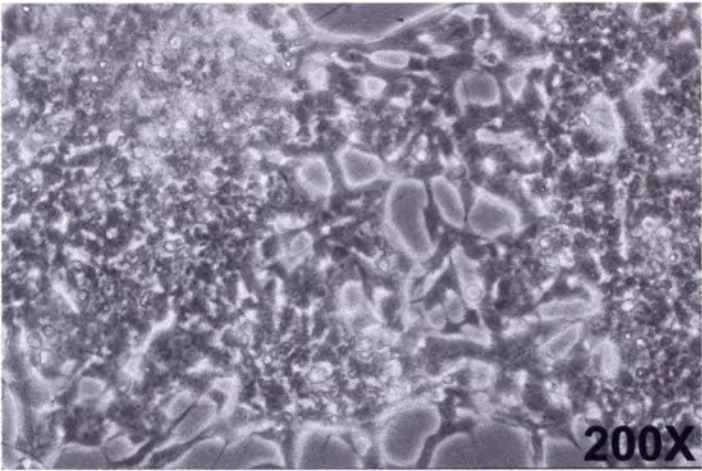
**Figure 4.** Phase micrographs of atRA and untreated CMN-1, CMN-2 and SK-N-SH neuroblastoma cells. **A**, untreated SK-N-SH neuroblastoma cells; **B**, SK-N-SH cells treated for 72 hours with 1  $\mu$ M atRA; **C**, untreated cellular CMN-1 cells; **D**, CMN-1 cells treated for 72 hours with 1  $\mu$ M atRA; **E**, untreated cellular CMN-2 cells; **F**, CMN-2 cells treated for 72 hours with 1  $\mu$ M atRA. **A** shows marked cellular clumping of SK-N-SH cells and contrasts greatly with the differentiated phenotype (evidenced by the formation of neurites) in cells exposed to atRA for 72 hours (**B**). Arrows indicate neurite formation in **B**. There were no microscopically evident changes visualized in atRA treated CMN-1 cells (**C&D**) or CMN-2 cells (**E&F**). All micrographs at 200X.

w/o retinoic acid

w/ retinoic acid

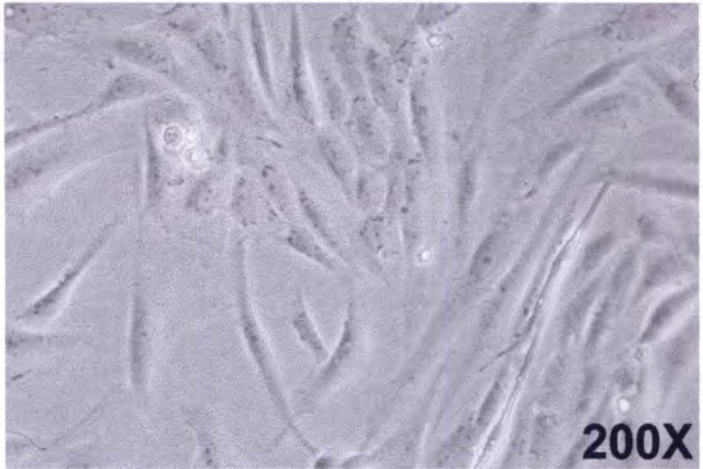
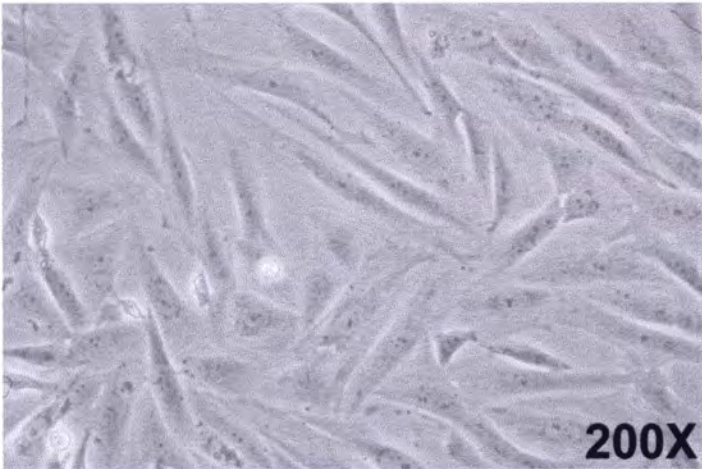
**A.**

**B.**



**C.**

**D.**



**E.**

**F.**

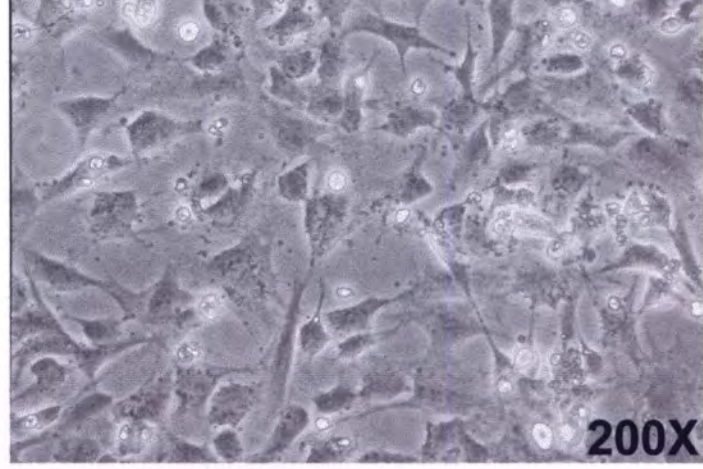
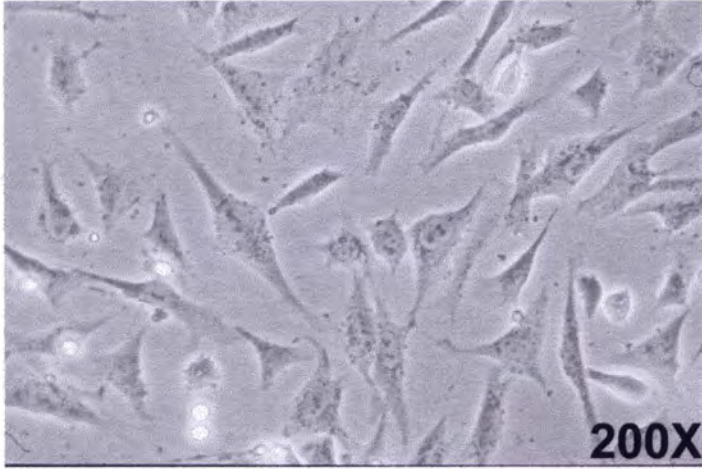
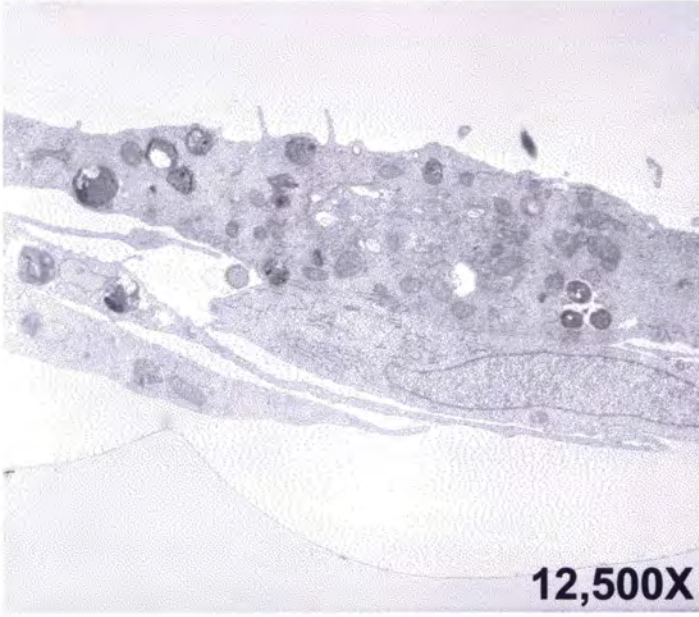


**Figure 5.** TEM and SEM micrographs of untreated and atRA treated CCSK-2 primary cell cultures. **A**, TEM micrograph of untreated CCSK-2 cells growing in multiple layers with stromal morphology. **B**, TEM micrograph of CCSK-2 cells exposed to 1  $\mu$ M at RA for 72 hours. **C**, SEM micrograph of untreated CCSK-2 cells. **D**, SEM micrograph of CCSK-2 cells treated with 1 $\mu$ M atRA for 72 hours. TEM and SEM analysis reveals marked cellular flattening in atRA treated cultures. TEM micrographs at 12,500X; SEM micrographs at 500X.

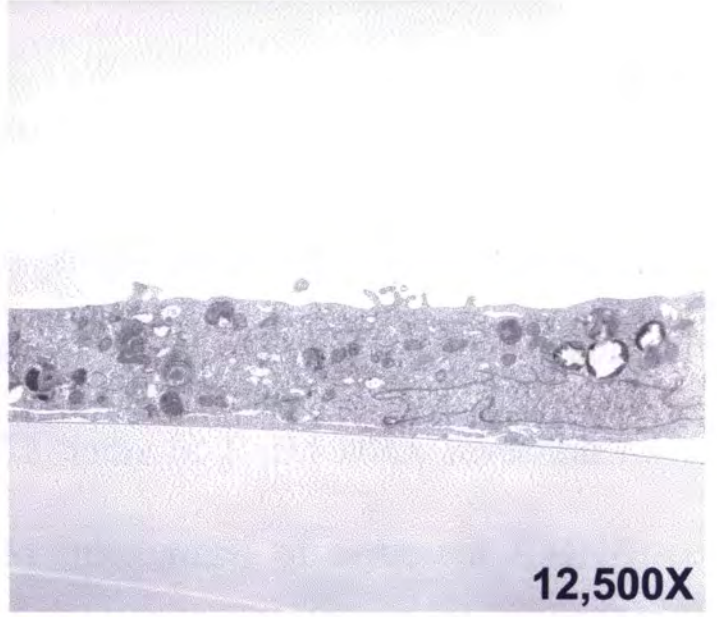
**A.**

w/o retinoic acid

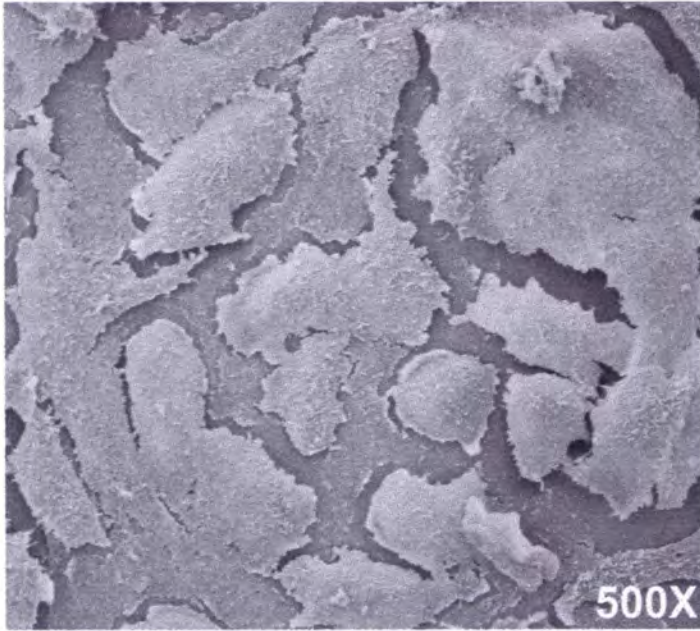


**B.**

w/ retinoic acid



**C.**



**D.**

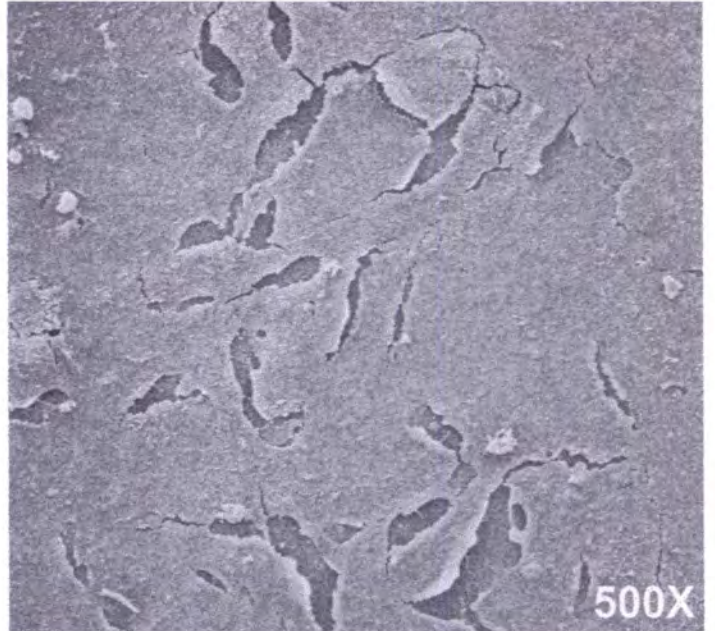
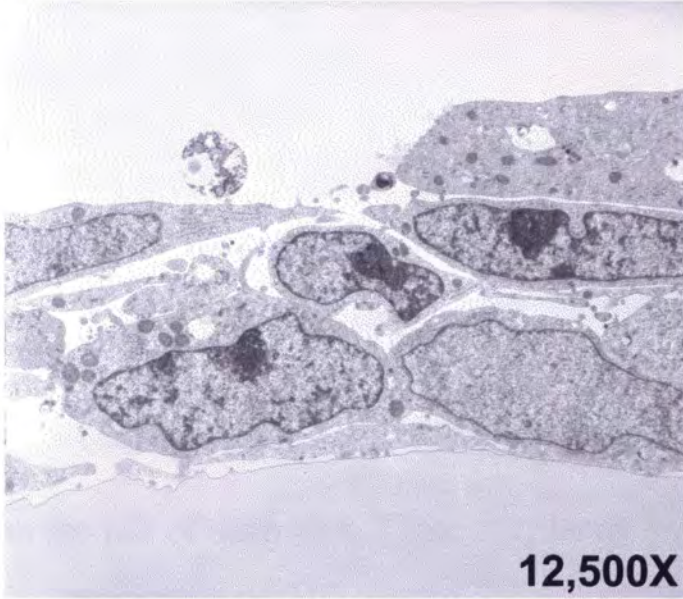
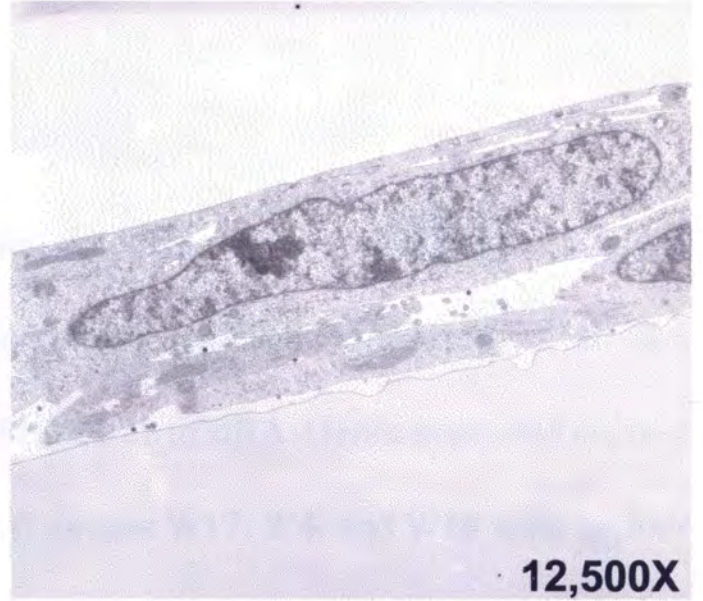


**Figure 6.** TEM and SEM micrographs of untreated and atRA treated cellular CMN-1 cells. **A**, TEM micrograph of untreated CMN-1 cells revealing multiple cell layers in culture. **B**, TEM micrograph CMN-1 cells treated for 72 hours in 1  $\mu$ M atRA revealing cellular flattening and closer juxtaposition. **C**, SEM micrograph of untreated CMN-1 cells demonstrating cellular disarray and multiple cell layers. **D**, SEM micrograph of CMN-1 cells exposed to 1 mM atRA for 72 hours showing interdigitation of tumor cells and cell flattening. TEM micrographs at 12,500X ;SEM micrographs at 2,000X.

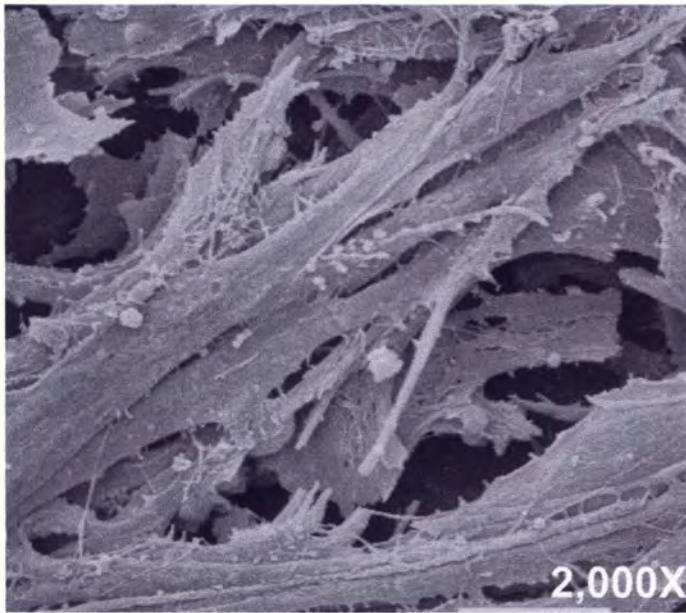
**A.** w/o retinoic acid



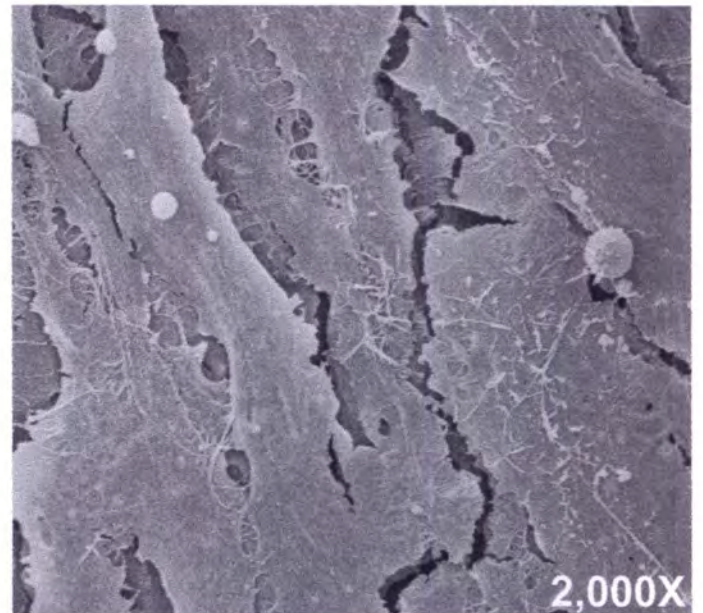
**B.** w/ retinoic acid



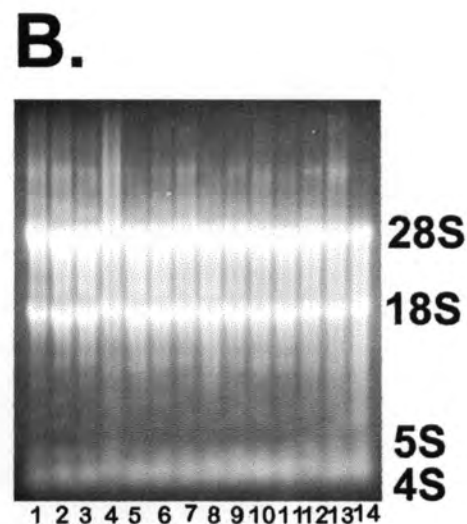
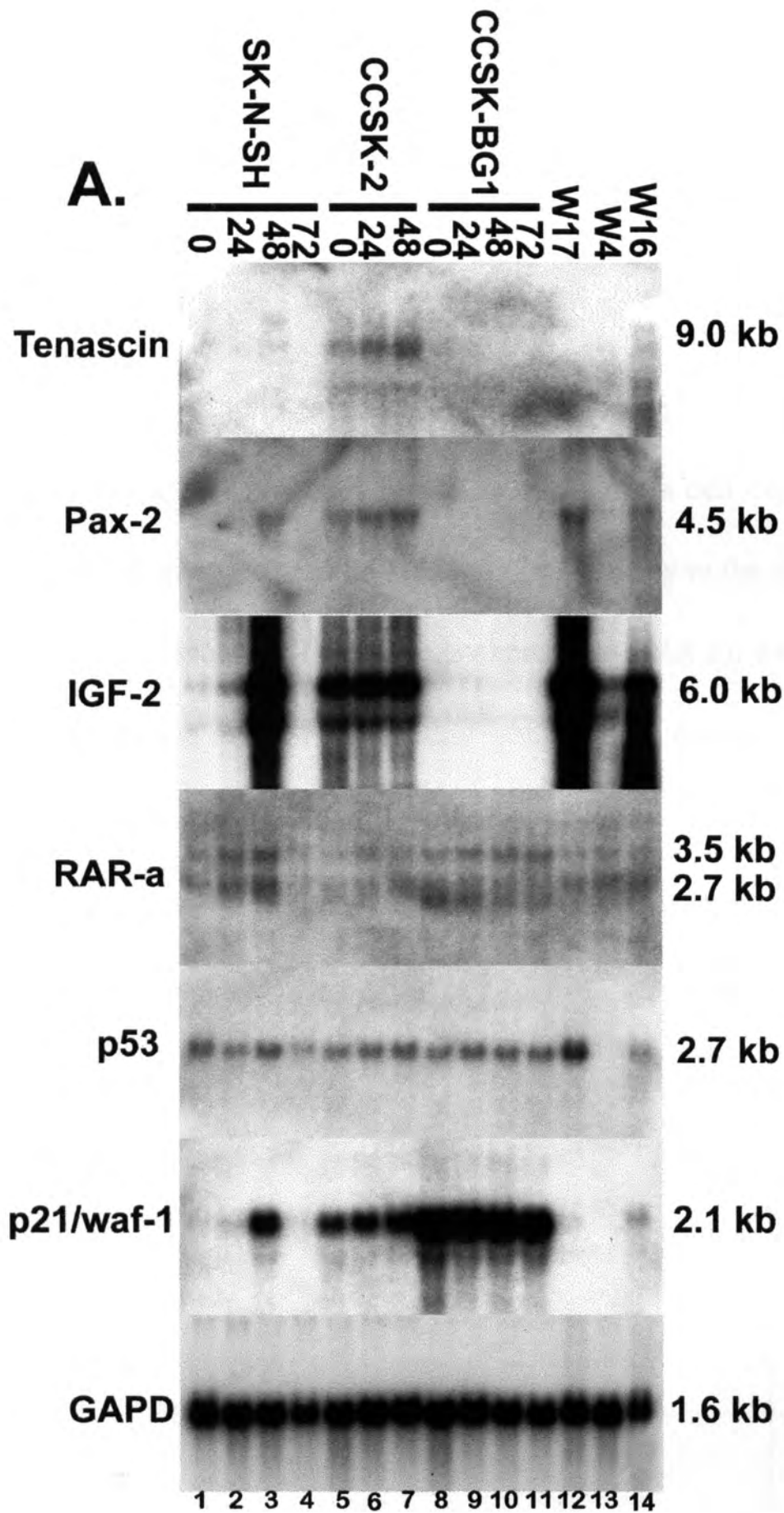
**C.**



**D.**

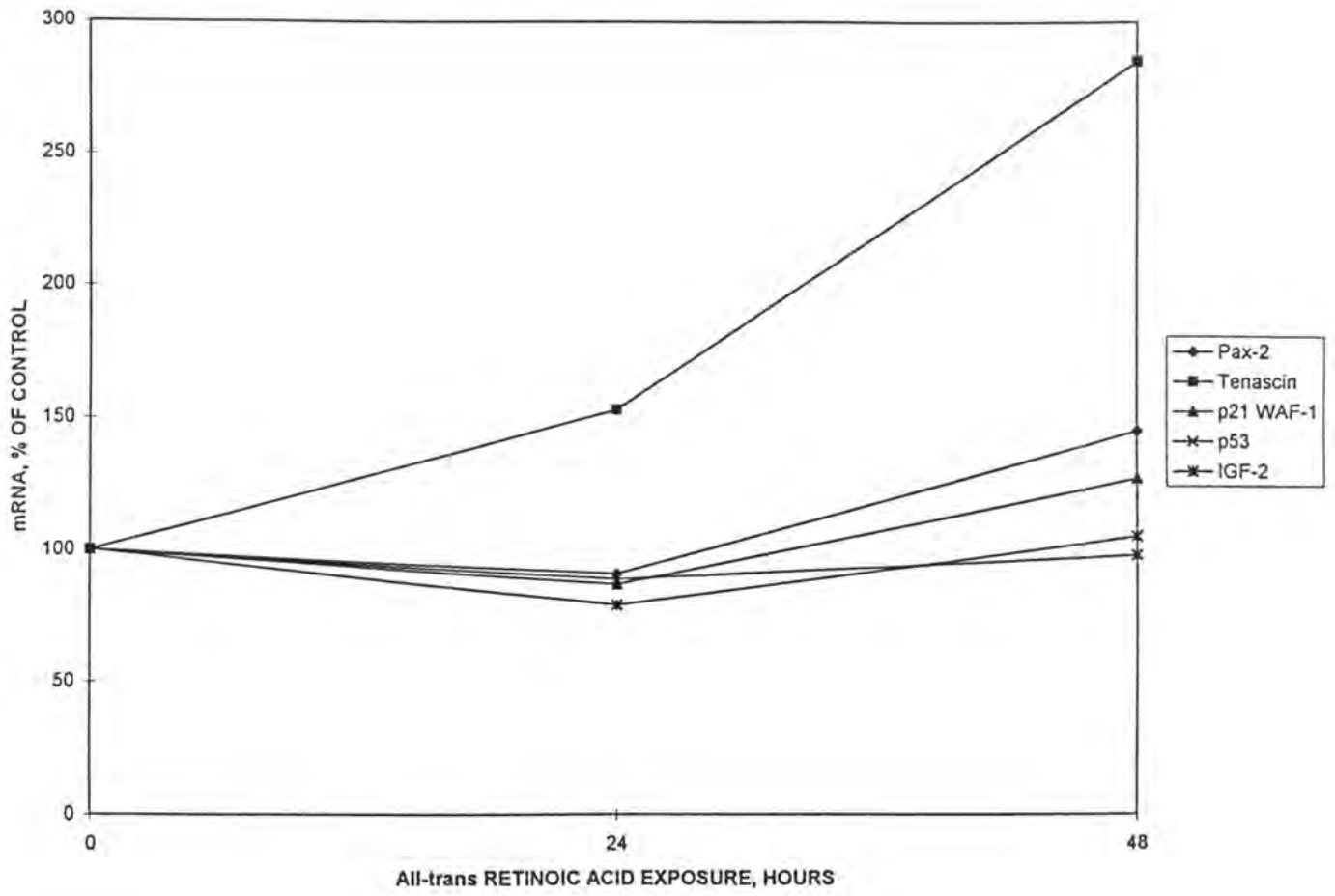
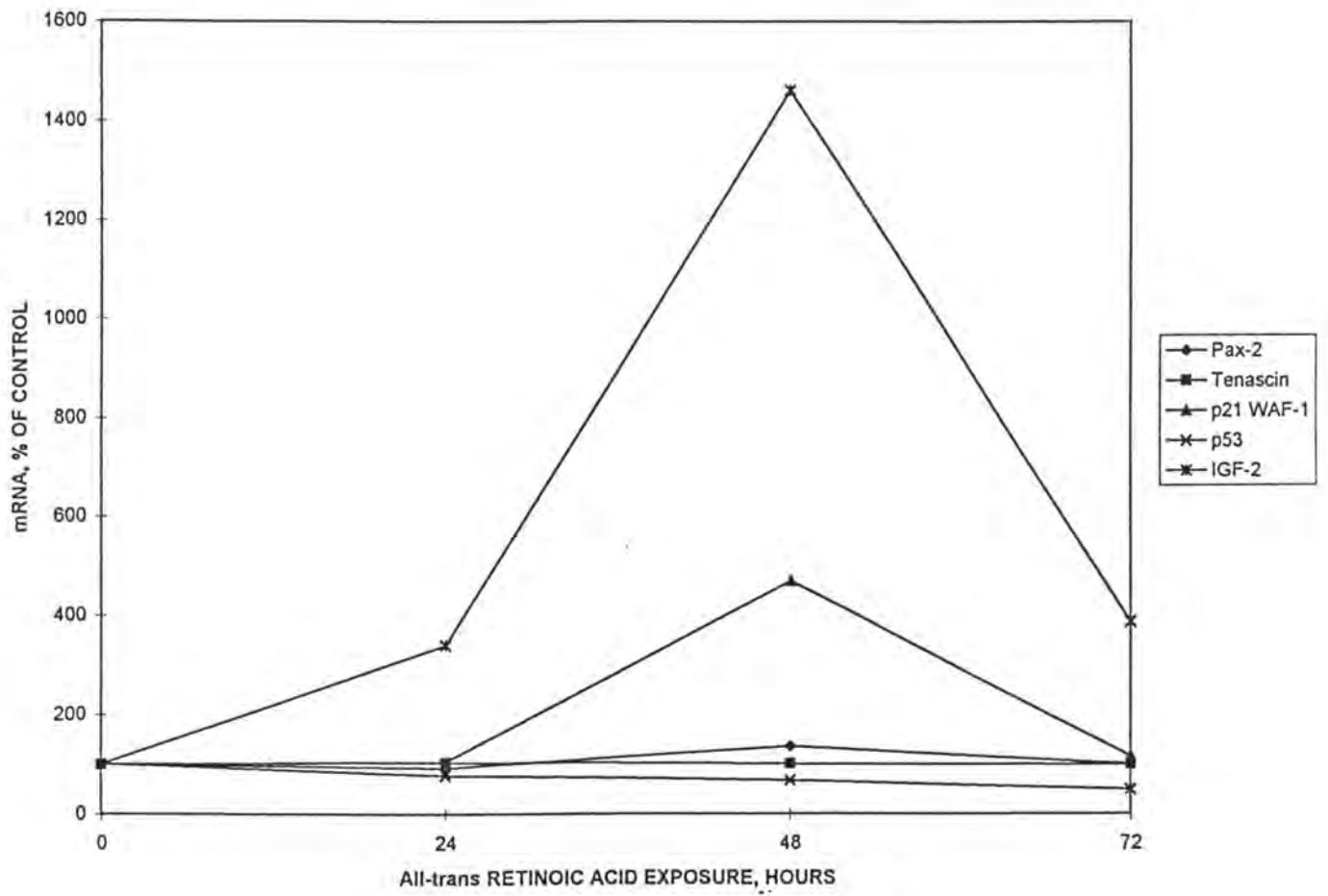


**Figure 7. A,** Modulation of gene expression in atRA treated CCSK and SK-N-SH neuroblastoma cell cultures. Cell lines evaluated are indicated at the top of the blots. Numbers over each lane correspond to hours of exposure to atRA. Genes evaluated are noted on the left of each blot. Three anaplastic Wilms' tumors W17, W4, and W16 were included as controls for Pax-2, p53, and p21. Hybridization with a GAPD cDNA probe was included as a indication of constitutive gene expression. **B,** ethidium bromide stained agarose gel of total cellular RNA.

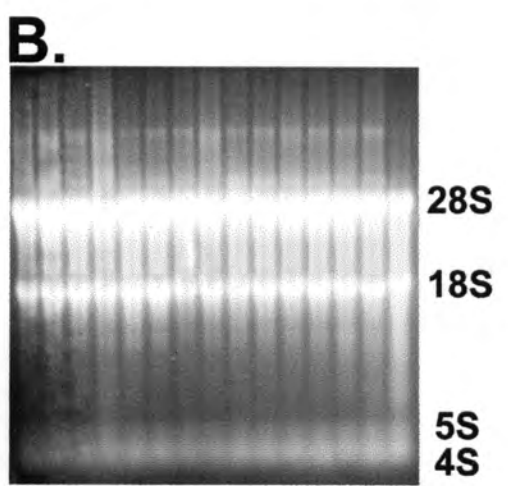
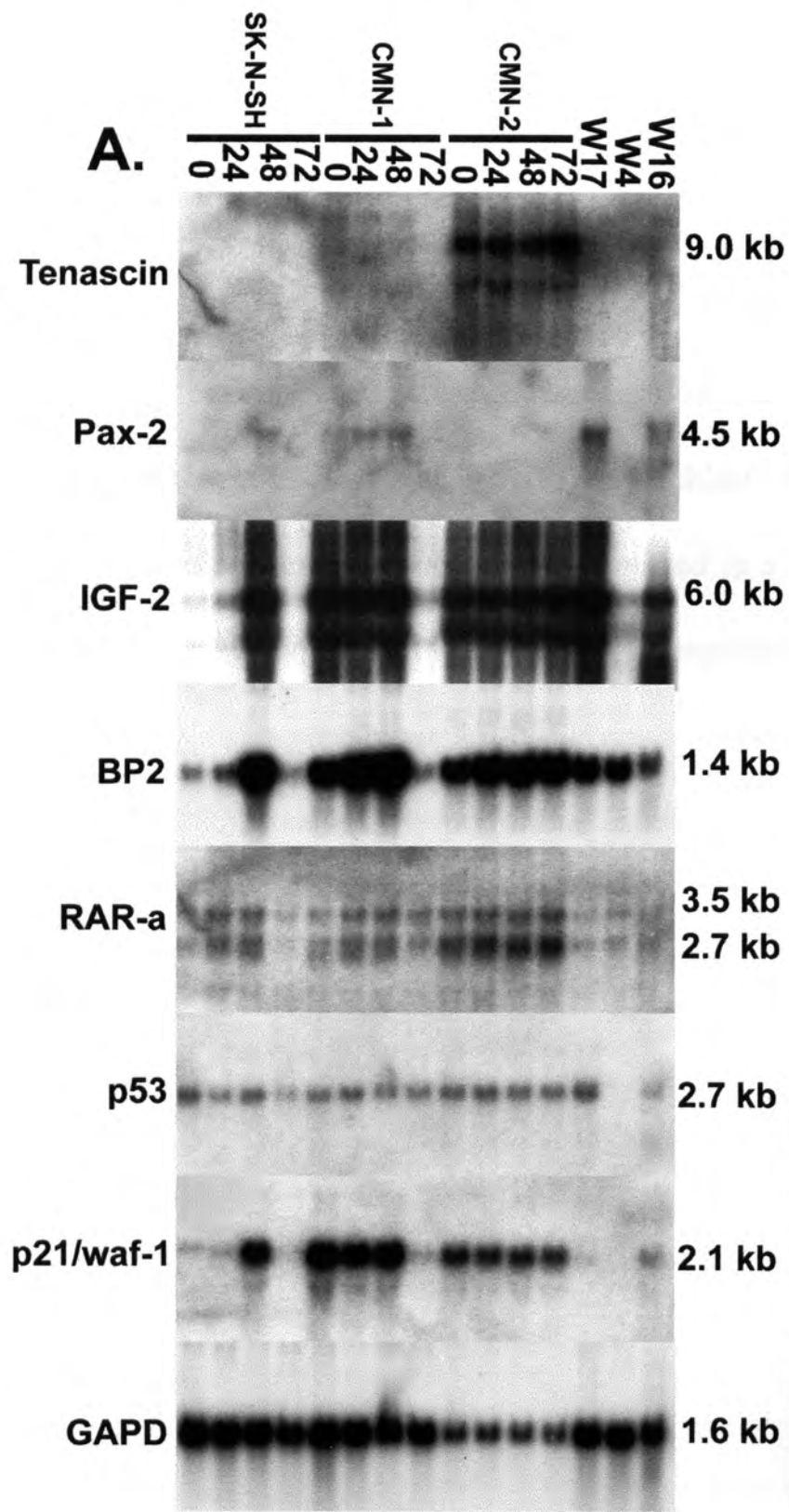




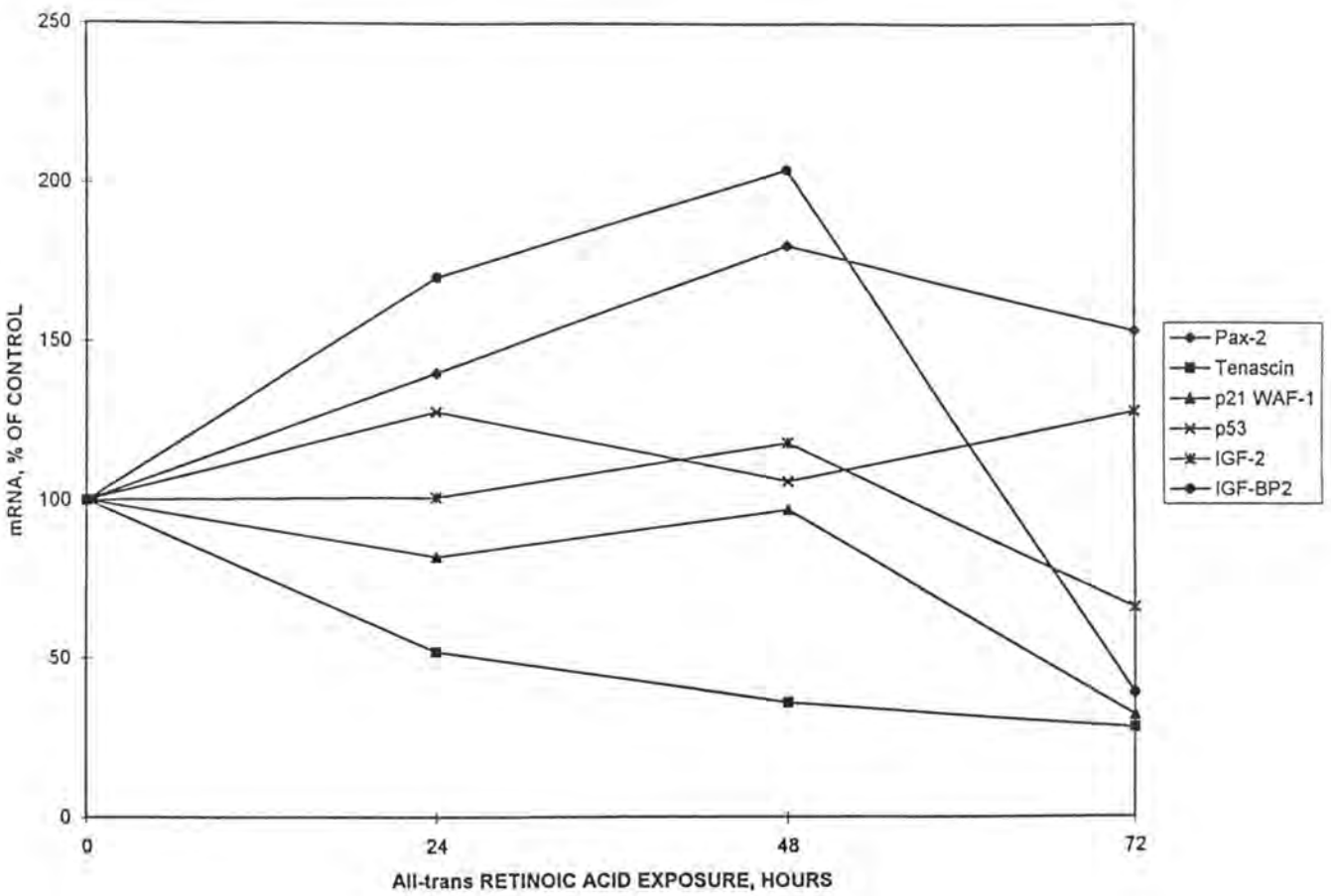
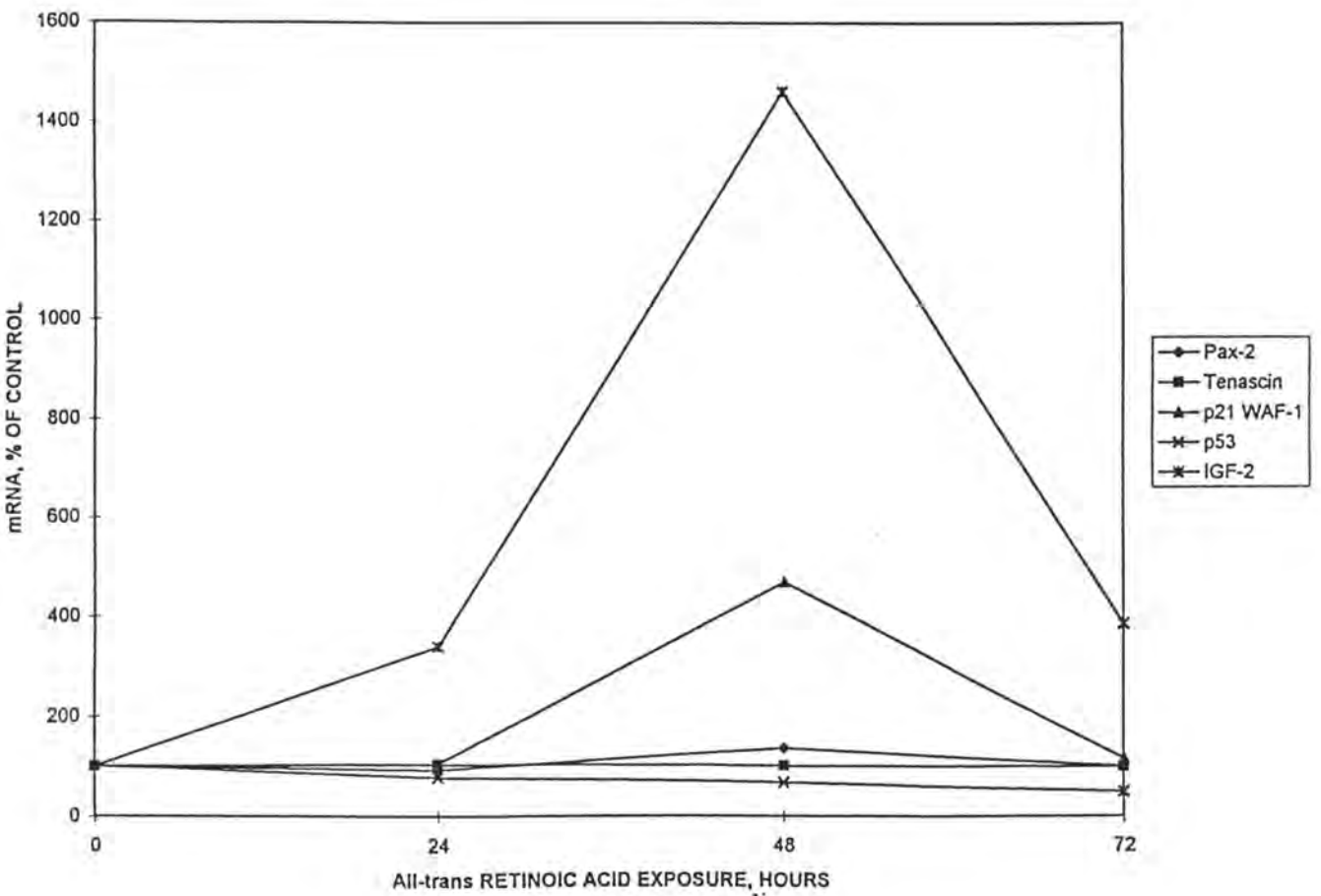
**Figure 8.** Line graph demonstrating quantification of Pax-2, tenascin, p21, p53, and IGF-2 mRNA in CCSK-2 and SK-N-SH neuroblastoma cell cultures treated with atRA. Lines representing gene expression are identified in a key to the right of the graph. **A,** Alterations of gene expression in CCSK-2 cells exposed to atRA for a 48 hour period. **B,** Alterations of gene expression in SK-N-SH neuroblastoma cells exposed to atRA over a 72 hour period. Quantification was performed using Adobe Photoshop Version 4.0 software.

**A.****B.**

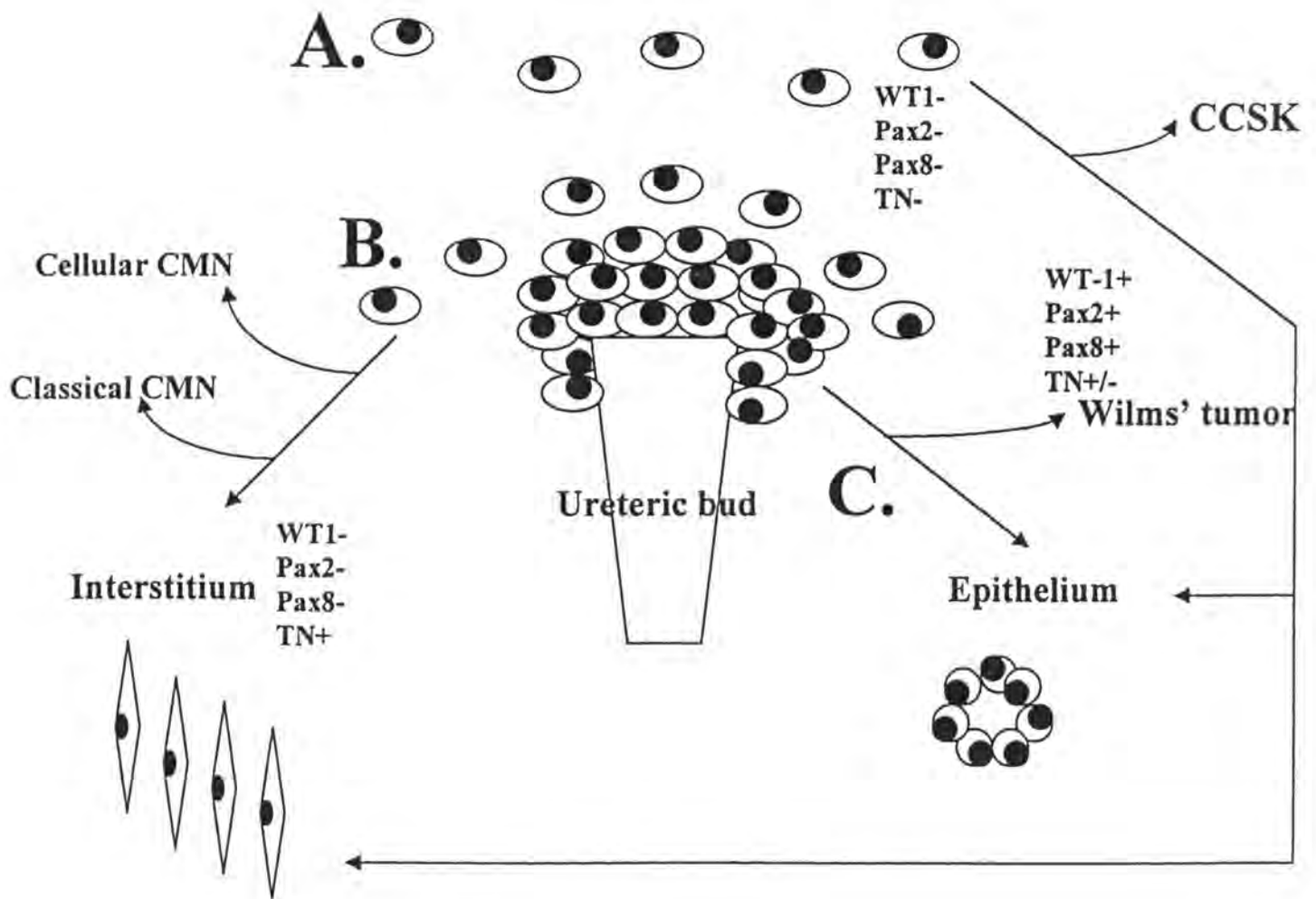
**Figure 9. A,** Modulation of gene expression in atRA treated cellular CMN and SK-N-SH neuroblastoma cell cultures. Cell lines evaluated are indicated at the top of the blots. Numbers over each lane correspond to hours of atRA exposure. Genes which were evaluated for RNA expression are noted at the left of each blot. Three anaplastic Wilms tumors, W17, W4, and W16 were included as controls for Pax-2, p53, and p21. Hybridization with a GAPD cDNA fragment was included to ensure equal loading of the gel. **B,** ethidium bromide stained agarose gel containing total cellular RNA.



**Figure 10.** Line graph demonstrating quantification of Pax-2, tenascin, p21, p53, IGF-2, and IGF-BP2 mRNA in CMN-1 and SK-N-SH neuroblastoma cell cultures treated with atRA. Lines representing gene expression are identified in a key to the right of the graph. **A,** Alterations of gene expression in CMN-1 cells exposed to atRA for a 72 hour period. **B,** Alterations of gene expression in SK-N-SH neuroblastoma cells exposed to atRA over a 72 hour period. Quantification was performed using Adobe Photoshop Version 4.0 software.

**A.****B.**

**Figure 11.** Model of CCSK and CMN histogenesis during normal fetal kidney development. **A**, the uninduced renal mesenchymal tissue which does not express the WT-1, Pax-2, Pax-8, or tenascin genes. A tumorigenic event in these cells may lead to CCSK. **B**, Secondary Mesenchyme destined to differentiate into elements of the renal interstitium. Cellular and classical CMN may derive be derived from this tenascin expressing tissue. **C**, Condensed, or induced renal mesenchyme which expressed WT-1, Pax-2, and Pax-8 during the inductive process. This tissue forms elements of the renal tubular system.





## **Chapter 6**

### **Summary and Conclusions**

The study of CCSK and CMN in the past has been difficult due to the rarity of these tumor types and the inability of one research group to attain a sufficient number of these tumors types for evaluation. This study reports, for the first time, the development of both an *in vivo* and *in vitro* model system by which to study these rare renal neoplasms of childhood in relation to Wilms' tumor and other pediatric malignancies.

Both cell cultures and nude mouse heterotransplants demonstrate similarities with their respective primary tumor specimens when evaluated histologically, ultrastructurally, and molecularly. Immunohistochemical characterization of cell lines has novelly demonstrated SMA immunoreactivity in both CCSK cultures. The latter findings may suggest that CCSK is a tumor derived from smooth muscle or a tumor which is derived from glomerular mesangial cells of the kidney, as both are positive for the smooth muscle actin protein. Interestingly, SMA immunoreactivity was limited to arterial smooth muscle cells in Carnoy's fixed paraffin embedded CCSK primary tumor tissue. The latter suggests that the cell culture environment (i.e. a collagen matrix) may have a differentiating effect upon CCSK cells. An origin in one of these cell types is consistent with northern analysis data which has shown negativity for markers of early induced mesenchyme such as WT-1, Pax-2 and Pax-8. Further, CCSK tumor specimens demonstrated low levels of tenascin mRNA, a gene expressed only in the immature stroma and renal interstitium of the kidney. In contrast, immunochemical findings in CMN are consistent with their primitive mesenchymal origins and supportive of a histogenetic origin in the early stromagenic cells. A panel of CMN primary tumor specimens expressed high levels

of tenascin mRNA. The latter may be indicative a early stromagenic origin for this tumor type and supports previous light and electron microscopic studies implicating fibroblasts and myofibroblasts as the cell of origin for this tumor type. Like CCSK, CMN failed to demonstrate mRNA for markers of induced mesenchyme and early epithelial progenitor cells such as WT-1.

Due to the their similarity in histologic appearance, it has long been speculated that CCSK and CMN may be linked in a tumor progression pathway (i.e. CMN may represent the benign counterpart of the potentially aggressive CCSK). A similar association between classical and anaplastic Wilms' tumors has suggested that the tumor suppressor protein, p53, may be involved in progression. Karyotypic and immunohistochemical analysis of p53 has suggested that this tumor suppressor may be involved in the pathogenesis of CCSK. Immunohistochemical analysis of a large panel of CCSK and CMN in this study, however, does not indicate that p53 is involved in CCSK pathogenesis. In fact, p53 immunoreactivity was only demonstrated in cell cultures of the benign CMN and not in the CCSK cells, contradictory to the supposed role of p53 in tumor progression. Further analysis of CCSK and CMN cells using a DNA damage response assay confirms our previous immunohistochemical findings in primary tumors that p53 is functional in these two tumor types. Functioning p53 molecules in CCSK suggests the possibility of another mechanism for the clinical aggressiveness of this tumor type. Other mechanisms which might contribute to p53 dysfunction were also examined in this study. Pathologic overexpression of the p53 binding protein, MDM-2, a protein which renders p53 inactive, was not present in a large panel of CCSK, CMN, and Wilms' tumors. Even though the increased p53 protein stability in CMN

cells remains unresolved, there may be several alternative explanations. For example, the cell culture environment may cause an upregulation of p53 mRNA translation as a protective effect, or p53 protein is rendered more stable due to a post-translational mechanism. Alternatively, p53 protein stability might be associated with the presence of an as yet unidentified p53 binding protein in these cells. These two model cell lines may be useful in identifying such a protein or proteins.

The functional analysis of p53 may also have prognostic utility as cells with mutations are sometimes more sensitive to chemotherapeutic agents which render DNA damage such as cisplatin and doxorubicin. Preliminary results in this laboratory have suggested that the multidrug resistant anaplastic Wilms' tumor cell line W4, containing a p53 null genotype, is particularly sensitive to cisplatin. The latter may be explained by the tumor cell's inability to arrest and repair DNA damage. Thus, when enough damage has accumulated, cells will die. The use of platinum agents (which are non-MDR drugs) in anaplastic tumors that are multidrug resistant and p53 null may be clinically useful.

CCSK and CMN undoubtedly represent aberrations of normal kidney development as children aged newborn through four years of age are most likely to be afflicted by this neoplasm. The study of the *in vivo* and *in vitro* model of these tumor types has potential usefulness in understanding normal nephrogenesis. The cellular and molecular mechanisms for the development of the renal stroma/ interstitium remains relatively unexplored. The latter contrasts greatly with the amount of information concerning the development of the renal tubular cell system. Renal interstitial cells and renal mesangial cells only comprise a small component of the normal adult kidney and their embryology remains unexplained. However,

both of cell types are associated with significant pathologies. For example, pathological deposition of extracellular matrix material is associated with glomerulosclerosis in disease states such as diabetes mellitus and lupus erythematosus. Interestingly, immunohistochemical analysis of CCSK cells in this study demonstrated smooth muscle actin positivity, a protein which is expressed in normal human mesangial cells. Further, one of the hallmark histologic features of CCSK is the deposition of collagenous extracellular matrix. Therefore, it follows that CCSK may be a pathological proliferation of early, precursor mesangial cells. If so, CCSK cell lines and tumor heterotransplants may be important models for better understanding the mechanisms of abnormal extracellular matrix deposition in diabetic and autoimmune compromised human mesangial cells. Therefore, *in vitro* and *in vivo* models of CCSK will be useful in understanding the mechanisms of neoplasia in this tumor type as well as a potentially useful model in the study of renal embryology, diabetic glomerulosclerosis, membranoproliferative glomerulonephritis, lupus nephritis, IgA nephropathy, as well as others.

Several additional experiments would continue to address the histogenesis of CCSK and CMN and mechanisms of normal kidney development. Using our developed cell lines, cell co-culture experiments including CMN cells and renal mesenchyme may provide evidence for the origin of this tumor. That is, if CMN is truly of secondary mesenchymal origin, then cultured tumor cells may express a soluble factor which orchestrates the development of renal vesicles, and eventually normal tubular epithelium. Secondly, both CCSK and CMN cells would be useful in transfection experiments. Several genes have important roles in the mesenchymal to epithelial transformation of the kidney and include E-cadherin, ovumorulin, hepatocyte growth factor, WT-1, Pax-2, and wnt-4. CCSK and CMN should be examined for

their mRNA and protein expression of these genes. Furthermore, cellular transfection of these genes may provide important clues for the origins of both tumor types. For example, would Wilms' tumor-1 transfection initiate epithelial differentiation of CMN or CCSK tumor cells? Lastly, tumor cells or xenografts derived from these tumor types should be treated with other inducers of kidney development such as low concentrations of lithium. Or, more importantly, these cells should be exposed to a biological inducer such as developing bone tissue to evaluate morphological and molecular alterations.

More recent findings in the genetic control of normal kidney development may also provide clues to the origins of pediatric renal tumors. For example, the BF-2 transcription factor is expressed in early stromal cells and is thought to mediate their development in a mouse model. A logical experiment would be to evaluate tumors which supposedly represent aberrations of stromal development for defects in this gene. In BF-2 knockout mice, stromal cells appear to develop normally, however, the kidney itself is smaller than normal, ducts have limited branching, and fewer mesenchymal aggregates to differentiate. CCSK, CMN, and Wilms' tumor, characterized by the apparent arrest of differentiation, may be a useful model for the study of BF-2 abnormalities. And, more importantly, CMN and CCSK cell lines will hopefully provide tools for a more complete understanding of the molecular basis of normal kidney development.

## **Chapter 7**

### **List of References**

Armstrong JF, Pritchard-Jones K, Bickmore WA, Hastie ND, and Bard JBL. The Expression of the Wilms' Tumor Gene, WT-1, in the Developing Mammalian Embryo. *Mechanisms of Development* 40: 85-97, 1992.

Aufderheide E, Chiquet-Ehrismann R, and Ekblom P. Epithelial-Mesenchymal Interactions in the Developing Kidney Lead to Expression of Tenascin in the Mesenchyme. *Journal of Cell Biology*. 105:599-608, 1987.

Babajko S and Binoux M. Modulation by Retinoic Acid of Insulin-like Growth Factor (IGF) and IGF Binding Protein Expression in Human SK-N-SH Neuroblastoma Cells. *European Journal of Endocrinology* 134(4): 474-480, 1996.

Baird PN, Groves N, Haber DA, Housman DE, and Cowell JK. Identification of Mutations in the WT-1 Gene in Tumours from Patients with the WAGR Syndrome. *Oncogene* 7: 2141-2149, 1992.

Bardeesy N, Falkoff D, Petruzzi MJ, Nowak N, Zabel B, Adam M, Aguiar MC, Grundy P, Shows T, and Pelletier J. Anaplastic Wilms' Tumor, a Subtype displaying poor prognosis, harbors p53 mutations. *Nature Genetics* 7: 91-97, 1994.

Beckwith JB. Mesenchymal Renal Neoplasms of Infancy Revisited. *Journal of Pediatric Surgery* 9: 803-805, 1974.

Beckwith JB and Palmer NF. Histopathology and Prognosis of Wilms' Tumors: Results from the First National Wilms' Tumor Study. *Cancer* 41: 1937-1948, 1978.

Beckwith JB and Weeks, D. Congenital Mesoblastic Nephroma: When Should we Worry? *Archives of Pathology and Laboratory Medicine* 110: 98-99, 1986.

Bolande RP, Brough J, and Izont RJ. Congenital Mesoblastic Nephroma of Infancy. *Pediatrics* 40: 272-278, 1967.

Brietman TR, Selonick SE, and Collins SJ. Induction of Differentiation of the Human Promyelocytic Leukemia Cell Line (HL-60) by Retinoic Acid. *Proceedings of the National Academy of Sciences USA* 77: 2936-2940, 1980.

Burak Y, Junen T, Haffner R, and Oren M. MDM-2 Expression is induced by wild-type p53 activity. *EMBO Journal* 12: 461-468, 1993.

Call KM, Glaser T, Ito CY, Buckler AJ, Pelletier J, Haber DA, Rose EA, Kral A, Yeger H, and Lewis WH. Isolation and Characterization of a Zinc Finger Polypeptide Gene at Human Chromosome 11 Wilms' Tumor Locus. *Cell* 60(3): 509-520, 1990.



- Cheah PL and Looi LM. Implications of p53 Protein Expression in Clear Cell Sarcoma of the Kidney. *Pathology* 28: 229-231, 1996.
- Chen CY, Oliner JD, Zhan Q, Fornace AJ Jr., Vogelstein B, and Kastan MB. Interactions Between p53 and MDM-2 in a mammalian cell cycle checkpoint pathway. *Proceedings of the National Academy of Sciences USA* 91: 2684-2688, 1994.
- Chin KV, Ueda K, Pastan I, and Gottesman MM. Modulation of Activity of the Promoter of the Human MDR-1 Gene by Ras and p53. *Science* 255: 459-462, 1992.
- Chiquet-Ehrismann R, Mackie EJ, Pearson CA, and Sakakura T. Tenascin: An Extracellular Matrix Protein Involved in Tissue Interactions During Fetal Development and Oncogenesis. *Cell* 47: 131-139, 1986.
- Chomczynski P and Sacchi N. Single-step Method of RNA Isolation by Acid Guanidinium Thiocyanate-Phenol-Chloroform Extraction. *Analytical Biochemistry* 162: 156-159, 1987.
- Crossin KL. Tenascin: A Multifunctional Extracellular Matrix Protein with a Restricted Distribution in Development and Disease. *Journal of Cellular Biochemistry* 61: 592-598, 1996.
- Davidoff AM, Pence JC, Shorter NA, Inglehart JD, and Marks JR. Expression of p53 in Human Neuroblastoma and Neuroepithelioma-Derived Cell Lines. *Oncogene* 7:127-133, 1992.
- Dehbi M and Pelletier J. Pax-8 Mediated Activation of the WT-1 Tumor Suppressor Gene. *EMBO Journal* 15(16): 4297-4306, 1996a.
- Dehbi M, Ghahremani M, Lechner M, Dressler G, and Pelletier J. The Paired-box Transcription Factor, Pax-2, Positively Modulates Expression of the Wilms' Tumor Suppressor Gene (WT-1). *Oncogene* 13(3): 447-453, 1996b.
- Dey BR, Sukhatme VP, Roberts AB, Sporn MB, Rauscher FJ III, and Kim SJ. Repression of the Transforming Growth Factor Beta -1 Gene by the Wilms' Tumor Suppressor WT-1 Gene Product. *Molecular Endocrinology* 8(5): 595-602, 1994.
- Dony C, Kessel M, and Gruss P. Post-transcriptional Control of myc and p53 Expression During Differentiation of the Embryonal Carcinoma Cell Line F9. *Nature* 317: 636-639, 1985.
- Douglass EC, Valentine M, Rowe ST, Parham DM, Williams JA, Sanders JM, and Houghton PJ. Malignant Rhabdoid Tumor: A Highly Malignant Childhood Tumor with Minimal Karyotypic Changes. *Genes Chromosomes Cancer* 2: 210-216, 1990.

Dressler GR, Deutsch U, Chowdhury K, Nornes HO, and Gruss P. Pax-2, a New Murine Paired Box Containing Gene and its Expression in the Developing Excretory System. *Development* 109: 787-795, 1990.

Dressler GR and Douglass EC. Pax-2 is a DNA-binding Protein Expressed in Embryonic Kidney and Wilms' Tumor. *Proceedings of the National Academy of Sciences USA* 89: 1179-1183, 1992.

Drummond IA, Madden SL, Rohwer-Nutter P, Bell GI, Sukhatme VP, and Rauscher FJ III. Repression of the Insulin-like Growth Factor II Gene by the Wilms' Tumor Suppressor. *Science* 257(5070):674-678, 1992.

Eccles MR, Yun K, Reeve AE, and Fidler AE. Comparative In situ Hybridization Analysis of Pax-2, Pax-8, and WT-1 Gene Transcription in Human Fetal Kidney and Wilms' Tumor. *American Journal of Pathology* 146(1): 40-50, 1995.

Ekblom P and Weller A. Ontogeny of Tubulointerstitial Cells. *Kidney International* 39: 394-400, 1991.

El Bahtimi R, Hazen-Martin DJ, Re GG, Willingham MC, Garvin AJ. Immunophenotype, mRNA Expression, and Gene Structure of p53 in Wilms' Tumor. *Modern Pathology* 9(3):238-244, 1996.

El-Diery WS, Tokino T, Velculescu DB, Levy DB, Parsons R, Trent JM, Lin D, Mercer WE, Kinzler KW, and Vogelstein B. WAF-1, a Potential Mediator of p53 Tumor Suppression. *Cell* 75: 817-825, 1993.

El-Diery WS, Harper JA, O'Connor PM, Velculescu VE, Canman CE, Jackman J, Pietenpol JA, Hill DE, Wang Y, Wiman KG, Mercer WE, Kastan MB, Kohn KW, Elledge SJ, Kinzler KW, and Vogelstein B. WAF-1/CIP-1 is Induced in p53-mediated G1 Arrest and Apoptosis. *Cancer Research* 54: 1169-1174, 1994.

Englert C, Hou X, Maheswaran S, Bennett P, Ngwu C, Re GG, Garvin AJ, Rosner MR, and Haber DA. WT-1 Suppresses Synthesis of the Epidermal Growth Factor Receptor and Induces Apoptosis. *EMBO Journal* 14(19): 4662-4675, 1995.

Englert C, Maheswaran S, Garvin AJ, Kreidberg J, and Haber DA. Induction of p21 by the Wilms' Tumor Suppressor, WT-1. *Cancer Research* 57(8): 1429-1434, 1997.

Esrig D, Spruch CH III, Nichols PW et al. p53 Nuclear Protein Accumulation Correlates with Mutations in p53, Tumor Grade, and Tumor Stage in Bladder Cancer. *American Journal of Pathology* 143: 1389-1397, 1993.

- Fearon ER, Vogelstein B, and Feinberg AP. Somatic Deletion and Duplication of Genes on Chromosome 11 in Wilms' Tumor. *Nature* 309(5964): 176-178, 1984.
- Feinberg AP and Vogelstein BA. Technique for Radiolabelling DNA Restriction Endonuclease Fragments to High Specific Activity. *Analytical Biochemistry* 132: 6-13, 1983.
- Gansler T, Furlanetto R, Gramling TS, Robinson KA, Blockner N, Buse MG, Sens DA, and Garvin AJ. Antibody to Type I Insulin-like Growth Factor Inhibits Growth of Wilms' Tumor in Culture and in Athymic Mice. *American Journal of Pathology* 135; 961-966, 1989.
- Garvin AJ, Congleton L, Inabnett T, Gansler T, and Sens DA. Growth Characteristics of Human Wilms' Tumor in Nude Mice. *Pediatric Pathology* 8: 599-615, 1988.
- Gonzalez-Crussi F. *Wilms' Tumor (Nephroblastoma) and Related Renal Neoplasms of Childhood*. CRC Press, Boca Raton, Florida, 1984.
- Gorina S and Pavletich NP. Structure of the p53 Tumor Suppressor Bound to the Ankyrin and SH3 Domains of 53BP2. *Science* 274: 1001-1004, 1996.
- Gould VE, Martinez-Lacabe V, Virtanen I, Sahlin KM, and Schwartz MM. Differential Distribution of Tenascin and Cellular Fibronectin in Acute and Chronic Renal Allograft Rejection. *Laboratory Investigation* 67: 71-79, 1992.
- Green DM, Breslow NE, Beckwith JB, Moksness J, Finklestein JZ, and D'Angio GJ. Treatment of Children with Clear Cell Sarcoma of the Kidney: A Report from the National Wilms' Tumor Study Group. *Journal of Clinical Oncology* 12(10): 2132-2137, 1994.
- Grundy RE, Telzerow PE, Breslow N, Moksness J, Huff V, and Paterson MC. Loss of Heterozygosity for Chromosome 16q and 1p in Wilms' Tumor Predicts an Adverse Outcome. *Cancer Research* 54: 2331-2333, 1994.
- Grundy P, Coppes MJ, and Haber D. Molecular Genetics of Wilms' Tumor. *Hematology - Oncology Clinics of North America* 9(6): 1201-1215, 1995.
- Gruss P and Walther C. Pax in Development. *Cell* 69: 719-722, 1992.
- Haas JE, Bonadio JF, and Beckwith JB. Clear Cell Sarcoma of the Kidney with Emphasis on Ultrastructural Studies. *Cancer* 54: 2978-2987, 1984.
- Haber DA, Buckler AJ, Glaser T, Call KM, Pelletier J, Sohn RL, Douglass EC, and Housman DE. An Internal Deletion within an 11p13 Zinc Finger Gene Contributes to the Development of Wilms' Tumor. *Cell* 61(7): 1257-1269, 1990.

- Haber DA, Sohn RI, Buckler AJ, Pelletier J, Call KM, and Housman DE. Alternative Splicing and Genomic Structure of the Wilms' Tumor Gene WT-1. *Proceedings of the National Academy of Sciences USA*. 88: 9618-9622, 1991.
- Hao Y, Crenshaw T, Moulton T, Newcomb E, and Tycko B. Tumor-Suppressor Activity of H19 RNA. *Nature* 365: 764-767, 1993.
- Hatada H, Ohashi Y, Fukushima Y, Kaneko M, Inoue Y, Komota A, and Okada S, An Imprinted Gene p57Kip2 is Mutated in Beckwith-Wiedemann Syndrome. *Nature Genetics* 14: 171-173, 1996.
- Hatini V, Huh SO, Herzlinger D, Soares VC, and Lai E. Essential Role of Stromal Mesenchyme in Kidney Morphogenesis Revealed by Targeted Disruption of Winged Helix Transcription Factor BF-2. *Genes and Development* 10: 1467-1478, 1996.
- Hawkins DS, Demers GW, and Galloway DA. Inactivation of p53 Enhances Sensitivity to Multiple Chemotherapeutic Agents. *Cancer Research* 56(4): 892-898, 1996.
- Haupt Y, Maya R, Kazaz A, and Oren M. MDM-2 Promotes the Rapid Degradation of p53. *Nature* 387: 296-299, 1997.
- Hawley RS and Friend SH. Strange Bedfellows in Even Stranger Places: The Role of ATM in Meiotic Cells, Lymphocytes, Tumors, and Functional Links to p53. *Genes and Development* 10: 2383-2388, 1996.
- Hazen-Martin DJ, Chao CC, Wang IY, Sens DA, Garvin AJ, and Wang AC. Developmental Pattern of Thy-1 Immunoreactivity in the Human Kidney and Application to Pediatric Renal Neoplasms. *Pediatric Pathology* 13: 37-52, 1993.
- Hazen-Martin DJ, Tarnowski BI, Todd JH, Sens MA, Bylander JE, Smyth BJ, Garvin AJ, and Sens DA. Serum-free Culture and Characterization of Renal Epithelial Cells Isolated from Human Fetal Kidney of Varying Gestational Ages. *In Vitro Cell and Developmental Biology* 30A: 356-365, 1994.
- Henry I, Bonaiti-Pelletier C, Chehensse V, Beldjord C, Schwartz C, Uttermam G, and Junien C. Uniparental Disomy in Genetic Cancer Predisposing Syndrome. *Nature* 351: 665-667, 1991.
- Herzlinger D, Koseki C, Mikawa T, and Al-Aqwati Q. Metanephric Mesenchyme Contains Multipotent Stem Cells Whose Fate is Restricted After Induction. *Development* 114: 565-572, 1992.

Hewitt SM, Hamada S, McDonnell TJ, Rauscher FJ III, and Saunders GF. Regulation of the Proto-Oncogene Bcl-2 and c-myc by the Wilms' Tumor Suppressor Gene WT-1. *Cancer Research* 55(22): 5386-5389, 1995.

Hoovers JMN, Kalikin LM, Johnson LA, Alders M, Redeker B, Law DJ, and Bliet J. Multiple Genetic Loci within 11p15 defined by Beckwith-Wiedemann Syndrome Breakpoints and Sub-chromosomal Transferrable Fragments. *Proceedings of the National Academy of Sciences USA*. 92: 12456-12460, 1995.

Huff V, Miwa H, Haber DA, Call KM, Housman D, Strong LC, and Saunders GF. Evidence for WT-1 as a Wilms' Tumor Gene: Intragenic Germinal Deletion in Bilateral Wilms' Tumor. *American Journal of Human Genetics* 48(5): 997-1003, 1991.

Ishii E, Fujimoto J, Hara S, Tanaka S, and Hata J. Human Sarcomatous Wilms' Tumor Cell Lines: Evidence for Epithelial Differentiation in Clear Cell Sarcoma of the Kidney. *Cancer Research* 49: 5392-5399, 1989.

Jones JI and Clemmons DR. Insulin-like Growth Factors and Their Binding Proteins: Biological Actions. *Endocrine Reviews* 16(1): 3-34, 1995.

Joshi VV, Kasznica J, and Walters WR. Atypical Mesoblastic Nephroma: Characterization of a Potentially Aggressive Variant of Conventional Congenital Mesoblastic Nephroma. *Archives of Pathology and Laboratory Medicine* 110: 100-106, 1986.

Junien C. Beckwith-Wiedemann Syndrome, Tumorigenesis, and Imprinting. *Current Opinion Genetics and Development* 2: 431-438, 1992.

Junquiera LC, Carneiro J, and Kelley RO. *Basic Histology*. Appleton and Lange, Norwalk, Connecticut, 1992.

Kaleti J, Quezado MM, Abaza MM, Raffeld M, and Tsokos M. The MDM-2 Oncoprotein is Over-expressed in Rhabdomyosarcoma Cell Lines and Stabilizes Wild-Type p53 Protein. *American Journal of Pathology* 149(1): 143-151, 1996.

Kaneko Y, Homma C, Maseki N, Masaharu S, and Hata J. Correlation of Chromosome Abnormalities with Histological and Clinical Features of Wilms' Tumor and Other Childhood Renal Tumors. *Cancer Research* 51: 5937-5942, 1991.

Kastan MB, Onyekwere O, Sidransky D, Vogelstein B, and Craig RW. Participation of p53 in the Cellular Response to DNA Damage. *Cancer Research* 51: 6304-6311, 1991.

Kidd JM. Exclusion of Certain Renal Neoplasms from the Category of Wilms' Tumor. *American Journal of Pathology*. 59: 16A, 1970.

Kikuchi H, Akasaka Y, Nagai T, Umezawa A, Iri H, Kato S, and Hata J. Genomic Changes in the WT Gene (WT-1) in Wilms' Tumor and Their Correlation with Histology. *American Journal of Pathology* 140: 781-786, 1992.

Ko LJ and Prives C. p53: Puzzle and Paradigm. *Genes and Development* 10: 1054-1072, 1996.

Koufos A, Hansen MF, Lampkin BC, Workman ML, Copeland NG, Jenkins NA, and Cavenee WK. Loss of Alleles at Loci on Human Chromosome 11 During Genesis of Wilms' Tumor. *Nature* 309(5964): 170-172, 1984.

Koukoulis GK, Gould VE, Bhattacharyya A, Gould JE, Howedy AA, and Virtanen I. Tenascin in Normal, Reactive, and Neoplastic Tissue: Biologic and Pathologic Implications. *Human Pathology* 22:636-643, 1991.

Knudson AG Jr. and Strong LC. Mutation and Cancer: A Model for Wilms' Tumor of the Kidney. *Journal of the National Cancer Institute* 48(2): 313-324, 1972.

Kreidberg JA, Sariola H, Loring JM, Maeda M, Masahiro M, Pelletier J, Housman D, and Jaenisch R. WT-1 is Required for Early Kidney Development. *Cell* 74(4): 679-691, 1993.

Kuhnelt, Koveker G, and Muller GH. Drying with Hexamethyldisilizane- a Time-saving Alternative to the Critical Point Method. *Handchirurgie, Mikrochiurgie, Plastische Chirurgie* 21(3): 164-165, 1989.

Kumar S, Carr T, Marsden HB, and Calabuig-Crespo MC. Study of Childhood Renal Using Antisera to Fibronectin, Laminin, and Epithelial Membrane Antigen. *Journal of Clinical Pathology* 39: 51-57, 1986.

Kussie PH, Gorina S, Marechal V, Elenbas B, Moreau J, Levine AJ, and Pavletich NP. Structure of the MDM-2 Oncoprotein Bound to the p53 Tumor Suppressor Transactivation Domain. *Science* 274: 948-953, 1996.

Laemmli UK. Cleavage of Structural Proteins During the Assembly of the Head of Bacteriophage T4. *Nature* 227: 280-285, 1970.

Lahoti C, Thorner P, Malkin D, and Yeger H. Immunohistochemical Detection of p53 in Wilms' Tumor Correlates with Unfavorable Outcome. *American Journal of Pathology* 148(5): 1577-1589, 1996.

Larsen WJ. *Essentials of Human Embryology*, New York, Churchill Livingstone, 1998.

Lechner MS and Dressler GR. The Molecular Basis of Embryonic Kidney Development. *Mechanisms of Development* 62: 105-120, 1997.

- Lee MP, Debraun M, Gurvanset R, Reichard BA, Elledge SJ, Feinberg AP. Low Frequency of p57Kip2 Mutations in Beckwith-Wiedemann Syndrome. *American Journal of Human Genetics* 61: 304-309, 1997.
- Leid M, Kastner P, and Chambon P. Multiplicity Generates Diversity in the Retinoic Acid Signalling Pathways. *Trends in Biochemical Sciences* 17: 427-433, 1992.
- Leroy P, Krust A, Zelent A, Mendelsohn C, Garnier JM, Kastner P, Dierich A, and Chambon P. Multiple Isoforms of the Mouse Retinoic Acid Receptor Alpha are Generated by Alternative Splicing and Differential Induction by Retinoic Acid. *EMBO Journal* 10: 59-69, 1991.
- Levine AJ, Momand J, and Finlay CA. The p53 Tumor Suppressor Gene. *Nature* 351: 453-456, 1991.
- Linnala A, Lehto VP, and Virtanen I. Neuronal Differentiation in SH-SY5Y Human Neuroblastoma Cells Induces Secretion of Tenascin and Upregulation of Alpha (V) Integrin Receptors. *Journal of Neuroscience Research* 49(1): 53-63, 1997.
- Liu M, Iavarone A, and Freedman LP. Transcriptional Activation of the Human p21 waf-1/cip-1 Gene by Retinoic Acid Receptor. *Journal of Biological Chemistry* 271(49): 31723-31728, 1996.
- Looi L and Cheah P. An Immunohistochemical Study Comparing Clear Cell Sarcoma of the Kidney and Wilms' Tumor. *Pathology* 25: 106-109, 1993.
- Maden M. Retinoids and the Control of Pattern Limb Development and Regeneration. *Trends in Genetics* 1: 103-107, 1985.
- Maheswaran S, Park S, Bernard A, Morris JF, Rauscher FJ III, Hill DE, and Haber DA. Physical and Functional Interaction Between WT-1 and p53 Proteins. *Proceedings of the National Academy of Sciences USA*. 90: 5100-5104, 1993.
- Maheswaran S, Englert C, Bennett P, Heinrich G, and Haber DA. The WT-1 Gene Product Stabilizes p53 and Inhibits p53 Mediated Apoptosis. *Genes and Development* 9(17):2143-2156, 1995.
- Malkin D, Sexsmith E, Yeger H, Williams BRG, and Coppes MJ. Mutations of the p53 Tumor Suppressor Gene Occur Infrequently in Wilms' Tumor. *Cancer Research* 54: 2077-2079, 1994.
- Marsden HB, Lawler W, and Kumar PM. Bone Metastasizing Renal Tumor of Childhood: Morphological and Clinical Features, and Differences from Wilms' Tumor. *Cancer* 42: 1922-1928, 1978.

- Marsden HB and Lawler W. Bone Metastasizing Renal Tumor of Childhood: Histopathological and Clinical Review of 38 Cases. *Virchows Archiv A* 387: 341-351, 1980.
- Matsuoka S, Edwards M, Bai C, Parker S, Zhang P, Baldini A, Harper J, Elledge S. p57Kip2, a Structurally Distinct Member of the p21Cip1 cdk Inhibitor Family, is a Candidate Tumor Suppressor Gene. *Genes and Development* 9: 650-662, 1995.
- Maw MA, Grundy PE, Millow LJ, Eccles MR, Dunn RS, Smith PJ, Feinberg AP, Law DJ, Paterson MC, Telzerow PE, Callen DF, Thompson AD, Richards RI, and Reeve AE. A Third Wilms' Tumor Locus on Chromosome 16q. *Cancer Research* 52: 3094-3098, 1992.
- Mierau GW, Weeks DA, and Beckwith JB. Anaplastic Wilms' Tumor and Other Clinically Aggressive Childhood Renal Neoplasms: Ultrastructural and Immunocytochemical Features. *Ultrastructural Pathology* 13: 225-248, 1989.
- Miyashita T and Reed JC. Tumor Suppressor p53 is a Direct Transcriptional Activator of the Human Bax Gene. *Cell* 80: 293-299, 1995.
- Momand J, Zambetti GP, Olson DC, George D, and Levine AJ. The MDM-2 Oncogene Product Forms a Complex with the p53 Protein and Inhibits p53-mediated Transactivation. *Cell* 69: 1237-1245, 1992.
- Morgan E and Kidd JM. Undifferentiated Sarcoma of the Kidney. *Cancer* 41: 1937-1948, 1978.
- Moulton T, Chung WY, Yuan L, Nensle T, Waber P, Nisen P, and Tycko B. Genomic Imprinting and Wilms' Tumor. *Medical and Pediatric Oncology* 27: 476-483, 1996.
- Mugrauer G and Ekblom P. Contrasting Expression Patterns of Three Member of the Myc Family of Proto-oncogenes in the Developing and Adult Mouse Kidney. *Journal of Cell Biology* 112(1): 13-25, 1991.
- Murphy WM, Beckwith JB, and Farrow GM. *Atlas of Tumor Pathology: Tumors of the Kidney, Bladder, and Related Urinary Structures*. Third Series, Fascicle 11, Armed Forces Institute of Pathology, Washington, DC, 1994.
- Nigro JM, Baker SJ, Preisinger AC, Jessup JM, Hostetter R, Cleary K, Bigner SH, Davidson N, Baylin S, Devilee P, Glover T, Collins T, Collins FC, Weston A, Modali R, Harris CC, and Vogelstein B. Mutations in the p53 Gene Occur in Diverse Human Tumor Types. *Science* 342: 705-708, 1989.



Nguyen KT, Liu B, Ueda K, Gottesman MM, Pastan I, Chin KV. Transactivation of the Human Multidrug Resistance (MDR-1) Gene Promoter by p53 Mutants. *Oncology Research* 6: 71-77, 1994.

O'Connor PM, Jackman J, Bae I, Myers TG, Fan S, Mutoh M, Scudiero DA, Monks A, Sausville EA, Weinstein JN, Friend S, Fornace AJ Jr., and Kohn KW. Characterization of the p53 Tumor Suppressor Pathway in Cell Lines of the National Cancer Institute Anticancer Drug Screen and Correlation with the Growth-Inhibitory Potency of 123 Anticancer Agents. *Cancer Research* 37: 4285-4300, 1997.

Oesterling JE, Eggleston JC, Jeffs RD, and Leventhal BG. Anaplastic Sarcoma Arising in a Mature Metachronous Bilateral Wilms' Tumor after Irradiation and Chemotherapy: Spontaneous versus Malignant Change. *Cancer* 59(12): 2000-2005, 1987.

O'Keefe D, Dao D, Zhao L, Sanderson R, Warburton D, Weiss L, Anyane-Yeboah K, and Tycko B. Coding Mutations in p57Kip2 are Present in Some Cases of Beckwith-Wiedemann Syndrome but are Rare or Absent in Wilms' Tumor. *American Journal of Human Genetics* 61: 295-303, 1997.

Oliner JD, Kinzler KW, Meltzer PS, George DL, and Vogelstein B. Amplification of a Gene Encoding a p53-associated Protein in Human Sarcomas. *Nature* 358: 80-83, 1992.

Oliner JD, Pietsenpol JA, Thiagalingam S, Gyuris J, Kinzler KW, and Vogelstein B. Oncoprotein MDM-2 Conceals the Activation Domain of Tumor Suppressor p53. *Nature* 362: 857-860, 1993.

Olsson IL, Breitman TR, and Gallo RC. Priming of Human Myeloid Leukemic Cell Lines HL-60 and U-937 with Retinoic Acid for Differentiation Effects of Cyclic Adenosine 3'-5'-Monophosphate -Inducing Agents. *Cancer Research* 42: 3928-3933, 1982.

Oltvai ZN, Millman CL, and Korsmeyer SJ. Bcl-2 Heterodimerizes *in vivo* with a Conserved Homolog, Bax, that Accelerates Programmed Cell Death. *Cell* 74: 609-619, 1993.

O'Malley DP, Mierau GW, Beckwith JB, and Weeks DA. Ultrastructure of Cellular Congenital Mesoblastic Nephroma. *Ultrastructural Pathology* 20: 417-427, 1996.

Orita M, Suzuki Y, Sekiya T, and Hayashi K. Rapid and Sensitive Detection of Point Mutations and DNA Polymorphisms Using the Polymerase Chain Reaction. *Genomics* 5: 874-879, 1989.

Parham DM. *Pediatric Neoplasia Morphology and Biology*, New York, Lippincott-Raven, 1996.

Park S, Bernard A, Bove K, Sens DA, Hazen-Martin DJ, Garvin AJ, and Haber DA. Inactivation of WT-1 in Nephrogenic Rests, Genetic Precursors to Wilms' Tumor. *Nature Genetics* 5: 363-367, 1993.

Pelletier J, Bruening W, Kashtan CE, Mauer SM, Manivel JC, Striegel JE, Houghton DC, Junien C, and Habib R. Germline Mutations in the Wilms' Tumor Suppressor Gene are Associated with Abnormal Urogenital Development. *Cell* 67(2): 437-447, 1991.

Pettinato G, Manivel JC, Wick MR, and Dehner LP. Classical and Cellular (Atypical) Congenital Mesoblastic Nephroma : A Clinicopathologic, Ultrastructural, Immunohistochemical, and Flow Cytometric Study. *Human Pathology* 20: 682-690, 1989.

Poleev A, Fickenscher H, Mundlos S, Winterpacht A, Zabel B, Fidler A, Gruss P, and Plachov D. Pax-8, a Human Paired Box Gene: Isolation and Expression in Developing Thyroid, Kidney, and Wilms' Tumor. *Development* 116: 611-623, 1992.

Pritchard-Jones K, Fleming S, Davidson N, Bickmore WA, Porteous D, Gosden C, Bard J, Buckler A, Pelletier J, Housman D, van Heyningen V, and Hastie N. The Candidate Wilms' Tumor Gene is Involved in Genitourinary Development. *Nature* 346: 194-197, 1990.

Pritchard-Jones K and Fleming S. Cell Types Expressing the Wilms' Tumour Gene (WT-1) in Wilms' Tumours: Implications for Tumor Histogenesis. *Oncogene* 6: 2211-2220, 1991.

Pritchard-Jones K and Hawkins MM. Biology of Wilms' Tumour. *Lancet* 349(9053):663-664, 1997.

Punnett HH, Halligan GE, Nayere Z, and Karmazin N. Translocation 10;17 in Clear Cell Sarcoma of the Kidney: A First Report. *Cancer Genetics and Cytogenetics* 41: 123-128, 1989.

Rahman N, Arbour L, Tonin P, Renshaw J, Pelletier J, Baruchel S, Pritchard-Jones K, Stratton MR, and Narod S. Evidence of a Familial Wilms' Tumor Gene (FWT1) on Chromosome 17q12-q21. *Nature Genetics* 13: 461-463, 1996.

Rauscher FJ III, Morris JF, Tournay OE, Cook DM, and Curran T. Binding of the Wilms' Tumor Locus Zinc Finger Protein to the EGR-1 Consensus Sequence. *Science* 250: 1259-1262, 1990.

Re GG, Hazen-Martin DJ, Sens DA, and Garvin AJ. Nephroblastoma (Wilms' Tumor): A Model System of Aberrant Renal Development *Seminars in Diagnostic Pathology* 11(2): 126-135, 1994.

- Re GG, Willingham MC, El Bahtimi R, Brownlee NA, Hazen-Martin DJ, and Garvin AJ. Anaplasia and Drug-Selection Independent Overexpression of the Multidrug Resistance Gene, MDR-1, in Wilms' Tumor. *Modern Pathology* 10(2): 129-136, 1997.
- Reeve AE, Eccles MR, Wilkins RJ, Bell GI, and Millow LJ. Expression of Insulin-like Growth Factor II Transcripts in Wilms' Tumor. *Nature* 317: 258-260, 1985.
- Robson JA and Sidell N. Ultrastructural Features of a Human Neuroblastoma Cell Line Treated with Retinoic Acid. *Neuroscience* 14(4): 1149-1162, 1985.
- Rothenpieler UW and Dressler GR. Pax-2 is Required for Mesenchyme to Epithelium Conversion During Kidney Development. *Development* 119: 711-720, 1993.
- Ryan G, Steele-Perkins V, Morris J, Rauscher FJ III, and Dressler GR. Repression of Pax-2 by WT-1 During Normal Kidney Development. *Development* 121: 867-875, 1995.
- Saga Y, Yagi T, Ikawa Y, Sakahura T, and Aizawa S. Mice Develop Normally Without Tenascin. *Genes and Development* 6: 592-598, 1992.
- Sanger F, Nicklen S, and Coulson AR. DNA Sequencing with Chain Terminating Inhibitors. *Proceedings of the National Academy of Sciences USA* 74: 5463-5467, 1977.
- Saxen L. *Organogenesis of the Kidney*. Cambridge University Press, Cambridge, United Kingdom, 1987.
- Schofield DE, Yunis EJ, and Fletcher JA. Chromosome Aberrations in Mesoblastic Nephroma. *American Journal of Pathology* 143(3): 714-724, 1993.
- Schofield DE, Beckwith JB, and Sklar J. Loss of Heterozygosity at Chromosome Regions 22q11-12 and 11p15.5 in Renal Rhabdoid Tumors. *Genes Chromosomes Cancer* 15: 10-17, 1996.
- Scott J, Cowell J, Robertson ME, Priestly LM, Wadey R, Hopkins B, Pritchard J, Bell GI, Rall LB, Graham CF, and Knott TJ. Insulin-like Growth Factor II Gene Expression in Wilms' Tumor and Embryonic Tissues. *Nature* 365: 764-767, 1985.
- Southern EM. Detection of Specific Sequences Among DNA Fragments Separated by Gel Electrophoresis. *Journal of Molecular Biology* 98(3): 503-517, 1975.
- Stein CA. Suramin: A Novel Antineoplastic Agent with Multiple Potential Mechanisms of Action. *Cancer Research* 53: 2239-2248, 1993.

- Steinman RA, Hoffman B, Ino A, Guillouf C, Lieberman DA, and El-Houseini ME. Induction of p21 (WAF-1/CIP-1) During Differentiation. *Oncogene* 9:3389-3396,1994.
- Tagge EP, Hanson P, Re GG, Othersen HB Jr., Smith CD, and Garvin AJ. Paired Box Gene Expression in Wilms' Tumor. *Journal of Pediatric Surgery* 29(2): 134-141, 1994.
- Thiele CJ, Cohen PS, and Israel MA. Regulation of the c-myb Expression in Human Neuroblastoma Cells During Retnoic Acid Induced Differentiation. *Molecular Cellular Biology* 8: 1677-1683, 1988.
- Tomlison GE, Argyle JC, Velasco S, and Nisen PD. Molecular Characterization of Congenital Mesoblastic Nephroma and its Distinction from Wilms' Tumor. *Cancer* 70: 2358-2361, 1992.
- Torres M, Gomez-Pardo E, Dressler GR, and Gruss P. Pax2 Controls Multiple Steps of Urogenital Development. *Development* 121: 4057-4065, 1995.
- Truong LD, Pindur J, Foster S, Majesky M, and Suki W. Tenascin Expression in Nephrogenesis and in Normal or Pathologic Glomerulus: Morphologic Features and Functional Implications. *Nephron* 72: 499-506, 1996.
- Ueno T, Suita S, and Zaizen Y. Retinoic Acid Induces Insulin-like Growth Factor II Expression in a Neuroblastoma Cell Line. *Cancer Letters* 71: 177-182, 1993.
- Vilar J, Gilbert T, Moreau E, and Merlet-Benichou C. Metanephros Organogenesis is Highly Stimulated by Vitamin A Derivatives in Organ Culture. *Kidney International* 49(5): 1478-1487, 1996.
- Vincent TS, Garvin AJ, Gramling TS, Hazen-Martin DJ, Re GG, and Sens DA. Expression of Insulin-like Growth Factor Binding Protein 2 (IGFBP2) in Wilms' Tumor. *Pediatric Pathology* 14: 723-730, 1994.
- Vincent TS, Hazen-Martin DJ, and Garvin AJ. Inhibition of Insulin-like Growth Factor II Autocrine Growth of Wilms' Tumor by Suramin *in vitro* and *in vivo*. *Cancer Letters* 103: 49-56, 1996a.
- Vincent TS, Re GG, Hazen-Martin DJ, Tarnowski BI, Willingham MC, and Garvin AJ. All-trans- Retnoic Acid Induced Growth Suppression of Blastemal Wilms' Tumor. *Pediatric Pathology and Laboratory Medicine* 16: 777-789, 1996b.
- Waber PG, Chen J, and Nisen PD. Infrequency of MDM-2 Gene Amplification in Pediatric Solid Tumors and Lack of Association with p53 Mutations in Adult Squamous Cell Carcinomas. *Cancer Research* 6028-6030, 1993.

- Wada RK, Seeger RC, Reynolds CP, Alloggiamento T, Yamashiro JM, Ruland C, Black AC, and Rosenblatt JD. Cell-type Specific Expression and Negative Regulation by Retinoic Acid of the Human N-Myc Promoter in Neuroblastoma Cells. *Oncogene* 7: 711-717, 1992.
- Waga S, Hannon GJ, Beach D, and Stillman B. The p21 Inhibitor of Cyclin-dependent Kinases Controls DNA Replication by Interaction with PCNA. *Nature* 369: 574-578, 1994.
- Wang ZY, Madden SL, Deuel TF, and Rauscher FJ III. The Wilms' Tumor Gene Product, WT-1 Represses Transcription of the Platelet-Derived Growth Factor A-Chain Gene. *Journal of Biological Chemistry* 267(31): 21999-22002, 1992.
- Wang-Wuu S, Soukup S, Bove K, Gotwals B, and Lampkin B. Chromosome Analysis of 31 Wilms' Tumors. *Cancer Research* 50: 2786-2793, 1990.
- Weksberg R, Shen DR, Fei YL, Song QL, and Squire J. Disruption of Insulin-like Growth Factor 2 Imprinting in Beckwith-Wiedemann Syndrome. *Nature Genetics* 5: 143-150, 1993.
- Werner H, Re GG, Drummond IA, Sukhatme VP, Rauscher FJ III, Sens DA, Garvin AJ, LeRoith D, and Roberts CT Jr. Increased Expression of the Insulin-like Growth Factor I Receptor Gene, IGF-1R, in Wilms' Tumor is Correlated with Modulation of IGF-1R Promoter Activity by the Wilms' Tumor Gene Product. *Proceedings of the National Academy of Sciences USA* 90(12): 5828-5832, 1993.
- Wigger HJ. Fetal Hamartoma of the Kidney: A Benign, Symptomatic, Congenital Tumor, not a Form of Wilms' Tumor. *American Journal of Clinical Pathology* 51: 323-327, 1969.
- Wu X, Bayle JH, Olson D, and Levine AJ. The p53-MDM-2 Autoregulatory Feedback Loop. *Genes and Development* 7: 1126-1132, 1993.
- Xiong Y, Hannon GJ, Zhang H, Casso D, Kobayashi R, and Beach D. p21 is a Universal Inhibitor of Cyclin Kinases. *Nature* 366: 701-704, 1993.
- Yoon-Jung C, Jung W, Soon J, and Park C. Clear Cell Sarcoma of the Kidney Immunohistochemical Study and Flow Cytometric Analysis of 7 Cases. *Yonsei Medical Journal* 35(3): 336-343, 1994.
- Yun K. Clear Cell Sarcoma of the Kidney Expresses Insulin-like Growth Factor II but not WT-1 Transcripts. *American Journal of Pathology* 142(1): 39-47, 1993.
- Zhan Q, Pan S, Bae I, Guillouf C, Lieberman DA, O'Connor PM, and Fornace AJ Jr. Induction of Bax by Genotoxic Stress in Human Cells Correlates with Normal p53 Status and Apoptosis. *Oncogene* 9: 3743-3751, 1994.